CPC(HEP & NP), 2012, **36**(12): 1287–1602 **Chinese Physics C** Vol. 36, No. 12, Dec., 2012

The AME2012 atomic mass evaluation *

(I). Evaluation of input data, adjustment procedures

G. Audi[1,§], M. Wang[1,2,3], A.H. Wapstra[4,†], F.G. Kondev[5], M. MacCormick[6], X. Xu[2,7], and B. Pfeiffer[8,‡]

[1] Centre de Spectrométrie Nucléaire et de Spectrométrie de Masse, CSNSM, CNRS/IN2P3, Université Paris-Sud, Bât. 108, F-91405 Orsay Campus, France

[2] Institute of Modern Physics, CAS, 509 Nanchang Rd., Lanzhou 730000, China

[3] Max-Planck-Institut für Kernphysik, Saupfercheckweg 1, D-69117 Heidelberg, Germany

[4] National Institute of Nuclear Physics and High-Energy Physics, NIKHEF, 1009DB Amsterdam, The Netherlands

[5] Argonne National Laboratory, 9700 S. Cass Avenue, Argonne, IL 60439, USA

[6] Institut de Physique Nucléaire, CNRS/IN2P3, Université Paris-Sud, F-91406 Orsay cedex, France

[7] Graduate University of Chinese Academy of Sciences, Beijing, 100049, People's Republic of China

[8] GSI Helmholtzzentrum für Schwerionenforschung, Planckstr. 1, D-64291 Darmstadt, Germany

Abstract This paper is the first of two articles (Part I and Part II) that presents the results of the new atomic mass evaluation, AME2012. It includes complete information on the experimental input data (including not used and rejected ones), as well as details on the evaluation procedures used to derive the tables with recommended values given in the second part. This article describes the evaluation philosophy and procedures that were implemented in the selection of specific nuclear reaction, decay and mass-spectrometer results. These input values were entered in the least-squares adjustment procedure for determining the best values for the atomic masses and their uncertainties. Calculation procedures and particularities of the AME are then described. All accepted and rejected data, including outweighed ones, are presented in a tabular format and compared with the adjusted values (obtained using the adjustment procedure). Differences with the previous AME2003 evaluation are also discussed and specific information is presented for several cases that may be of interest to various AME users. The second AME2012 article, the last one in this issue, gives a table with recommended values of atomic masses, as well as tables and graphs of derived quantities, along with the list of references used in both this AME2012 evaluation and the NUBASE2012 one (the first paper in this issue).

AMDC: http://amdc.in2p3.fr/ and http://amdc.impcas.ac.cn/

1 Introduction

The last complete evaluation of experimental atomic mass data AME2003 [1, 2] was published in 2003. Since then an uncommonly large amount of new, high quality, data has been published in the scientific literature. This is substantiated by the fact that as much as 53% of the data used in the present AME2012 evaluation were not available in 2003.

The large number of new data with high quality that are continuously produced render updates of the atomic mass table on a regular basis and a frequency of two or three years necessary. This also corresponds to the demand expressed by the extended nuclear research community. Actually, just after the publication of the AME1993 evaluation [3, 4, 5, 6], the intention was to produce interim updates every two years, followed by a full publication every six to eight years. As a result, the AME1995 update [7] was indeed published two years later. However, due to the necessity to create the NUBASE evaluation (see below), the planned AME updates were not completed. A certain stabilization was reached in 2003, encouraging the publication of the full AME2003 evaluation [1, 2], which was for the first time synchronized with the complementary evaluation of nuclear structure properties, NUBASE2003.

At the same time, renewal and extension of the manpower devoted to these two evaluations was clearly needed, while effective support from institutions was declining and the main authors in the AME2003 were com-

* This work has been undertaken with the encouragement of the IUPAP Commission on Symbols, Units, Nomenclature, Atomic Masses and Fundamental Constants (SUNAMCO).

§ Corresponding author. *E-mail address:* amdc.audi@gmail.com (G. Audi).

† Deceased, December 2006.

‡ Present address: II. Physikalisches Institut, Justus-Liebig-Universität, Heinrich-Buff-Ring 16, D-35392 Gießen.

ing close to retirement for one, stopping for the other one. In 2007, the evaluation was about to disappear. Fortunately, this work was revived in November 2008 when the Institute of Modern Physics at Lanzhou decided to ascertain the future of this long tradition, for the benefit of the physics community worldwide. From the dynamics thus created, other collaborators from all around the world joined gradually.

In order to accomodate the strong demand from the international physics community, a preliminary version of AME, the AME2011 preview, was released from the Atomic Mass Data Center website in April 2011. It was the first time for the mass tables to be disseminated through internet without an accompanying hardcopy.

In this article, general aspects of the development of AME2012 are presented and discussed. In doing this, we will mention several local analyses intended, partly, to study points elaborated further below. Other local analyses may be found on the AMDC web site [8].

The main AME2012 evaluation table (Table I) is presented in this Part I. All accepted and rejected experimental data are given and compared with the adjusted values deduced using a least-squares fit analysis.

Similarly to the previous AME evaluations, the uncertainties quoted in the present tables are one-standard deviation (1 σ).

There is no strict literature cut-off date for the data used in the present AME2012 evaluation: all data, available to the authors until the material was sent to the publisher (November 18, 2012), were included. Those results which could not be included for particular reasons, such as the need for a heavy revision of the evaluation at too late a development stage, were added in remarks to the relevant data. The final mass-adjustment calculations were performed on November 16, 2012.

The present publication updates and includes all the information presented in the previous atomic mass evaluations (since AME1983), including those which are not contributing to the final adjustment results presented here.

Aaldert H. Wapstra, the founder of AME, is among the co-authors of the AME2012 publication. Unfortunately, he passed away at the end of 2006, but he made enormous contributions to the AME2012 development during the two years following the publication of the previous AME2003 evaluation. And more than those two years, the present work is composed of his spirit and wisdom.

1.1 Isomers in the AME and the emergence of NUBASE

During the development of the previous atomic mass evaluations, a computer file (called *Mfile*) that contains the approximate mass values for nuclides in their ground and selected excited isomeric states was maintained. It was used as an approximate input to the computer adjustment program, which essentially uses the differences between the input and these approximate values in order to improve the precision of the calculations. The other reason for the existence of this file was that, where isomers occur, one has to be careful to check which one is involved in reported experimental data, such as α- and β-decay energies. In fact, several cases exist in the literature where the authors were not aware that complications occurred due to presence of isomers. For that reason, our *Mfile* contained known data on such isomeric pairs (half-lives, excitation energies and spin-parities). The issue of isomerism became even more important, when considering new mass-spectrometer methods that were developed to measure masses of exotic nuclides far from the valley of β-stability, which have, in general, relatively short lifetimes. Since the mass resolution of such spectrometers is limited, it is often experimentally impossible to separate isomers. As a consequence, only an average mass value for a particular isomeric pair can be obtained. Since the mass of the ground state is the primary aim of the present evaluation, it can be derived only in cases where one has information on the excitation energies and production rates of the isomers. When the excitation energy of a particular isomer is not experimentally known, it was estimated from trends in neighboring nuclides, as outlined below. Therefore, it was judged necessary to make the *Mfile* as complete as possible, which turned out to be a major effort. However, the resulting NUBASE evaluation, published for the first time in 1997 [9], was greeted with interest from many colleagues working in the areas of nuclear structure physics, nuclear astrophysics and applied nuclear physics, which made the effort worthwhile. In 2003, the NUBASE2003 and AME2003 were published jointly for the first time. Similarly, accompanying the present AME, the NUBASE2012 is published in the first part of this issue.

1.2 Highlights

The backbone Nowadays, the highest precision values presently measured for the atomic masses are concurrently obtained by two different experimental techniques. The first one comprises of direct mass-spectrometry measurements using Penning traps, while the second one utilizes γ-ray energy measurements following neutron capture reactions.

In the present work, results obtained by both methods are combined consistently (with a very few exceptions) to improve considerably the precision of the atomic masses for nuclides along the line of stability in a diagram of the

atomic number Z versus neutron number N [10], thus resulting in a reliable 'backbone'.

The highest precision of 7×10^{-12} presently achieved for mass measurements has been obtained by the Penning trap method. The masses of some stable alkali-metal nuclides and noble-gas nuclides have been determined to 10^{-10} or even better, providing reliable reference standards for other mass measurements.

While most stable nuclides, and some long-lived ones, could have their mass accuracy improved using Penning traps, the priority was given to cases where there is a strong motivation from the physics point of view. For example, the $Q_{\beta\beta}$ values for some nuclides relevant to neutrino properties have been determined with very high precision, strengthening at the same time the backbone.

The exotic species The extent of the domain of nuclides with experimentally known masses has increased impressively over the last few years. Penning traps together with storage rings have played an important role in this extension.

Penning trap mass measurement facilities exist in many nuclear physics laboratories all around the world. They contribute not only in obtaining precise mass values for nuclides near the stability line, but together with the two storage rings facilities, one at the GSI-DARMSTADT and the other at the IMP-LANZHOU, provide valuable experimental results for a wealth of unstable, short-lived nuclides. Until recently, masses of such unstable nuclides were only known from Q_β end-point measurements, which have severe drawbacks owing to the pandemonium effect [11], more specially for high Q_β-values (see Section 6.7). In the present work, the masses for such nuclides have changed considerably compared to AME2003. It can be concluded that the shape of the atomic mass surface, and hence understanding of nuclear interactions, has changed significantly over the last 10-20 years.

It is somewhat ironical, but not unexpected, that the new results showed that several older data are not as good as thought earlier, but the reverse is also true. For example, while reactivating mass-spectrometer measurements performed by the group of Demirkhanov (laboratory labels R04-R13 in Table I), we were positively surprised to notice that their accuracy is much better than thought in the past.

The Isobaric Analogue States - IAS Isobaric Analogue States (IAS) have not been considered with the attention they require and included in the mass evaluation since AME1993. In this issue we have updated and included these masses since they are important states from the nuclear interaction point of view (see Section 6.4). As for any excited state (see also the discussion about isomers in NUBASE, Section 2.2, p. 1161), the mass of an IAS can be derived either from an internal relation (amongst levels within the same nuclide) where the best evaluations are in ENSDF, or from external relations (to other nuclides). In the latter case, only the AME's method can treat with accurateness the data to derive a mass value. It was therefore considered important and also our duty to have these data included in the main mass table, hence providing the users of our tables with the best mass values for the IAS.

Recalibrations Gamma-ray energies measured with bent-crystal spectrometers following neutron capture provide highly-accurate energy relations, e.g. the one-neutron separation energies. However, energies deduced in several (p,γ) reactions are also known with a similar precision. In fact, the accuracies achieved in both cases are so high that one of us [AHW] has re-examined all calibrations. In addition, several α-particle decay energies are also known with a high precision; and here too it was found necessary to harmonize the calibrations.

Differential reactions Another feature near the line of stability is the increased number of measurements of reaction energy differences, which can often be measured with a much higher precision compared to the absolute reaction energies. The AME2012 computer program accepts this type of input data which are given in their original shape in the present table of input data (Table I). This may be another incentive for presenting *primary* results in published literature: in later evaluations those results could be corrected automatically if calibration values change due to new experimental results.

Bare and highly ionized atoms As a result of availability of high-energy accelerators that produce highly ionized atoms, the number of nuclides for which experimental mass values are now known is substantially larger compared to our previous atomic mass tables. These measurements are sometimes made on deeply ionized particles, even up to bare nuclides. The results for masses reported in the literature are converted by the authors to values for neutral (and un-excited) atoms. The needed electron binding energies are taken from tables, like those of Huang et al. [12] (see also the discussion in Part II, Section 2, p. 1604).

At the proton drip-line A further significant development of the presented work is the inclusion of many new data on proton disintegrations that allowed a significant extension of the knowledge of proton binding en-

ergies. In several cases such data are also useful in determining the excitation energies of isomers, as well as in gaining information about the spins and parities of the parent and daughter states. The latter two developments are reasons why it is necessary to pay even more attention to relative positions of isomers than was necessary in our early evaluations. Spatial and time-correlated studies using double-sided silicon strip detectors were especially useful in studying long chains of α-decaying nuclides. The measured α-decay energies often provided precise information on mass differences between the individual chain members. It is fortunate that such new experimental data are produced regularly mainly at laboratories in Finland, Germany, Japan and USA.

Remark: in the following text, several data of general interest will be discussed. Mention of references that can be found in Table I will be avoided. When it is necessary to provide a specific reference, those will be given using the key-numbers (e.g. [2002Aa15]), listed at the end of Part II, under "References used in the AME2012 and the NUBASE2012 evaluations", p. 1863.

Table A. Constants used in this work or resulting from the present evaluation.

1 u	=	$M(^{12}\mathrm{C})/12$	=		atomic mass unit			
1 u	=	1 660 538.921	±	0.073	$\times 10^{-33}$ kg	44	ppb	*a*
1 u	=	931 494.061	±	0.021	keV	22	ppb	*a*
1 u	=	931 494.0023	±	0.0007	keV_{90}	0.7	ppb	*b*
$1\ \mathrm{eV}_{90}$	=	1 000 000.0063	±	0.022	μeV	22	ppb	*a*
1 MeV	=	1 073 544.150	±	0.024	nu	22	ppb	*a*
$1\ \mathrm{MeV}_{90}$	=	1 073 544.2174	±	0.0007	nu	0.7	ppb	*b*
M_e	=	548 579.90946	±	0.00022	nu	0.4	ppb	*a*
	=	510 998.928	±	0.011	eV	22	ppb	*a*
	=	510 998.89581	±	0.00041	eV_{90}	0.8	ppb	*b*
M_p	=	1 007 276 466.92	±	0.09	nu	0.09	ppb	*c*
M_α	=	4 001 506 179.127	±	0.060	nu	0.015	ppb	*c*
$M_n - M_H$	=	839 883.71	±	0.51	nu	610	ppb	*d*
	=	782 346.64	±	0.48	eV_{90}	610	ppb	*d*

a) derived from the work of Mohr and Taylor [13].
b) for the definition of V_{90}, see text.
c) derived from this work combined with M_e and total ionization energies for ^{1}H and ^{4}He from [13].
d) this work.

2 Units; recalibration of α- and γ-ray energies

Atomic mass determination for a particular nuclide can be generally performed by establishing an energy relation between the mass we want to deduce and that for a well known nuclide. This energy relation is then expressed in electron-volts (eV). Mass values can also be obtained as an inertial mass from the movement characteristics of an ionized atom in an electro-magnetic field. The mass, is then derived from a ratio of masses and it is then expressed in 'unified atomic mass' (u). Those two units are used in the present work.

The mass unit is defined, since 1960, as one twelfth of the mass of one free atom of carbon-12 in its atomic and nuclear ground states, $1\ \mathrm{u} = M(^{12}\mathrm{C})/12$. Before 1960, two mass units were used: the physics one, defined as $^{16}\mathrm{O}/16$, and the chemical one which considered one sixteenth of the average mass of a standard mixture of the three stable oxygen isotopes. This difference was considered as being not at all negligible, when taking into account the commercial value of all concerned chemical substances. Physicists could not convince the chemists to drop their unit off; "The change would mean millions of dollars in the sale of all chemical substances", said the chemists, which is indeed true! Kohman, Mattauch and Wapstra [14] then calculated that, if $^{12}\mathrm{C}/12$ was chosen, the change would be ten times smaller for chemists, and in the opposite direction ... This led to an unification; 'u' stands therefore, officially, for 'unified mass unit'! It is worth mentioning that the chemical mass-spectrometry community (e.g. bio-chemistry, polymer chemistry) widely use the dalton unit (symbol Da, named after John Dalton [15]). It allows to express the number

of nucleons in a molecule, at least as it is presently used in these domains. It is thus not strictly the same as 'u'.

The unit for energy is the electron-volt. Until the end of last century, the relative precision of $M-A$ expressed in keV was for several nuclides less accurate than the same quantity expressed in mass units. The choice of the volt for the energy unit (the electronvolt) is not unambiguous. For example, one may use the *international* volt V, but other can choose the volt V_{90} as *maintained* in national metrology laboratories and defined by adopting an exact value for the constant $(2e/h)$ in the relation between frequency and voltage in the Josephson effect. Since 1990, by definition $2e/h = 483597.9$ (exact) GHz/V_{90} (see Table B). Already in 1983, an analysis by Cohen and Wapstra [16] showed that all precision measurements of reaction and decay energies were calibrated in such a way that they can be more accurately expressed in *maintained* volt. Also, as seen in Table A, the precision of the conversion factor between mass units and *maintained* volt (V_{90}) is more accurate than that between the former and *international* volt. In fact, the accuracy is so high that the relative precision of $M-A$ expressed in eV_{90} is the same as that expressed in mass units. For example, the mass excess of ^{4}He is 2 603 254.13±0.06 nu in mass units, 2 424 915.63±0.06 eV_{90} in *maintained* volt units and 2 424 915.78±0.08 eV in *international* volt units. Due to the increase of precision, the relative precision of $M-A$ expressed in keV_{90} is as good as the same quantity expressed in mass units, whereas the uncertainties expressed in *international* volts are larger than in V_{90}. Therefore, as already adopted in our previous mass evaluations, the V_{90} (*maintained* volt) unit is used in the present work.

In the most recent (2012) evaluation by Mohr et al. [13], the relation between *maintained* and *international* volts is given as V_{90}=[1+6.3(2.2)$\times 10^{-8}$]V, that could be expressed as a difference of 63(22) ppb.

In Table A the relations between *maintained* and *international* volts, and several constants of interest, obtained from the evaluation of Mohr et al. [13] are given. Given also are the ratio of mass units to electronvolts for the two Volt units, and also the ratio of the two Volts. In addition, values for the masses of the proton, neutron and α particle, as derived from the present evaluation, are also given, together with the mass difference between the neutron and the light hydrogen atom.

In earlier mass tables (e.g. AME1993), we used to give values for the binding energies, $ZM_H + NM_n - M$. The main reason for this was that the uncertainty (in keV_{90}) of this quantity was larger than that of the mass excess, $M-A$. However, due to the increased precision in the neutron mass, this is no longer important. Similarly to AME2003, we now give instead the binding energy per nucleon for educational reasons, connected to the Aston curve and the maximum stability around the 'Iron-peak' of importance in astrophysics (see also the note in Part II, Section 2, p. 1605).

The defining values and the resulting mass-energy conversion factors are given in Table B. Since 2003 the definition has not been modified. Therefore, no recalibration has been necessary in the present AME2012 compared to AME2003, except in one case where the precicion in the obtained data is better than a few hundred ppb.

This case is the ^{1}H(n,γ)^{2}H reaction which has the highest energy precision in the input data with relative uncertainty of 180 ppb, where the wave length of the emitted γ ray is determined by using the ILL silicon crystal spectrometer. In AME2003, the recommended value was 2224.5660(4) keV_{90}, based on the work of [1999Ke05] at the NBS. In a later work from the same group [2006De21], the value was corrected to be 2224.55610(44) keV with new evaluation on the lattice spacing of the crystal and fundamental constants at that time. The value of the crystal lattice spacing is used as an adjusted parameter in the new evaluation of Mohr et al., but not expressed explicitly. Using the same value of the wave length in [2006De21], and the new length-energy conversion coefficient, we derive 2224.55600(44) keV_{90} as input to our evaluation. Note that the value expressed in eV_{90} is 0.14 smaller than expressed in *international* eV, about one third of the uncertainty.

Table B. Definition of Volt units, and resulting mass-energy conversion constants.

	$2e/h$			u		
1983	483594.21	(1.34)	GHz/V	931501.2	(2.6)	keV
1983	483594	(exact)	GHz/V_{86}	931501.6	(0.3)	keV_{86}
1986	483597.67	(0.14)	GHz/V	931494.32	(0.28)	keV
1990	483597.9	(exact)	GHz/V_{90}	931493.86	(0.07)	keV_{90}
1999	483597.9	(exact)	GHz/V_{90}	931494.009	(0.007)	keV_{90}
2010	483597.9	(exact)	GHz/V_{90}	931494.0023	(0.0007)	keV_{90}

Some more historical points are worth mentioning.

It was in 1986 that Taylor and Cohen [17] showed that the empirical ratio between the two types of volts, which had of course been selected to be nearly equal to 1, had changed by as much as 7 ppm. For this reason, in 1990 a new value was chosen [18] to define the *maintained* volt V_{90}. In their 1998 evaluation, Mohr and Taylor [19] had to revise the conversion constant to *international* eV. The result was a slightly higher (and 10 times more precise) value for V_{90}.

Since older high-precision, reaction-energy measurements were essentially expressed in keV_{86}, we had to take into account the difference in voltage definition that causes a systematic error of 8 ppm. We were therefore obliged, for the AME2003 tables, to adjust the older precise data to the new keV_{90} standard. For α-particle energies, Rytz [20] has taken this change into account, when updating his earlier evaluation of α-particle energies. We have used his values in the present input data table (Table I) and indicated this by adding in the reference field the symbol "Z".

A considerable number of (n,γ) and (p,γ) reactions has a precision not much worse than 8 ppm. In 1990, one of us [21] has discussed the need for necessary recalibration for several γ rays that are often used as calibration standards. This work has been updated in AME2003 (in a special file dedicated to this study, available from the AMDC Web-site [22]) to evaluate the influence of new calibrators, as well as of the new Mohr and Taylor fundamental constants on γ-ray and particle energies used in (n,γ), (p,γ) and (p,n) reactions. In doing this, the calibration work of Helmer and van der Leun [23], based on the fundamental constants at that time, was used. For each of the data concerned, the changes were relatively minor. However, we judged it necessary, in AME2003, to make such recalibrations, since otherwise they add up to systematic uncertainties that are non-negligible. We also reconsidered the calibration for proton energies (see below). As in the case of Rytz' recalibrations for α-decay energies, such data are marked by "Z" behind the reference key-number. If it was not possible to do so, for example when this position was used to indicate that a remark was added, the same "Z" symbol was added to the uncertainty value mentioned in the remark.

The list of input values (Table I) for our calculations includes many excitation energies that are derived from γ-ray measurements that are generally evaluated in the Nuclear Data Sheets (NDS) [24]. Only in exceptional cases, it made sense to change them to recalibrated results.

For higher γ-ray energies, the AME1995 adjustment used several data recalibrated with results from Penning trap measurements for initial and final atoms involved in (n,γ) reactions. The use of the newer constants and of additional, or revised, Penning trap results, made it necessary, in AME2003, to revise again the recalibrated results. One of the consequences was that the energy coming free in the ^{14}N(n,γ)^{15}N reaction, playing a crucial role in these calibrations, was changed from $10\,833\,301.6\pm2.3\,eV_{90}$ to $10\,833\,296.2\pm0.9\,eV_{90}$ in AME2003, and $10\,833\,295.33\pm0.77\,eV_{90}$ in present AME. For more details and discussion, see [22].

Several old neutron binding energies were improved in unexpected ways. For example, a value with a somewhat large uncertainty of 650 eV was reported for the neutron binding energy of ^{54}Cr. Careful examination of the original article showed that this value was essentially the sum of the energies of two capture γ-rays. For their small energy difference a smaller error was reported. Later work yielded a much improved value for the transition to the ground state, allowing to derive a considerably improved neutron binding energy. Also, in some cases, observed neutron resonance energies could be combined with the latest measurements of the excitation energies of the resonance states. Further discussions can be found on the AMDC web site [22].

In AME2003, we also recalibrated proton energies, more particularly those involved in resonance energies and thresholds. An unfortunate development here was that the data for the 991 keV ^{27}Al+p resonance [1994Br37] (used frequently for calibration) were reported with higher precision than older ones, but they differed more than expected [22]. The value most often used in earlier work was 991.88 ± 0.04 keV from the work of Roush *et al.* [25]. In 1990, Endt *et al.* [26] averaged it with the later result by Stoker *et al.* [27], thus obtaining a slightly modified value of 991.858 ± 0.025 keV. By doing this, changes in the values of natural constants used in the derivation of these values were not taken into account. By correcting for this omission and by critically evaluating earlier data, one of us [28] derived in 1993 a value 991.843 ± 0.033 keV for this standard, and, after the 2003 revision, 991.830 ± 0.050 keV [22]. The measurement of [1994Br37] yielded 991.724 ± 0.021 keV, which is two standard deviations from the above adopted value (labeled 'B' in Table 1).

3 Input data, representation in a connections diagram

As mentioned above, there are two methods that are used in measurements of atomic masses: the mass-spectrometry one (often called a "direct method"), where the inertial mass is determined from the trajectory of the ion in a magnetic field, or from its time-of-flight, and

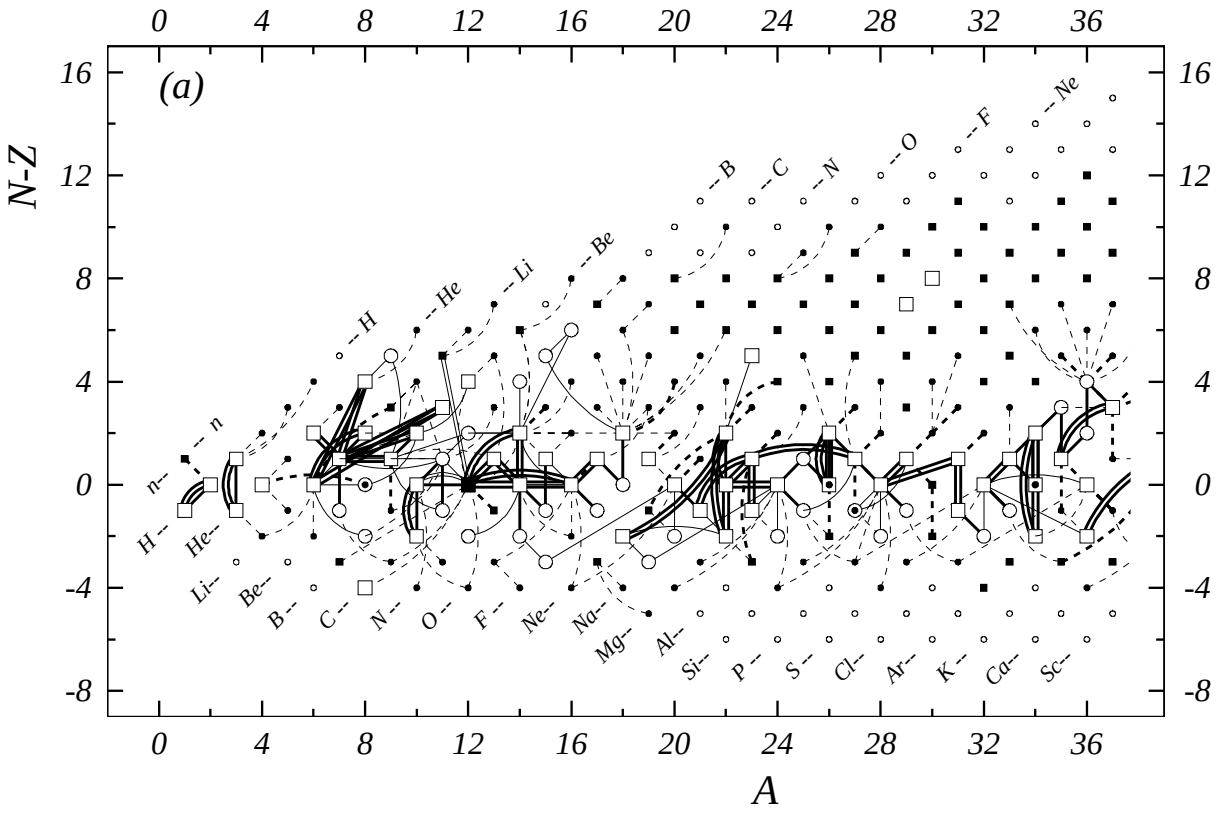

Figure 1: (a)–(j). Diagram of connections for input data.

For *primary data* (those checked by other data):

- □ absolute mass-doublet nuclide (i.e. connected to ^{12}C, ^{35}Cl or ^{37}Cl); (or nuclide connected by a unique secondary relative mass-doublet to a remote reference nuclide);
- ◯ other primary nuclide;
- ⊡ ⊙ primary nuclide with relevant isomer;
- // mass-spectrometer connection;
- ——— other primary reaction connection.

Primary connections are drawn with two different thicknesses. Thicker lines represent the highest precision data in the given mass region (limits: 1 keV for $A < 36$, 2 keV for $A = 36$ to 165 and 3 keV for $A > 165$).

For *secondary data* (cases where masses are known from one type of data and are therefore not checked by a different connection):

- ■ secondary experimental nuclide determined from mass-spectrometry;
- ● secondary experimental nuclide determined by a reaction or a decay;
- ○ nuclide for which mass is estimated from trends in the Mass Surface TMS;
- – – – – – connection to a secondary nuclide. Note that an experimental connection may exist between two estimated TMS nuclides when neither of them is connected to the network of primaries.

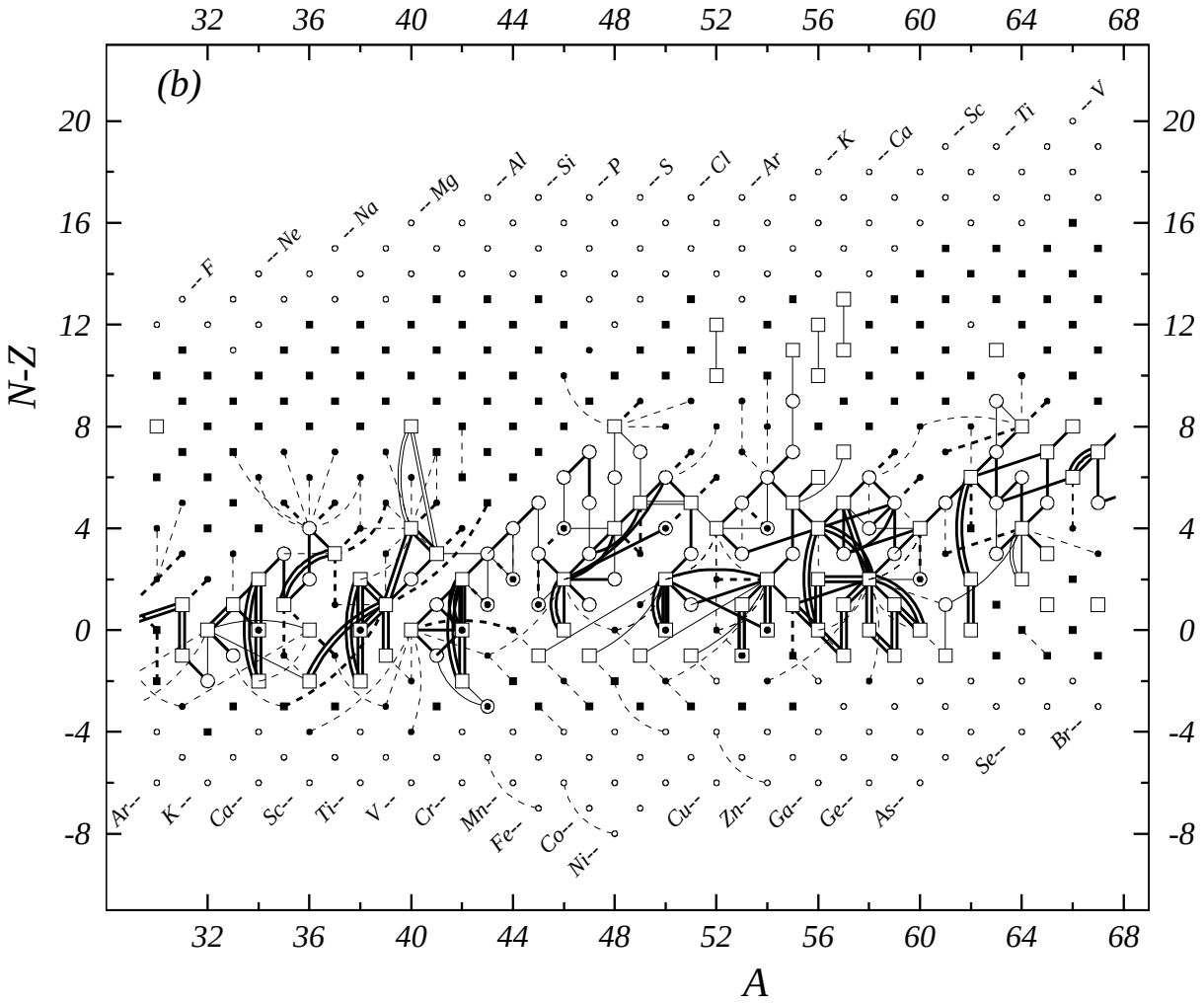

Figure 1 (b). Diagram of connections for input data —- continued.

the so-called "indirect method" where the reaction energy, i.e. the difference between several masses, is determined using a specific nuclear reaction or a decay process. In the present work all available experimental data related to atomic masses (both energy and mass-spectrometry data) are considered. The input data are extracted from the available literature, compiled in an appropriate format and then carefully evaluated.

In AME data treatment, we try our best to use the primary experimental information. In this way, the masses can be recalibrated automatically for any future changes, and the original correlation information can be properly preserved.

One example that illustrates our policy of data treatment is the following. In the [1986Ma40] publication, the Q value of the ^{148}Gd(p,t)^{146}Gd reaction was measured relative to that for the ^{65}Cu(p,t)^{63}Cu reference reaction. The latter value was adopted from the AME1995 mass table, but it was changed by 1.8 keV in the present mass table. In AME2003, the corresponding equation was ^{148}Gd(p,t)^{146}Gd = –7843±4 keV. However, in the present work, it is presented and used as a differential reaction equation: ^{148}Gd(p,t)^{146}Gd−^{65}Cu(p,t)^{63}Cu = 1500±4 keV. Strictly speaking, those equations are not exact either. What is measured in the experiment is the energy spectra of the ejected particles. Since there are differences between the masses of the measured nuclides and the reference, the response of the ejected particles to the Q values are different for the measured nuclides and the reference, depending also on the angle where the spectra are obtained. While the exact equations are quite complex, we believe that the treatment by differential reaction equation represents the original data more reliably and that most of the primary information is preserved.

Nuclear reaction $A(a,b)B$ and decay $A(b)B$ energy measurements connect the initial (A) and final (B) nuclides with one or two reaction or decay particles. With the exception of some reactions between very light nuclides, the precision with which the masses of reaction particles a and b are known is much higher than that of the measured reaction and decay energies. Thus, these reactions and decays can each be represented as a link be-

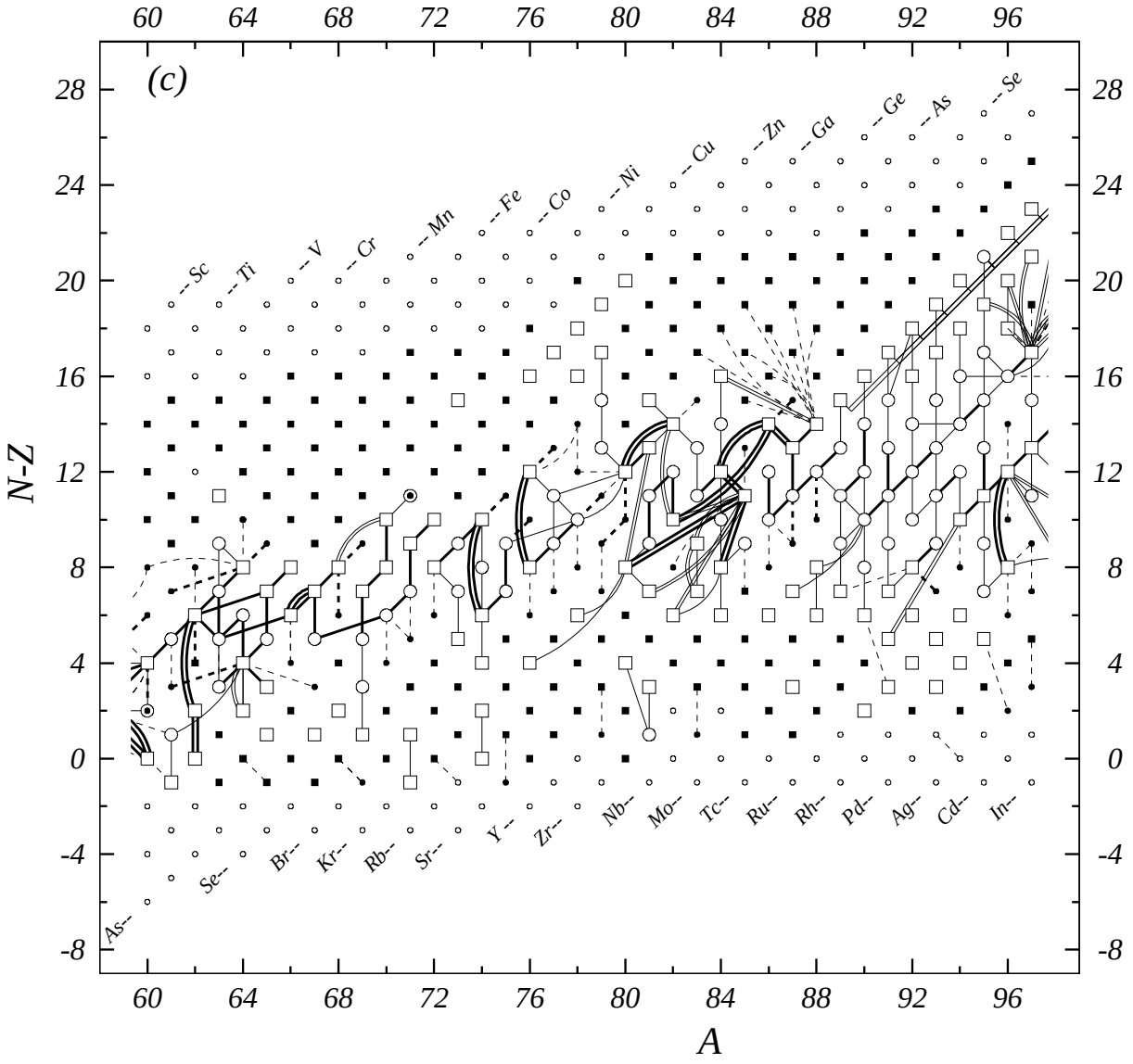

Figure 1 (c). Diagram of connections for input data —- continued.

tween two nuclides A and B. Differential reaction energies $A(a,b)B-C(a,b)D$ are in principle represented by a combination of four masses.

Direct mass-spectrometry measurements, again with exception of a few cases between very light nuclides, can be separated in a class of connections between two or three nuclides, and a class essentially determining an absolute mass value (see Section 5). Penning trap measurements, almost always give a ratio of masses between two nuclides (inversely proportional to their cyclotron frequencies in the trap). Sometimes these two nuclides can be very far apart. Thus, those measurements are in most cases best represented as a combination of two masses. Other types of direct experimental methods, such as 'Smith-type', 'Schottky', 'Isochronous' and 'time-of-flight' mass-spectrometers, are calibrated in a more complex way, and are thus published by their authors as absolute mass doublets. They are then presented in Table I as a difference: ^{A}El-u.

For completeness we mention that early mass-spectrometer "triplet" measurements on unstable nuclides can best be represented as linear combinations of masses of three isotopes, with non-integer coefficients [29].

This situation allows us to represent the input data graphically in a diagram of $(N-Z)$ versus $(N+Z)$ as shown in Fig. 1. This is straightforward for absolute mass-doublets and for two-nuclide difference cases; but not for spectrometer triplets and differential reaction energies (see Section 1.2., p. 1289). The latter are in general more important for one of the two reaction energies than for the other one; in the graphs we therefore represent them simply by the former. (For computational reasons, these data are treated as primaries even though the diagrams then show only one connection.)

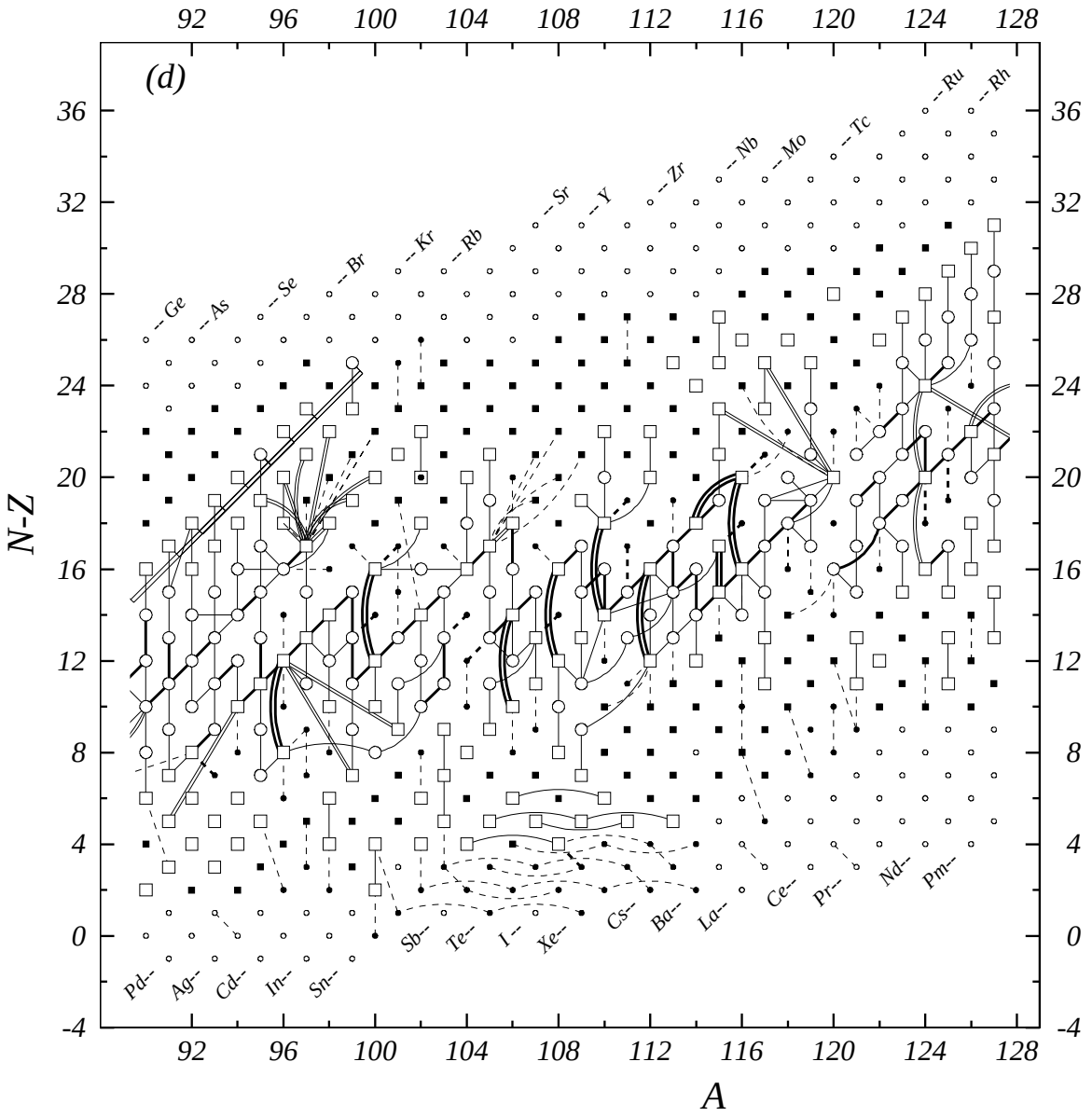

Figure 1 (d). Diagram of connections for input data —- continued.

In the present work, all input data are evaluated, i.e. calibrations are checked if necessary, and the data are compared with other results and with the trends in the mass surface (TMS) in the region. As a consequence, several input data are changed or even rejected. All input data, including the rejected ones (not presented in Fig. 1), are given in Table I. As can be seen from Fig.1, the accepted data may allow determination of the mass of a particular nuclide using several different routes; such a nuclide is called *primary*. The mass values in the table are then derived by least squares methods. In the other cases, the mass of a nuclide can be derived only from a connection to another one; it is called a *secondary* nuclide. This classification is of importance for our calculation procedure (see Section 5, p. 1305).

The diagrams in Fig. 1 also show many cases where the relation between two atomic masses is accurately known, but not the values of the masses. Since our policy is to include all available experimental results, we have produced in such cases estimated mass values that are based on the trends in the mass surface in the neighborhood (TMS). In the resulting system of data representations, vacancies occur, which were filled using the same TMS procedure. Estimates of unknown masses are further discussed in the next section.

Some care should be taken in the interpretation of Fig. 1, since excited isomeric states and data relations involving such isomers are not completely represented on these drawings. This is not considered a serious defect; those readers who want to update such values can conve-

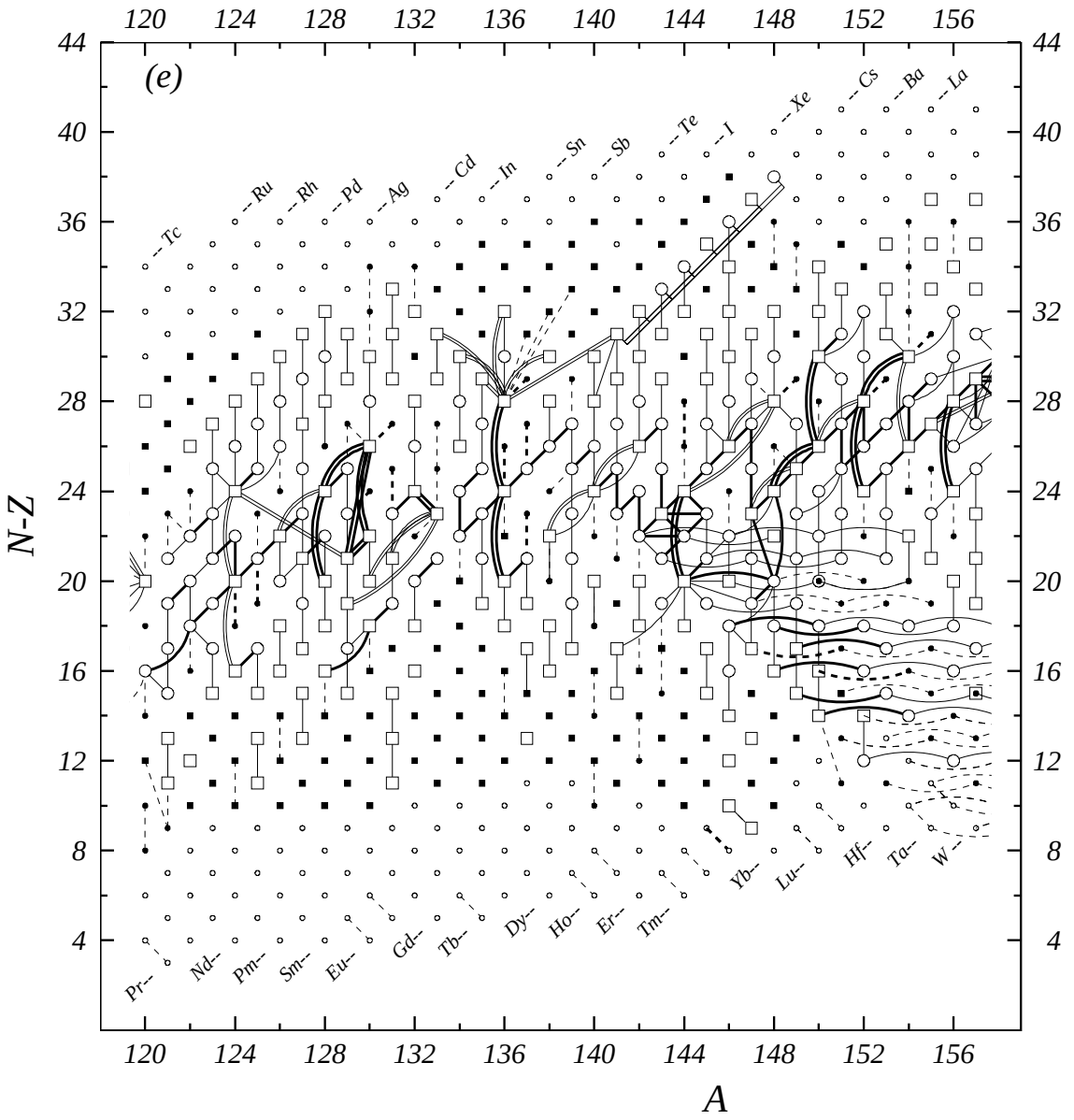

Figure 1 (e). Diagram of connections for input data —- continued.

niently consult Table I, where all relevant information is given.

4 Regularity of the mass-surface and use of trends in the Mass Surface (TMS)

When atomic masses are displayed as a function of N and Z, one obtains a *surface* in a 3-dimensional space. However, due to the pairing energy, this surface is divided into four *sheets*. The even-even sheet lies lowest, the odd-odd highest, the other two nearly halfway in-between, as shown in Fig. 2. The vertical distances from the even-even sheet to the odd-even and even-odd ones are the proton and neutron pairing energies Δ_{pp} and Δ_{nn}. They are nearly equal. The distances of the last two sheets to the odd-odd sheet are equal to $\Delta_{nn} - \Delta_{np}$ and $\Delta_{pp} - \Delta_{np}$, where Δ_{np} is the proton-neutron pairing energy due to the interaction between the two odd nucleons, which are generally not in the same shell. These energies are represented in Fig. 2, where a hypothetical energy zero represents a nuclide with no pairing among the last nucleons.

Experimentally, it has been observed that: the four sheets run nearly parallel in all directions, which means that the quantities Δ_{nn}, Δ_{pp} and Δ_{np} vary smoothly and slowly with N and Z; and that each of the mass sheets varies also smoothly, but rapidly with N and Z [30]. The smoothness is also observed for first order derivatives (slopes, e.g. the graphs in Part II, p. 1826) and all second order derivatives (curvatures of the mass surface). They are only interrupted in places by cusps or bumps associ-

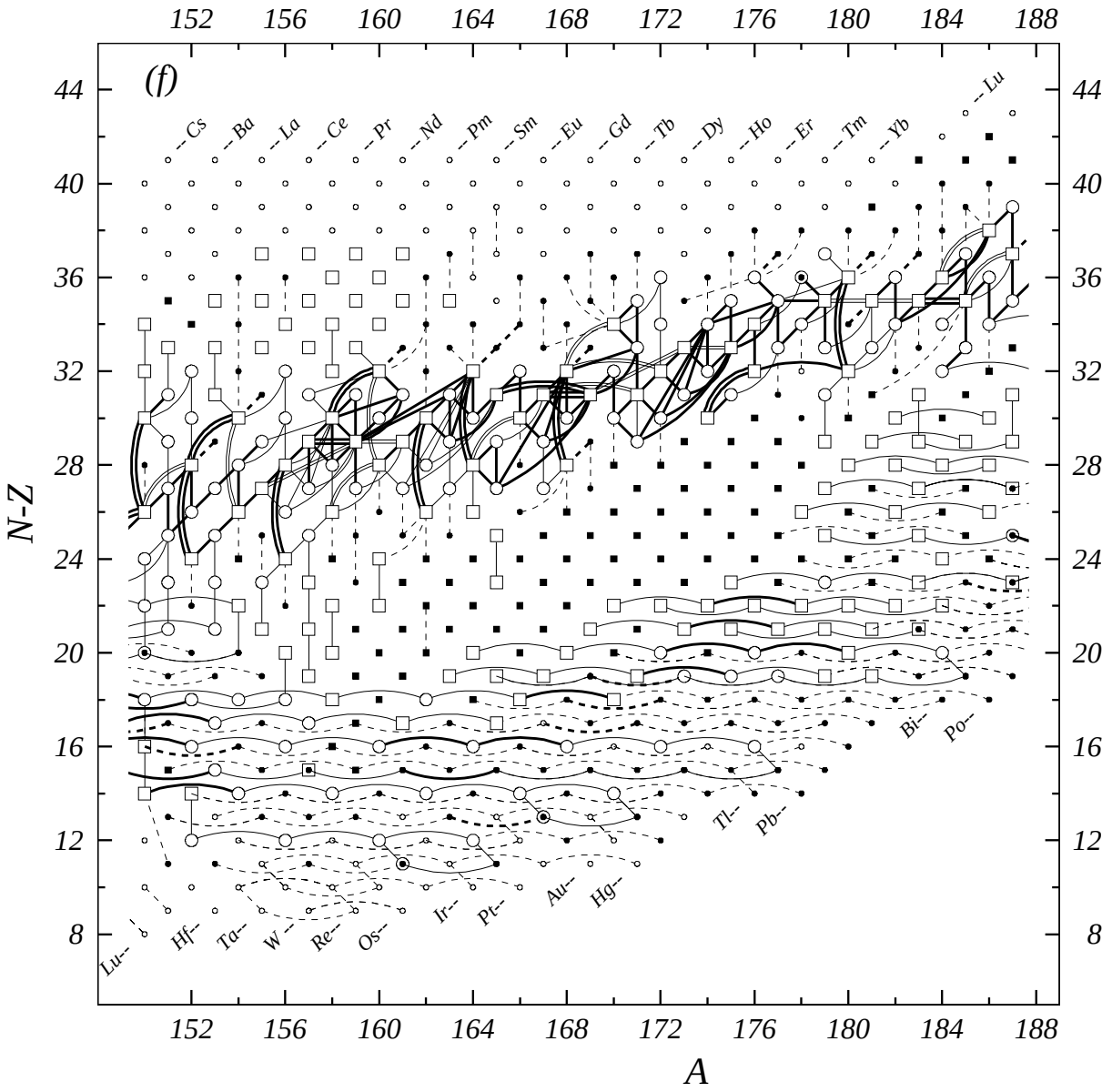

Figure 1 (f). Diagram of connections for input data —- continued.

ated with important changes in nuclear structure: shell or sub-shell closures, shape transitions (spherical-deformed, prolate-oblate), and the so-called 'Wigner' cusp along the $N = Z$ line.

This observed regularity of the mass sheets in all places where no change in the physics of the nucleus are known to exist, can be considered as one of the BASIC PROPERTIES of the mass surface. Thus, dependable estimates of unknown, poorly known or questionable masses can be obtained by extrapolation from well-known mass values on the same sheet. In the evaluation of masses the property of regularity and the possibility to make estimates are used for several purposes:

1. Any coherent deviation from regularity, in a region (N,Z) of some extent, could be considered as an indication that some new physical property is being discovered. However, if one single mass violates the trends in the mass surface given by neighboring nuclides, then one may seriously question the correctness of the related datum. There might be, for example, some undetected systematic [31] contribution to the reported result of the experiment measuring this mass. We then reexamine with extra care the available experimental information in literature for possible errors and often ask the corresponding authors for additional information. Such a process often leads to corrections.

2. There are cases where several experimental data disagree among each other, but no particular reason can be found for rejecting one or some of them by

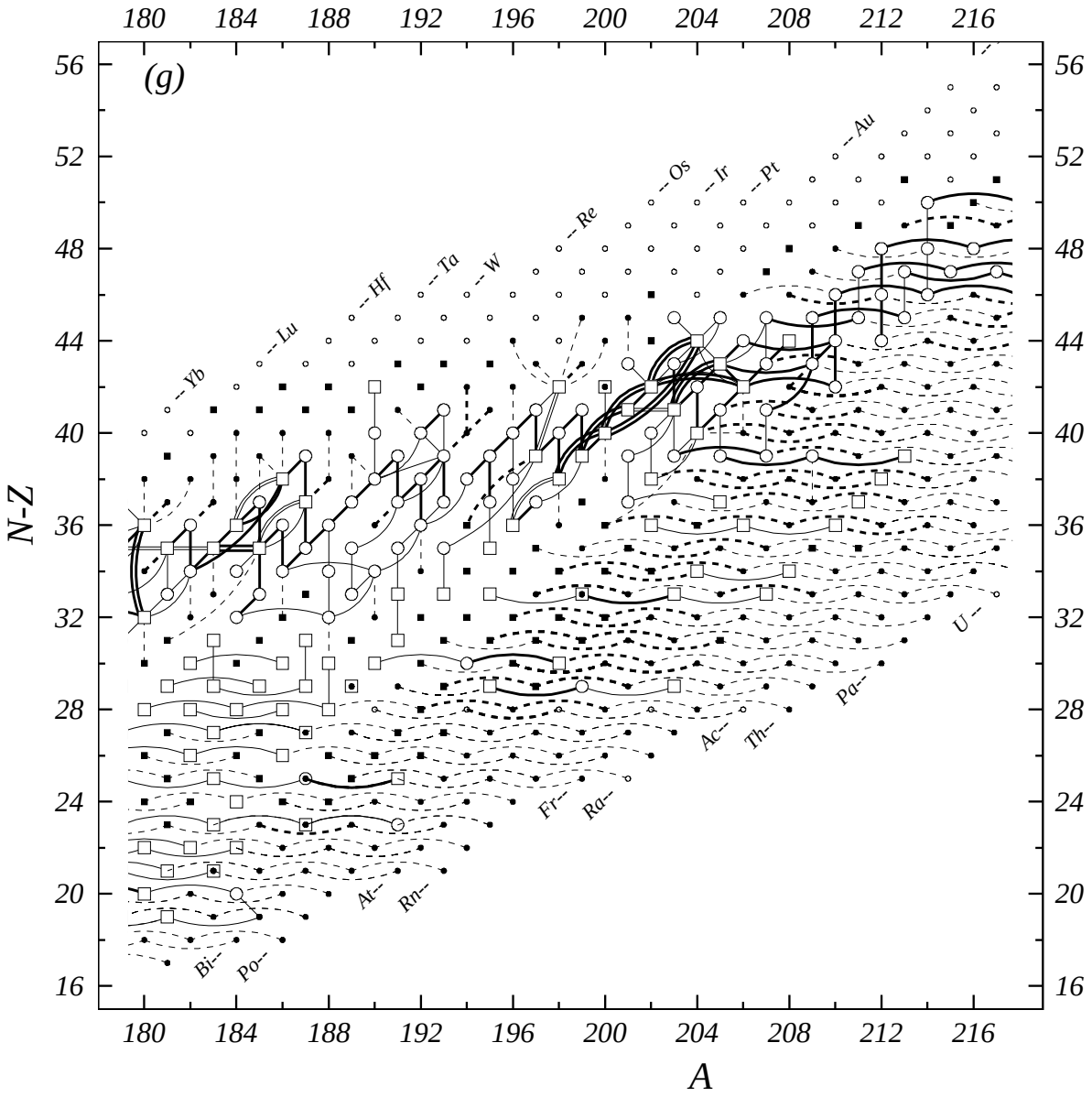

Figure 1 (g). Diagram of connections for input data —- continued.

studying the corresponding papers. In such cases, the measure of agreement with the just mentioned regularity can be used by the evaluators for selecting which of the conflicting data will be accepted and used in the evaluation, thus following the same policy that was used in our earlier work.

3. There are cases where masses determined from ONLY ONE experiment (or from same experiments) deviate severely from the smooth surface. Such cases are examined closely and are discussed extensively below (Section 4.1).

4. Finally, drawing the mass surface allows to derive estimates for the still unknown masses, either from interpolations or from short extrapolations (see below, Section 4.2).

4.1 Scrutinizing and manipulating the surface of masses

Direct representation of the mass surface is not convenient, since the binding energy varies very rapidly with N and Z. Splitting in four sheets, as mentioned above, complicates even more such a representation. There are two ways that allow to observe with some precision the surface of masses: one of them uses the *derivatives* of this surface, the other is obtained by *subtracting a simple function* of N and Z from the masses.

The derivatives of the mass surface By *derivative* of the mass surface we mean a specified difference between

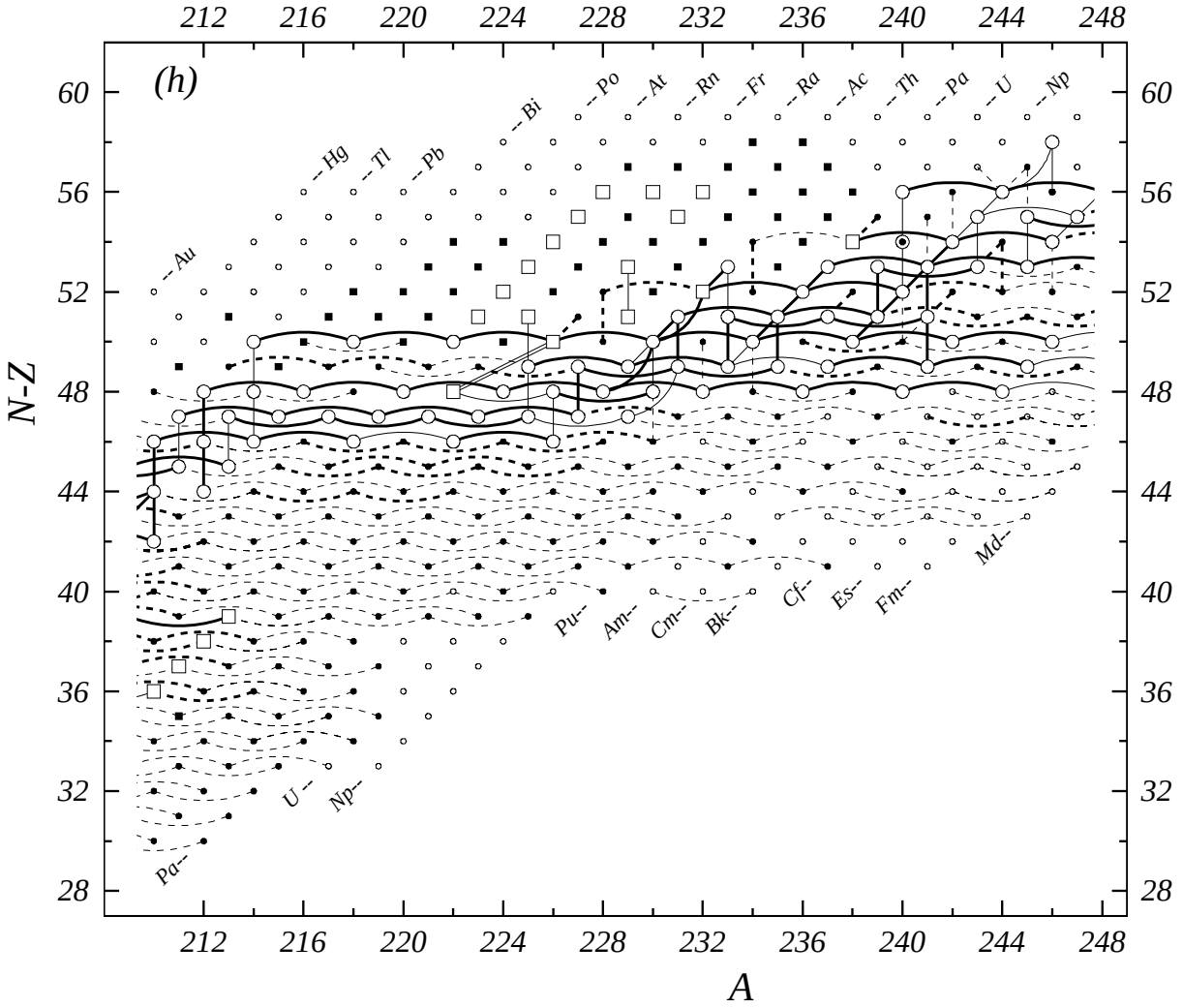

Figure 1 (h). Diagram of connections for input data —- continued.

the masses of two nearby nuclides. These functions are also smooth and have the advantage of displaying much smaller variations. For a derivative specified in such a way that differences are between nuclides in the same mass sheet, the near parallelism of these leads to an (almost) unique surface for the derivative, allowing thus a single display. Therefore, in order to visualize the trends in the mass surface, we found that such estimates could be obtained best in graphs such as α- and double-β-decay energies and separation energies of two protons and two neutrons. These four derivatives are plotted against N, Z or A in Part II, Figs. 1–36, p. 1826.

However, from the way these four derivatives are created, they give information only within one of the four sheets of the mass surface (e-e, e-o, o-e or e-e; e-o standing for even-N and odd-Z). When examining the mass surface, an increased or decreased spacing of the sheets cannot be observed. Also, when estimating unknown masses, divergences of the four sheets could be unduly created, which is unacceptable.

Fortunately, other various representations are possible (e.g. separately for odd and even nuclides: one-neutron separation energies versus N, one-proton separation energy versus Z, β-decay energy versus A, ...). We have prepared such graphs that can be obtained from the AMDC web site [8].

The method of 'derivatives' suffers from involving two masses for each point to be drawn, which means that if one mass is moved then two points are changed in opposite direction, causing confusion in the drawings. Also, reversely, the deviation of one point from regularity could be due to either the nuclide it represents or the related one in the difference, rendering the analysis rather complex.

Subtracting a simple function Since the mass surface is smooth, one can try to define a function of N and Z as

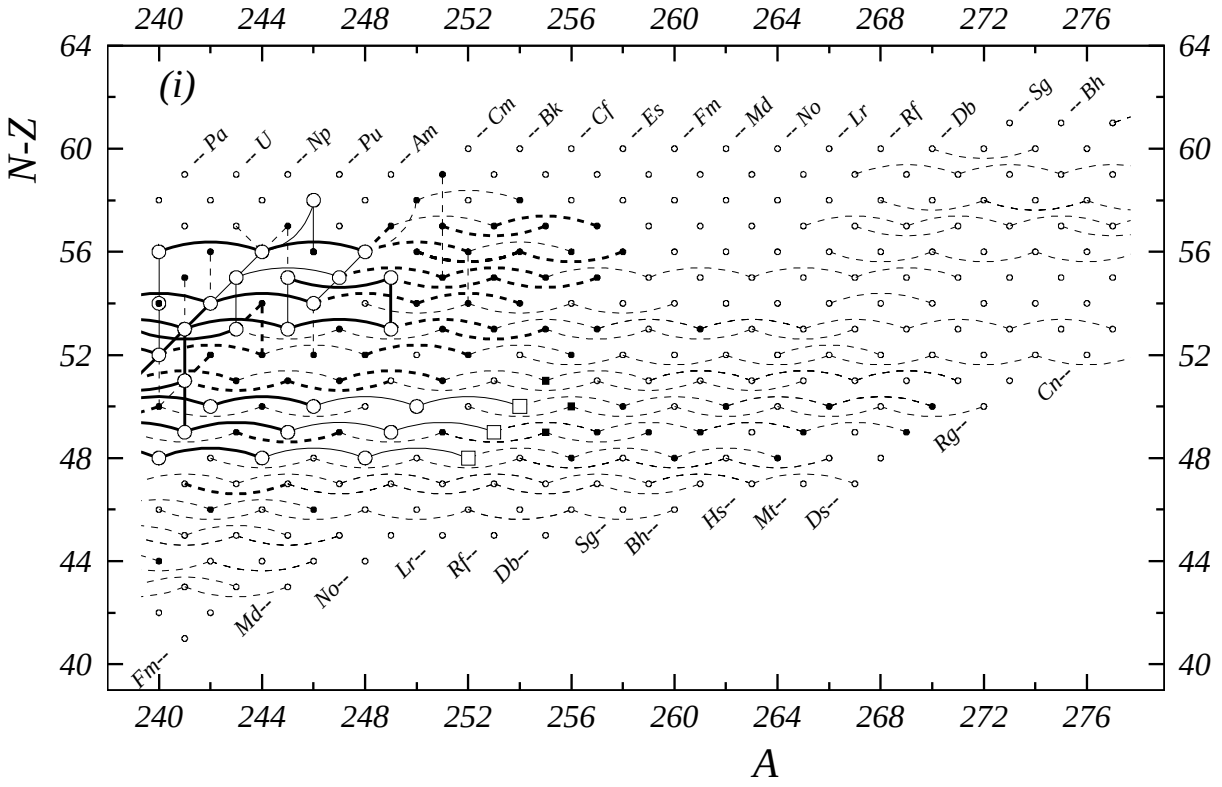

Figure 1 (i). Diagram of connections for input data —- continued.

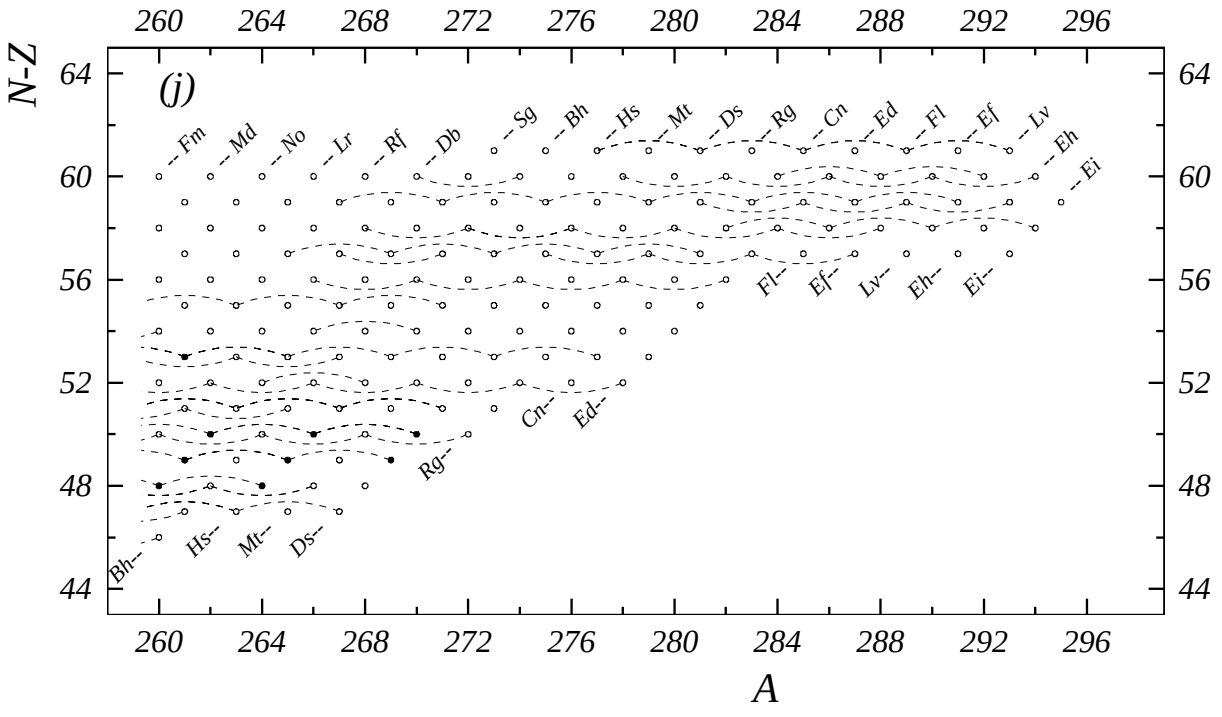

Figure 1 (j). Diagram of connections for input data —- continued.

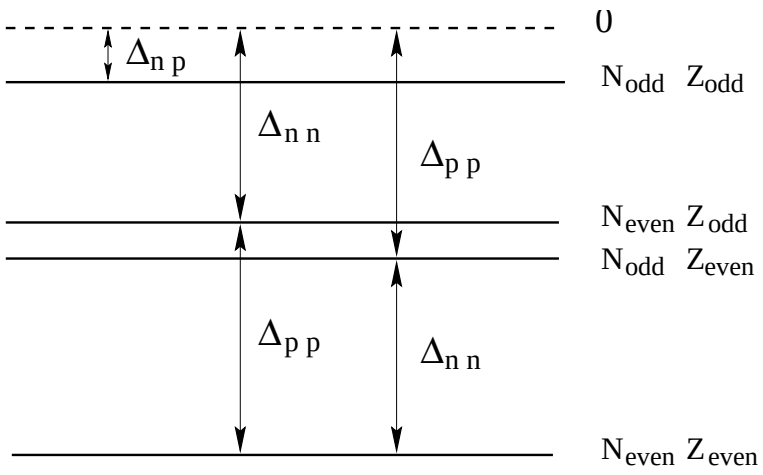

Figure 2: The surface of masses is split into four sheets. This scheme represents the pairing energies responsible for this splitting. The zero energy surface is purely hypothetical with no pairing at all among the outer nucleons.

simple as possible and not too far from the real surface of masses. The difference between the mass surface and this function, while displaying reliably the structure of the former, will vary less rapidly, thus improving its observation.

A first and simple approach is the semi-empirical *liquid drop* formula of Bethe and Weizsäcker [32] with the addition of a pairing term in order to fuse more or less the four sheets of the mass surface. Another possibility, that we prefer [30], is to use the results of the calculation of one of the modern models. However, we can use here only those models that provide masses specifically for the spherical part, forcing the nucleus to be not deformed. The reason is that the models generally describe quite well the shell and sub-shell closures, and to some extent the pairing energies, but not the locations of deformation. If the theoretical deformations were included and not located at exactly the same position as given by the experimental masses, the mass difference surface would show two dislocations for each shape transition. Interpretation of the resulting surface would then be very difficult. In the present work, we make use of such differences with models. The plots we have prepared can also be retrieved from the AMDC web site [8].

Manipulating the mass surface In order to make estimates of unknown masses or to test changes on measured ones, an interactive graphical program was developed [30, 33] that allows a simultaneous observation of four graphs, either from the 'derivatives' type or from the 'differences' type, as a function of any of the variables N, Z, A, $N-Z$ or $N-2Z$, while drawing iso-lines (lines connecting nuclides having same value for a parameter) of any of these quantities. The mass of a nuclide can be modified or created in any view and we can determine how much freedom is left in setting a value for this mass. At the same time, interdependence through secondary connections (Fig. 1) are taken into account. In cases where two tendencies may alternate, following the parity of the proton or of the neutron numbers, one of the parities may be deselected.

The replaced values for data yielding the 'irregular masses' as well as the 'estimated unknown masses' (see below) are thus derived by observing the continuity property in several views of the mass surface, with all the consequences due to connections to masses in the same chain. Comparisons with the predictions of 16 nuclear mass-models are presently available in this program.

With this graphical tool, the results of 'replacement' analyses are felt to be safer; and also the estimation of unknown masses is more reliable.

All mass values dependent on interpolation procedures, and indeed all values not derived from experimental data alone, have been clearly marked with the sharp (#) symbol in all tables, here and in Part II.

Since publication of AME1983 [34], estimates are also given for the precision of such data derived from trends in the mass surface (TMS). These precisions are not based on a formalized procedure, but on previous experience with such estimates.

In the case of extrapolation however, the uncertainty in the estimated mass will increase with the distance of extrapolation. These uncertainties are obtained by considering several graphs of TMS with a guess on how much the estimated mass may change without the extrapolated surface looking too much distorted. This recipe is unavoidably subjective, but has proven to be efficient through the agreement of these estimates with newly measured masses in a great majority of cases [35].

4.2 Irregular mass values

When a single mass deviates significantly from regularity with no similar pattern for nuclides with same N or with same Z values, then the correctness of the data determining this mass may be questioned.

Our policy, redefined in AME1995 [7], for those locally *irregular* masses, and only when they are derived from a unique mass relation (i.e., not confirmed by a different experimental method), is to replace them by values derived from trends in the mass surface (TMS). There are only 27 such physical quantities in the present evaluation, compared to 27 in AME2003, 59 in AME1995 and 67 in AME1993 that were selected, partly, in order to avoid too strongly oscillating plots. Although these numbers reflects a more strict use of this procedure, the user of our tables should not assume that the remaining 27 items are the same ones carried on from generation to generation. The opposite is true, most of the old ones have been replaced by new data showing that we were correct in our choice. Generally, in such unique mass relation, only one measurement is reported. But sometimes there are two measurements (2 cases) or three (in previous evaluations) that we still treat the same way, since use of the same method and the same type of relation may well lead to the same systematic uncertainty (for example a mis-assignment or ignorance of a final level). Taking into account the connecting chains for secondaries (Figs. 1a–1j) has the consequence that several more ground state masses are affected (and twice as many values in each type of plot of derivatives as given in Part II). It should be stressed that only the most striking cases have been treated this way, those necessary to avoid, as much as possible, confusions in the graphs in Part II. In particular, as happened previously, the plots of α-decay energies of light nuclides (Fig. 18 and 19 in Part II, p. 1844 and 1845) exhibit many overlaps and crossings that obscure the drawings; no attempt was made to locate possible origins of such irregularities.

Replacing these few irregular experimental values by ones we recommend, in all tables and graphs in this AME2012, means also that, as explained already in AME1995, we discontinued an older policy that was introduced in AME1993, where original irregular experimental values were given in all main tables, and 'recommended' ones given separately in secondary tables. This policy led to confusion for many users of our tables. Since AME1995, we only give what we consider the *"best recommended values"*, using, when we felt necessary and as explained above, *'values derived from TMS'*. Data which are not used following this policy, can be easily located in Table I where they are flagged 'D' and always accompanied by a comment explaining in which direction the value has been changed and by which amount.

Such data, as well as the other local irregularities that can be observed in the figures in Part II could be considered as incentive to remeasure the masses of the involved nuclides, preferably by different methods, in order to remove any doubt and possibly point out true irregularities due to physical properties.

The present authors insist that only the most striking irregularities have been replaced by estimates. In AME2003, p. 148, we gave as an example the case of ^{112}Te, which mass was determined from the reported delayed-proton energy measurement from ^{113}Xe with a precision of 150 keV. However, we felt that it was deviating 300 keV from the trends given by neighboring nuclides, but it was not been replaced by an estimated mass value. This was felt as an incentive to remeasure the mass of ^{112}Te, if possible using a different method. As a matter of fact, a group using a Penning trap at SHIPTRAP [2007Ma92], measured the mass of this nuclide and found its mass was to be moved from -77301$\pm$170 keV to -77567.5$\pm$8.4 keV, i.e. almost exactly where our estimate located it.

4.3 Estimates for unknown masses

Estimates for unknown masses are also made with use of trends in the mass surface, as explained above, by demanding that all graphs should be as smooth as possible, except where they are expected to show the effects of shell closures or nuclear deformations effects. Therefore, we warn the user of our tables that the present extrapolations, based on trends in known masses, will be wrong if unsuspected new regions of deformation or (semi-) magic numbers occur.

In addition to the rather severe constraints imposed by the requirement of simultaneous REGULARITY of all graphs, many further constraints result from knowledge of reaction or decay energies in the regions where these estimates are made. These regions and these constraints are shown in Figs. 1a–1j. Two kinds of constraints are present. In some cases the masses of (Z, A) and (Z, A+4) are known but not the mass of (Z, A+2). Then, the values of $S_{2n}(A+2)$ and $S_{2n}(A+4)$ cannot both be chosen freely from the graphs; their sum is known. In other cases, the mass differences between several nuclides (A+4n, Z+2n) are known from α-decays and also those of (A-2+4n, Z+2n). Then, the differences between several successive $S_{2n}(A+4n, Z+2n)$ are known. Similar situations exist for two or three successive S_{2p}'s or Q_α's.

Also, knowledge of stability or instability against particle emission, or limits on proton or α emission, yield upper or lower limits on the separation energies.

For proton-rich nuclides with $N < Z$, mass estimates can be obtained from the charge symmetry. This feature gives a relation between masses of isobars around the one with $N = Z$. In several cases, we make a correction by including the Thomas-Ehrman effect [36], which makes proton-unstable nuclides more bound than follows from the above estimate. For very light nuclides, we can use the estimates for this effect found by Comay *et al.* [37]. However, since the analysis of proton-unstable nuclides (see Section 6.5) showed that this effect is much smaller for $A = 100 - 210$, we use a correction that decreases with increasing mass number.

Another often good estimate can be obtained from the observation that masses of nuclidic states belonging to an isobaric multiplet are represented quite accurately by a quadratic equation of the charge number Z (or of the third components of the isospin, $T_3 = \frac{1}{2}(N-Z)$): the Isobaric Multiplet Mass Equation (IMME). Use of this relation is attractive since, otherwise than the relation mentioned above, it uses experimental information (i.e. excitation energies of isobaric analogues). The exactness of the IMME has regularly been a matter of discussion. At regular intervals of time, some new mass measurements question the validity of the IMME, followed soon by other works showing that another member of the same multiplet is to be questioned. For example, a measurement [2001He29] of the mass of ^{33}Ar has questioned the validity of the IMME at $A = 33$. The measured mass, with an uncertainty of about 4 keV, was 18 keV lower than the value following from IMME, with a precision of 3 keV. One year later, another measurement [38] showed that one of the other mass values entering in this equation was wrong. With the new value, the difference is only 3 keV, thus within uncertainties.

Up to the AME1983, we indeed used the IMME for deriving mass values for nuclides for which no, or little information was available. This policy was questioned with respect to the correctness in stating as 'experimental' a quantity that was derived by combination with a calculation. Since AME1993, it was decided not to present any IMME-derived mass values in our evaluation, but rather use the IMME as a guideline when estimating masses of unknown nuclides. We continue this policy here, and do not replace experimental values by an estimated one from IMME, even if orders of magnitude more precise. Typical examples are ^{28}S and ^{40}Ti, for which the IMME predicts masses with precisions of respectively 24 keV and 22 keV, whereas the experimental masses are known both with 160 keV precision, from double-charge exchange reactions.

The extension of the IMME to higher energy isobaric analogues has been studied by one of the present authors [39]. The validity of the method, however, is made uncertain by possible effects spoiling the relation. In the first place, the strength of some isobaric analogues at high excitation energies is known to be distributed over several levels with the same spin and parity. Even in cases where this interference effect has not been observed, it remains a possibility, and as such, it introduces an uncertainty in the energy level to be attributed to the IAS. In the second place, as argued by Thomas and Ehrman [36], particle-unstable levels must be expected to be shifted somewhat.

It also happens that information on excitation energies of $T_3 = -T + 1$ isobaric analogue states is available from measurements on proton emission following β-decays of their $T_3 = -T$ parents. Their authors, in some cases, derived from their results a mass value for the parent nuclide, using a formula derived by Antony et al. [40] from a study of known energy differences between isobaric analogues. We observe, however, that one obtains somewhat different mass values by combining Antony differences with the mass of the mirror nuclide of the mother. Also, earlier considerations did not take into account the difference between proton-pairing and neutron-pairing energies, which one of the present authors [AHW] noticed to have a not negligible influence on the constants in the IMME.

Another possibility is to use a relation proposed by Jänecke [41], as done for example by Axelsson *et al.* [42] in the case of ^{31}Ar. We have in several cases compared the results of different ways for extrapolating, in order to find a best estimate for the desired mass value.

Enough values have been estimated to ensure that every nuclide for which there is any experimental Q-value is connected to the main group of primary nuclides. In addition, the evaluators want to achieve continuity of the mass surface. Therefore an estimated value is included for any nuclide if it is between two experimentally studied nuclides on a line defined by either $Z =$ constant (isotopes), $N =$ constant (isotones), $N - Z =$ constant (isodiaspheres), or, in a few cases $N + Z =$ constant (isobars). It would have been desirable to give also estimates for all unknown nuclides that are within reach of the present accelerator and mass separator technologies. Unfortunately, such an ensemble is practically not easy to define. Instead, we estimate mass values for all nuclides for which at least one piece of experimental information is available (e.g. identification or half-life measurement or proof of instability towards proton or neutron emission). Then, the ensemble of experimental masses and estimated ones has the same contour as in the NUBASE2012 evaluation (see p. 1159).

5 Calculation Procedures

The atomic mass evaluation is unique when compared to the other evaluations of data [30], in a sense that almost all mass determinations are relative measurements, not absolute ones. Even those called 'absolute mass doublets' are relative to ^{12}C, ^{35}Cl or ^{37}Cl. Each experimental datum sets a relation in mass or in energy among two (in a few cases three or more) nuclides. It can be therefore represented by one link among these two nuclides. The ensemble of these links generates a highly entangled network. Figs. 1a–1j, in Section 3 above, show a schematic representation of such a network.

The masses of a large number of nuclides are multiply determined, entering the entangled area of the canvas, mainly along the backbone. Correlations do not allow to determine their masses straightforwardly.

To take into account these correlations we use a least-squares method weighed according to the precision with which each piece of data is known. This method allows to determine a set of adjusted masses.

5.1 Least-squares method

Each piece of data has a value $q_i \pm dq_i$ with the accuracy dq_i (one standard deviation) and makes a relation between 2, 3 or 4 masses with unknown values m_μ. An overdetermined system of Q data to M masses ($Q > M$) can be represented by a system of Q linear equations with M parameters:

$$\sum_{\mu=1}^{M} k_i^\mu m_\mu = q_i \pm dq_i \qquad (1)$$

e.g. for a nuclear reaction $A(a,b)B$ requiring an energy q_i to occur, the energy balance writes:

$$m_\mathrm{A} + m_\mathrm{a} - m_\mathrm{b} - m_\mathrm{B} = q_i \pm dq_i \qquad (2)$$

thus, $k_i^\mathrm{A} = +1$, $k_i^\mathrm{a} = +1$, $k_i^\mathrm{b} = -1$ and $k_i^\mathrm{B} = -1$.

In matrix notation, $\mathbf{K}$ being the (Q,M) matrix of coefficients, Eq. 1 writes: $\mathbf{K}|m\rangle = |q\rangle$. Elements of matrix $\mathbf{K}$ are almost all null: e.g. for $A(a,b)B$, Eq. 2 yields a line of $\mathbf{K}$ with only four non-zero elements.

We define the diagonal weight matrix $\mathbf{W}$ by its elements $w_i^i = 1/(dq_i dq_i)$. The solution of the least-squares method leads to a very simple construction:

$$^\mathbf{t}\mathbf{KWK}|m\rangle = {}^\mathbf{t}\mathbf{KW}|q\rangle \qquad (3)$$

the NORMAL matrix $\mathbf{A} = {}^\mathbf{t}\mathbf{KWK}$ is a square matrix of order M, positive-definite, symmetric and regular and hence invertible [43]. Thus the vector $|\overline{m}\rangle$ for the adjusted masses is:

$$|\overline{m}\rangle = \mathbf{A}^{-1}\,{}^\mathbf{t}\mathbf{KW}|q\rangle \qquad \text{or} \qquad |\overline{m}\rangle = \mathbf{R}|q\rangle \qquad (4)$$

The rectangular (M,Q) matrix $\mathbf{R}$ is called the RESPONSE matrix.

The diagonal elements of $\mathbf{A}^{-1}$ are the squared errors on the adjusted masses, and the non-diagonal ones $(a^{-1})_\mu^\nu$ are the coefficients for the correlations between masses m_μ and m_ν. Values for correlation coefficients for the most precise nuclides are given in Table B of Part II (p. 1605). Following the advice of B.N. Taylor, we now also give on the web-site of the AMDC [8] the full list of correlation coefficients, allowing thus any user to perform exact calculation of any combination of masses.

One of the most powerful tools in the least-squares calculation described above is the flow-of-information matrix, discovered in 1984 by one of us [GAu]. This matrix allows to trace back the contribution of each individual piece of data to each of the parameters (here the atomic masses). The AME uses this method since 1993.

The flow-of-information matrix $\mathbf{F}$ is defined as follows: $\mathbf{K}$, the matrix of coefficients, is a rectangular (Q,M) matrix, the transpose of the response matrix ${}^\mathbf{t}\mathbf{R}$ is also a (Q,M) rectangular one. The (i,μ) element of $\mathbf{F}$ is defined as the product of the corresponding elements of ${}^\mathbf{t}\mathbf{R}$ and of $\mathbf{K}$. In reference [44] it is demonstrated that such an element represents the *"influence"* of datum i on parameter (mass) m_μ. A column of $\mathbf{F}$ thus represents all the contributions brought by all data to a given mass m_μ, and a line of $\mathbf{F}$ represents all the influences given by a single piece of data. The sum of influences along a line is the *"significance"* of that datum. It has also been proven [44] that the influences and significances have all the expected properties, namely that the sum of all the influences on a given mass (along a column) is unity, that the significance of a datum is always less than unity and that it always decreases when new data are added. The significance defined in this way is exactly the quantity obtained by squaring the ratio of the uncertainty on the adjusted value over that on the input one, which is the recipe that was used before the discovery of the $\mathbf{F}$ matrix to calculate the relative importance of data.

A simple interpretation of influences and significances can be obtained in calculating, from the adjusted masses and Eq. 1, the adjusted data:

$$|\overline{q}\rangle = \mathbf{KR}|q\rangle. \qquad (5)$$

The i^{th} diagonal element of $\mathbf{KR}$ represents then the contribution of datum i to the determination of $\overline{q_i}$ (same datum): this quantity is exactly what is called above the *significance* of datum i. This i^{th} diagonal element of $\mathbf{KR}$ is the sum of the products of line i of $\mathbf{K}$ and column i of $\mathbf{R}$. The individual terms in this sum are precisely the *influences* defined above.

The flow-of-information matrix **F**, provides thus insight on how the information from datum *i* flows into each of the masses m_μ.

The flow-of-information matrix cannot be given in full in a printed table. It can be observed along lines, displaying thus, for each datum, the nuclides influenced by this datum and the values of these *influences*. It can be observed also along columns to display for each primary mass all contributing data with their *influence* on that mass.

The first display is partly given in the table of input data (Table I) in column 'Signf.' for the *significance* of primary data and 'Main infl.' for the largest *influence*. Since in the large majority of cases only two nuclides are concerned in each piece of data, the second largest *influence* could easily be deduced. It is therefore not felt necessary to give a table of all *influences* for each primary datum.

The second display is given in Part II, Table II (p. 1673) for the up to three most important data with their *influence* in the determination of each primary mass.

5.2 Consistency of data

The system of equations being largely over-determined ($Q >> M$) offers the evaluator several interesting possibilities to examine and judge the data. One might for example examine all data for which the adjusted values deviate significantly from the input ones. This helps to locate erroneous pieces of information. One could also examine a group of data in one experiment and check if the uncertainties assigned to them in the experimental paper were not underestimated.

If the precisions dq_i assigned to the data q_i were indeed all accurate, the normalized deviations v_i between adjusted $\overline{q}_i$ (Eq. 5) and input q_i data, $v_i = (\overline{q}_i - q_i)/dq_i$, would be distributed as a Gaussian function of standard deviation $\sigma = 1$, and would make χ^2:

$$\chi^2 = \sum_{i=1}^{Q} \left(\frac{\overline{q}_i - q_i}{dq_i} \right)^2 \qquad \text{or} \qquad \chi^2 = \sum_{i=1}^{Q} v_i^2 \qquad (6)$$

equal to $Q-M$, the number of degrees of freedom, with a precision of $\sqrt{2(Q-M)}$.

One can define as above the NORMALIZED CHI, χ_n (or 'consistency factor' or 'Birge ratio'): $\chi_n = \sqrt{\chi^2/(Q-M)}$ for which the expected value is $1 \pm 1/\sqrt{2(Q-M)}$.

Another quantity of interest for the evaluator is the PARTIAL CONSISTENCY FACTOR, χ_n^p, defined for a (homogeneous) group of p data as:

$$\chi_n^p = \sqrt{\frac{Q}{Q-M} \; \frac{1}{p} \; \sum_{i=1}^{p} v_i^2}. \qquad (7)$$

Of course the definition is such that χ_n^p reduces to χ_n if the sum is taken over all the input data. One can consider for example the two main classes of data: the reaction and decay energy measurements and the mass-spectrometry data (see Section 5.5). One can also consider groups of data related to a given laboratory and with a given method of measurement and examine the χ_n^p of each of them. There are presently 269 groups of data in Table I (among which 184 have at least one measurement used in determining the masses), identified in column 'Lab'. A high value of χ_n^p might be a warning on the validity of the considered group of data within the reported uncertainties. We used such analyses in order to be able to locate questionable groups of data. In bad cases they are treated in such a way that, in the final adjustment, no really serious cases occur. Remarks in Table I report where such corrections have been made.

5.3 Separating secondary data

In Section 3, while examining the diagrams of connections (Fig. 1), we noticed that, whereas the masses of *secondary* nuclides can be determined uniquely from the chain of secondary connections going down to a *primary* nuclide, only the latter see the complex entanglement that necessitated the use of the least-squares method.

In terms of equations and parameters, we consider that if, in a collection of equations to be treated with the least-squares method, a parameter occurs in only one equation, removing this equation and this parameter will not affect the result of the fit for all other data. We can thus redefine more precisely what was called *secondary* in Section 3: the parameter above is a *secondary* parameter (or mass) and its related equation a *secondary* equation. After solving the reduced set, the *secondary* equation can be used to find the value and uncertainty for that particular *secondary* parameter. The equations and parameters remaining after taking out all secondaries are called *primary*.

Therefore, only the system of *primary* data is overdetermined, and thus will be improved in the adjustment, so that each *primary* nuclide will benefit from all the available information. *Secondary* data will remain unchanged; they do not contribute to χ^2.

The diagrams in Fig. 1 show, that many *secondary* data exist. Thus, taking them out simplifies considerably the system. More importantly, if a better value is found for a *secondary* datum, the mass of the *secondary* nuclide can easily be improved (one has only to watch since the replacement can change other *secondary* masses down the chain, see Fig. 1). The procedure is more complicated for new *primary* data.

We define DEGREES for *secondary* nuclides and *sec-*

ondary data. They reflect their distances along the chains connecting them to the network of primaries. The first secondary nuclide connected to a primary one will be a nuclide of degree 2; and the connecting datum will be a datum of degree 2 as well. Degree 1 is for primary nuclides and data. Degrees for secondary nuclides and data range from 2 to 18. In Table I, the degree of data is indicated in column 'Dg'. In the table of atomic masses (Part II, Table I, p. 1608), each *secondary* nuclide is marked with a label in column 'Orig.' indicating from which other nuclide its mass value is determined.

To summarize, separating secondary nuclides and secondary data from primaries allow to significantly reduce the size of the system that will be treated by the least-squares method described above. After treatment of the primary data alone, the adjusted masses for primary nuclides can be easily combined with the secondary data to yield masses of secondary nuclides.

In the next section we will show methods for reducing further this system, but without allowing any loss of information. Methods that reduce the system of primaries for the benefit of the secondaries not only decrease computational time (which nowadays is not so important), but allows an easier insight into the relations between data and masses, since no correlation is involved.

Remark: the word *primary* used for these nuclides and for the data connecting them does not mean that they are more important than the others, but only that they are subject to the special treatment below. The labels *primary* and *secondary* are not intrinsic properties of data or nuclides. They may change from primary to secondary or reversely when other information becomes available.

5.4 Compacting the set of data

5.4.1 Pre-averaging

Two or more measurements of the same physical quantities can be replaced without loss of information by their average value and precision, reducing thus the system of equations to be treated. By extending this procedure, we consider *parallel* data: reaction data occur that give essentially values for the mass-difference between the same two nuclides, except in rare cases where the precision is comparable to that in the masses of the reaction particles. Example: ^{14}C(^{7}Li,^{7}Be)^{14}B and ^{14}C(^{14}C,^{14}N)^{14}B; or ^{22}Ne(t,^{3}He)^{22}F and ^{22}Ne(^{7}Li,^{7}Be)^{22}F.

Table C. Worst pre-averagings. n is the number of data in the pre-average.

Item	n	χ_n	σ_e	Item	n	χ_n	σ_e
^{249}Bk(α)^{245}Am	2	2.55	2.45	^{223}Pa(α)^{219}Ac	2	2.09	10.0
^{133}Te-^{130}Xe$_{1.023}$	2	2.54	4.4	^{27}P^{i}(2p)^{25}Al	2	2.08	75
^{144}Ce(β^-)^{144}Pr	2	2.44	2.18	^{177}Pt(α)^{173}Os	2	2.06	6
^{97}Mo(p,n)^{97}Tc	2	2.40	12.9	^{244}Cf(α)^{240}Cm	2	2.03	4.0
^{220}Fr(α)^{216}At	2	2.34	4.7	^{15}N(p,n)^{15}O	2	2.03	1.4
^{75}As(n,γ)^{76}As	2	2.32	0.17	^{58}Fe(t,p)^{60}Fe	4	2.03	7.4
^{176}Au(α)^{172}Ir	2	2.31	17.6	^{204}Tl(β^-)^{204}Pb	2	2.03	0.39
^{110}In(β^+)^{110}Cd	3	2.29	28.4	^{69}Co-u	2	2.02	413
^{43}Cl-u	2	2.28	233	^{167}Os(α)^{163}W	4	1.98	3.5
^{166}Os(α)^{162}W	2	2.24	10.5	^{106}Ag(ε)^{106}Pd	2	1.98	6.6
^{146}Ba(β^-)^{146}La	2	2.24	107	^{78}Se(n,γ)^{79}Se	3	1.96	0.28
^{154}Eu(β^-)^{154}Gd	2	2.22	4.0	^{46}Ca(n,γ)^{47}Ca	2	1.94	0.56
^{40}Cl(β^-)^{40}Ar	2	2.21	76	^{145}Sm(ε)^{145}Pm	2	1.92	7.9
^{219}U(α)^{215}Th	2	2.18	38	^{234}Th(β^-)^{234}Pam	3	1.90	2.10
^{153}Gd(n,γ)^{154}Gd	2	2.16	0.39	^{242}Pu(α)^{238}U	2	1.89	2.08
^{36}S(^{11}B,^{13}N)^{34}Si	3	2.13	32	^{230}Th(d,t)^{229}Th	2	1.89	8.6
^{113}Cs(p)^{112}Xe	3	2.11	5.8	^{99}Ag-^{85}Rb$_{1.165}$	2	1.87	12.6

Such data are represented together, in the main least-squares fit calculations, by one of them carrying their average value. If the Q data to be pre-averaged are strongly conflicting, i.e. if the consistency factor (or Birge ratio, or normalized χ) $\chi_n = \sqrt{\chi^2/(Q-1)}$ resulting in the calculation of the pre-average is greater than 2.5, the (internal) precision σ_i in the average is multiplied by the Birge ratio ($\sigma_e = \sigma_i \times \chi_n$). There are 2 cases where $\chi_n > 2.5$, see Table C (they were 6 in AME2003). The quantity σ_e is often called the 'external error'. However, this treatment is not

used in the very rare cases where the precisions in the values to be averaged differ too much from one another, since the assigned uncertainties lose any significance (only one case in AME2003, none here.) If such a case occurs, considering policies from the Particle Data Group [45] and some statistical-treatment methods reviewed by Rajput and MacMahon [46], we adopt an arithmetic average and the dispersion of values as an uncertainty, which is equivalent to assigning to each of these conflicting data the same uncertainty.

In the present evaluation, we have replaced 2961 data by 1182 averages. As much as 23% of those have values of χ_n (Birge ratio) beyond unity, 2.1% beyond two, none beyond 3, giving an overall very satisfactory distribution for our treatment. With the above choice of a threshold of χ_n^0=2.5 for the Birge ratio, only 0.17% of the cases are concerned by the multiplication by χ_n. As a matter of fact, in a complex system like the one here, many values of χ_n beyond 1 or 2 are expected to exist, and if errors were multiplied by χ_n in all these cases, the χ^2-test on the total adjustment would have been invalidated. This explains the choice we made here of a rather high threshold ($\chi_n^0 = 2.5$), compared e.g. to $\chi_n^0 = 2$ recommended by Woods and Munster [47] or $\chi_n^0 = 1$ used in a different context by the Particle Data Group [45], for departing from the rule of 'internal error' of the weighted average.

Besides the computer-automated pre-averaging, we found it convenient, in the case of some β^+-decays, to combine results stemming from various capture ratios in an average. These cases are ^{109}Cd(ε)^{109}Ag (average of 3 data), ^{139}Ce(ε)^{139}La (average of 10) and ^{195}Au(ε)^{195}Pt (5 results), and they are detailed in Table I. Four more cases occur in our list, but they carry no weight (they are then, as usual, labeled 'U' in Table I).

Used policies in treating parallel data In averaging β- (or α-) decay energies derived from branches observed in the same experiment, to or from different levels in the decay of a given nuclide, the uncertainty we use for the average is not the one resulting from the least-squares, but instead we use the smallest occurring one. In this way, we avoid decreasing artificially the part of the uncertainty that is not due to statistics. In some cases, however, when it is obvious that the uncertainty is dominated by weak statistics, we do not follow the above rule (e.g. ^{23}Al^i(p)^{22}Mg of [1997Bl04]).

Some quantities have been reported more than once by the same group. If the results are obtained by the same method in different experiments and are published in regular refereed journals, only the most recent one is used in the calculation, unless explicitly mentioned otherwise. There are two reasons for this policy. The first is that one might expect that the authors, who believe their two results are of the same quality, would have averaged them in their latest publication. The second is that if we accept and average the two results, we would have no control on the part of the uncertainty that is not due to statistics. Our policy is different if the newer result is published in a secondary reference (not refereed abstract, preprint, private communication, conference, thesis or annual report). In such cases, the older result is used in the calculations, except when the newer one is an update of the previous value. In the latter case, the original reference in our list mentions the unrefereed paper.

5.4.2 Replacement procedure

Large contributions to χ^2 have been known to be caused by a nuclide G connected to two other ones H and K by reaction links with errors large compared to the error in the mass difference between H and K, in cases where the two disagreed. Evidently, contributions to χ^2 of such local discrepancies suggest an unrealistically high value of the overall consistency parameter. This is avoided by a replacement procedure: one of the two links is replaced by an equivalent value for the other. The pre-averaging procedure then takes care both of giving the most reasonable mass value for G, and of not causing undesirably large contributions to χ^2.

5.4.3 Insignificant data

Another feature to increase the meaning of the final χ^2 is to not use, in the least-squares procedure, data with weights at least a factor 10 smaller than other data, or than combinations of *all* other data giving the same result. They are given in the list of input data but labeled 'U'; comparison with the output values allows to check our judgment. Earlier, data were labeled 'U' if their weight was 10 times smaller than that of a *simple* combination of other data. This concept has been extended since AME1993 to data that weigh 10 times less than the combination of *all* other accepted data. Until the AME2003 evaluation, our policy was not to print data labeled 'U' if they already appeared in one of our previous tables, reducing thus the size of the table of data to be printed. This policy is changed in the present publication, and we try as much as possible to give all relevant data, including insignificant ones. The reason for this is that it often happens that conflicts might appear amongst recent results, then accessibility to older ones might be of help or shed some light, when evaluating the new data.

5.5 Used policies - treatment of undependable data

The important interdependence of most data, as illustrated by the connection diagrams (Figs. 1a–1j) allows local and general consistency tests. These can indicate that

something may be wrong with the input values. We follow the policy of checking all significant data that differ by more than two (sometimes 1.5) standard deviations from the adjusted values. Fairly often, study of the experimental paper shows that a correction is necessary. Possible reasons could be that a particular decay has been assigned to a wrong final level or that a reported decay energy belongs to an isomer, rather than to a ground state, or even that the mass number assigned to a decay has been shown to be incorrect. In such cases, the values are corrected and remarks are added below the corresponding A-group of data in Table I, in order to explain the reasons for the corrections.

It can also happen that a careful examination of a particular paper can lead to serious doubts about the validity of the results within the reported precision, but could not permit making a specific correction. Doubts can also be expressed by the authors themselves. The results are given, however, in Table I and compared with the adjusted values. They are labeled 'F', and not used in the final adjustment, but always followed by a comment to explain the reason for this label. The reader might observe that in several cases the difference between the experimental and adjusted values is small compared to the experimental uncertainty: this does not disprove the correctness of the label 'F' assignment.

It happens quite often that two (or more) pieces of data are discrepant, leading to important contribution to the χ^2. A detailed examination of the papers may not allow correction or rejection, indicating that at least the result of one of them could not be trusted within the given uncertainties. Then, based on past experience, we use in the calculations the value that seems to us to be the most trustable, while the other is labeled 'B', if published in a regular refereed journal, or 'C' otherwise.

Data with labels 'F', 'B' or 'C' are not used in the calculations. We do not assign such labels if, as a result, no experimental value published in a regular refereed journal could be given for one or more resulting masses. When necessary, the policy defined for 'irregular masses' with 'D'-label assignment may apply (see Section 4.2). In some cases, detailed analysis of strongly conflicting data could not lead to reasons to assume that one of them is more dependable than the others or could not lead to a rejection of a particular data entry. Also, bad agreement with other data is not the only reason to doubt the correctness of reported data. As in previous AME, and as explained above (see Section 4), we made use of the property of regularity of the surface of masses in making a choice, as well as in further checks on the other data.

We do not accept experimental results if information on other quantities (e.g. half-lives), derived in the same experiment and for the same nuclide, were in strong contradiction with well established values.

5.6 The AME computer program

Our computer program in four phases has to perform the following tasks: **i)** decode and check the data file; **ii)** build up a representation of the connections between masses, allowing thus to separate primary masses and data from secondary ones, to pre-average same and parallel data, and thus to reduce drastically the size of the system of equations to be solved (see Section 5.3 and 5.4), without any loss of information; **iii)** perform the least-squares matrix calculations (see above); and **iv)** deduce the atomic masses (Part II, Table I), the nuclear reaction and separation energies (Part II, Table III), the adjusted values for the input data (Table I), the *influences* of data on the primary nuclides (Table I), the *influences* received by each primary nuclide (Part II, Table II), and display information on the inversion errors, the correlations coefficients (Part II, Table B), the values of the χ^2s and the distribution of the v_i (see below), ...

5.7 Results of the calculation

In this evaluation we have 12437 experimental data of which 5376 are labeled 'U' (see above), 765 are labeled 'O' (old result from same group) and 740 are not accepted and labeled 'B', 'C', 'D' or 'F' (respectively 416, 144, 29 and 151 items). In the calculation we have thus 5556 valid input data, compressed to 3777 in the pre-averaging procedure. Separating secondary data, leaves a system of 1947 primary data, representing 1117 primary reactions and decays, and 830 primary mass-spectrometer measurements. To these are added 821 data estimated from TMS trends (see Section 4, p. 1297), some of which are essential for linking unconnected experimental data to the network of experimentally known masses (see Figs. 1a–1j).

In the atomic mass table (Part II, Table I) there is a total of 3827 masses (including ^{12}C) of which 3353 are ground state masses (2438 experimental masses and 915 estimated ones), and 464 are excited isomers (336 experimental and 128 estimated). Among the 2438 experimental ground state masses, 87 nuclides have a precision better than 0.1 keV, 315 better than 1 keV and 1438 better than 10 keV (respectively 45, 192 and 1020 in AME2003). There are 123 nuclides known with uncertainties larger than 100 keV (231 in AME2003). Separating secondary masses in the ensemble of 3827, leaves 1176 primary masses (^{12}C not included).

Thus, we have to solve a system of 1947 equations with 1176 parameters. Theoretically, the expectation value for χ^2 should be 771$\pm$39 (and the theoretical $\chi_n =$

1 ± 0.025).

The total χ^2 of the adjustment is actually 765 ($\chi_n = 0.996$), thus showing that the ensemble of evaluated data was of excellent quality, and that the criteria of selection and rejection we adopted were adequate. In the past this was not always the case and in AME2003 we could observe that on average the uncertainties in the input values were underestimated by 23%. The distribution of the v_i's (the individual contributions to χ^2, as defined in Eq. 6, and given in Table I) is also acceptable. If we consider all the 10531 data that are used in the adjustment plus the 'obsolete' ones (label 'O') and the unweighed ones (label 'U'), the distribution of v_i's yields 21% of the cases beyond unity, 4% beyond two, and 6 items (0.06%) beyond 3.

Considering separately the two main classes of data, the partial consistency factors χ_n^p are respectively 1.021 and 0.962 for energy measurements and for mass-spectrometry data, showing that both types of input data, after selection, are of excellent quality.

As in our preceding works [1, 6], we have tried to estimate the average accuracy for 269 groups of data related to a given laboratory and with a given method of measurement, by calculating their partial consistency factors χ_n^p (see Section 5.2). In general, the experimental uncertainties appear to be correctly estimated, with as much as 37% of the groups of data having χ_n^p larger than unity, and 2.6% beyond $\chi_n^p = 2$.

6 Discussion of the input data

In most cases, values as given by authors in the original publication are accepted, but there are also exceptions. An example is the performed recalibration due to change in the definition of the volt, as discussed in Section 2. For somewhat less simple cases, a remark is added in Table I at the end of the concerned A-group. A curious example of combinations of data that cannot be accepted without change follows from the measurements of the Edinburgh-Argonne group. They report decay energies in α-decay series, where the ancestors are isomers between which the excitation energy is accurately known from their proton-decay energies. These authors give values for the excitation energies between isomeric daughter pairs with considerably smaller errors than follow from the errors quoted for the measured α-decay energies. The evident reason is, that these decay energies are correlated; this means that the errors in their differences are relatively small. Unfortunately, the presented data do not allow an exact calculation of both masses and isomeric excitation energies. This would have required that, instead of the two E_α values of an isomeric pair, they would have given the error in their difference (and, perhaps, a more exact value for the most accurate E_α of the pair). Instead, entering all their Q_α and E_1 (isomeric excitation energies) values in our input file would yield outputs with too small errors. And accepting any partial collection makes some errors rather drastically too large. We therefore do enter here a selection of input values, but sometimes slightly changed, chosen in such a way that our adjusted Q_α and E_1 values and errors differ as little as possible from those given by the authors. A further complication could occur if some of the Q_α's are also measured by other groups. But until now, we found no serious troubles in such cases.

Necessary corrections to recent mass-spectrometer data are mentioned in Section 6.2.

A change in errors, not values, is caused by the fact explained below that in several cases we do not necessarily accept reported α-energies as belonging to transitions between ground states. This also causes uncertainties in derived proton decay energies to deviate from those reported by the authors (e.g. in the α-decay chain of ^{170}Au), see also Section 7.10.

6.1 Improvements along the backbone

After the publication of AME2003, only a few new measurements for stable nuclides that used the classical mass-spectrometers were published.

Most of the new mass-spectrometry data were obtained from precision measurements of ratios of cyclotron frequencies of ions in Penning traps. Similarly to the classical measurements, where ratios of voltages or resistances were used, we found that the Penning trap results can be converted to a linear combination of masses of electrically neutral atoms in μu, without any loss of accuracy. A special mention is for the MIT-FSU group who give their original results as linear equations, including corrections for electron and molecular binding energies, which can be easily used in our computer code. Other groups give their results as ratio of cyclotron frequencies (see also next paragraph), which we convert to linear equations as described in Appendix C, and finally we add corrections for electron and molecular binding energies. In such cases, we added a remark to the equation used in the input data table (Table I), to describe the original data and our treatment. Some authors publish their results directly as masses, but this is not a recommended practice for high-precision mass measurements.

6.2 Mass-spectrometry away from β-stability

For the reader interested in the history of mass measurements by mass spectrometry, the resolving powers, resolutions and the discoveries they rendered possible in nuclear

physics as well as in cosmology, one of us has prepared a document [48].

6.2.1 Penning trap spectrometers

In addition to ISOLTRAP, the Penning trap spectrometer located at on-line mass separator facility ISOLDE at CERN, several others Penning traps have been operating at the major accelerators facilities around the world: CPT-Argonne, JYFLTRAP-Jyväskylä, LEBIT-East-Lansing, SHIPTRAP-Darmstadt, and TITAN-Vancouver. More are presently under construction. They produce experimental atomic masses for nuclides further away from the valley of β-stability, by using the cyclotron frequencies of charged ions captured in the trap. Such frequencies are always compared to that of a well know calibrator in order to determine the ratio of two masses, which is converted, without loss of accuracy, to a linear relation between the two masses (see also Section 6.1 above and Appendix C). Experimental methods that utilize measurements of cyclotron frequency have an advantage compared to volt or magnetic field measurements in a sense that the parameter that is needed in the former, namely the frequency, is the physical quantity that can be measured with the highest precision. In fact, very high resolving power (10^6) and accuracies (up to 10^{-8}) are routinely achieved for nuclides located quite far from the line of β-stability. Such high resolving power made it possible in 1991 [49], for the first time in the history of mass-spectrometry, to resolve nuclear isomers from their ground state (^{84}Rb^m) and to determine their excitation energies. Another beautiful demonstration was given in 2003 in [2004Va07] for ^{70}Cu, ^{70}Cu^m and ^{70}Cu^n, where in the same work the masses of the three isomers were determined by mass-spectrometry, and the excitation energies by $\beta\gamma$ spectroscopy. Typically, the precision can reach 100 eV or better (60 eV for the difference between ^{6}He and ^{7}Li at TITAN-Vancouver, [2012Br03]). Even the most exotic nuclides, such as ^{11}Li (8.75 ms) or ^{74}Rb (64.78 ms), could be measured with precisions of 600 eV and 4 keV at the TITAN-Vancouver [2008Sm03] and ISOLTRAP-Cern [2007Ke09] facilities, respectively.

In earlier evaluations we found it necessary to multiply uncertainties in values from some groups of mass-spectrometry data [50] with discrete factors (F =1.5, 2.5 or 4.0) following the partial consistency factors χ_n^p we found for these groups (see Section 5.2). Such a treatment is not necessary in the case of most the Penning trap which all have F =1 (except for the sub-group 'Ma8' [2006Mu05] from ISOLTRAP for which F =1.5).

6.2.2 Double-focussing mass-spectrometry

For nuclides far away from the valley of stability, mass-triplet measurements, in which undetectable systematic effects could build-up in large deviations when the procedure is iterated [1986Au02], could be recalibrated with the help of the Penning trap measurements. Recalibration was automatically obtained in the evaluation, since each mass-triplet was originally converted to a linear mass relation among the three nuclides, allowing both easy application of least-squares procedures, and automatic recalibration. In the present adjustment of data, most of the 181 original data, performed in the 80's, are now outweighed, except for the most exotic (and thus the most interesting) ones. There are still 12 of them that contribute to the present adjustment, essentially for the most exotic nuclides: ^{91}Rb for 12% of the determination of its mass, ^{95}Rb (48%), ^{99}Rb (13%), ^{143}Cs (24%), ^{144}Cs (30%), ^{146}Cs (18%), ^{147}Cs (21%) and the most exotic ^{148}Cs (100%). In Table I, the relevant equations are normalized to make the coefficient of the middle isotope unity, so that they read e.g.

$$^{97}\mathrm{Rb} - (0.490 \times {}^{99}\mathrm{Rb} + 0.511 \times {}^{95}\mathrm{Rb}) = 350 \pm 60 \text{ keV}$$

$$^{145}\mathrm{Cs} - (0.392 \times {}^{148}\mathrm{Cs} + 0.608 \times {}^{143}\mathrm{Cs}) = -370 \pm 90 \text{ keV}$$

(the ^{148}Cs symbol representing the mass excess of nuclide ^{148}Cs in keV). The other two coefficients are three-digit approximations of

$$\frac{A_2}{A_3 - A_1} \times \frac{A_2 - A_1}{A_3} \text{ and } \frac{A_2}{A_3 - A_1} \times \frac{A_3 - A_2}{A_1}$$

We took A instead of M in order to arrive at coefficients that do not change if the M-values change slightly. The difference is unimportant.

6.2.3 Radio-frequency mass-spectrometry

The Orsay Smith-type mass-spectrometer MISTRAL, also connected to ISOLDE, has performed quite precise measurements of very short-lived light nuclides, before the Penning traps could cover all the possibilities that were offered by a transmission mass-spectrometer in terms of instant measurements. There are still 8 of the measurements performed with MISTRAL that are used in this evaluation for the determination of the masses of ^{26}Ne, ^{26,27,28,29}Na and ^{29}Mg.

6.2.4 Classical time-of-flight

Mass measurements by time-of-flight mass spectrometry technique at SPEG (GANIL) and TOFI (Los Alamos), also apply to very short nuclides, due to instant measurements, but the precisions are much lower than with MISTRAL. Masses of almost undecelerated fragment products, coming from thin targets bombarded with heavy ions [51] or high energy protons [52] are measured from a combination of magnetic deflection and time of flight determination. Nuclides in an extended region in A/Z and Z are

analyzed simultaneously. Each individual ion, even if very short-lived ($1\mu s$), is identified and has its mass measured at the same time. In this way, mass values with accuracies of (3×10^{-6} to 5×10^{-5}) are obtained for a large number of neutron-rich nuclides of light elements, up to $A=70$. A difficulty is that the obtained value applies to an isomeric mixture where all isomers with half-lives of the order of, or longer than the time of flight (about 1 μs) may contribute. The resolving power, around 10^4, and cross-contaminations can cause significant shifts in masses. The most critical part in these experiments is calibration, since obtained from an empirically determined function, which, in several cases, had to be extrapolated rather far from the calibrating masses. It is possible that, in the future, a few mass-measurements far from stability may provide better calibration points and allow a re-analysis of the concerned data, on a firmer basis. Such recalibrations require analysis of the raw data and cannot be done by the evaluators. With new data from other methods allowing now comparison, we observed strong discrepancies for one of the two groups, and had to increase thus the associated partial consistency factor to $F=1.5$. We noted already earlier that important differences occurred between ensemble of results within this group of data. Using $F=1.5$ for data labeled 'TO1-TO6' in the 'Lab' column of Table I, allows to recover consistency.

6.2.5 Cyclotron time-of-flight

Longer time-of-flights (50 to 100 μs), thus higher resolving powers, can be obtained with cyclotrons. The accelerating radio-frequency is taken as reference to ensure a precise time determination, but this method implies that the number of turns of the ions inside the cyclotron, should be known exactly. This was achieved successfully at SARA-Grenoble for the mass of ^{80}Y. Measurements performed at GANIL with the CSS2 cyclotron, could not determine the exact number of turns. In a first experiment on ^{100}Sn, a careful simulation was done instead. In a second experiment on ^{68}Se, ^{76}Sr, ^{80}Sr and ^{80}Y, a mean value of the number of turns was experimentally determined for the most abundant species only, thus mainly the calibrants. Penning traps measurements at the CPT-Argonne, JYFLTRAP-Jyväskylä and ISOLTRAP revealed that this last method suffered serious systematic errors. Remeasurement at GANIL with the CSS2 cyclotron with improved method confirm the Penning trap data.

6.2.6 Storage ring time-of-flight

Similarly, long flight path can be obtained in a storage ring. The first set-up of this type is the GSI-ESR at Darmstadt. The precision of the measurements could be as good as 90 keV even for nuclides quite far from stability. The second one at the IMP-CSR at Lanzhou could achieve precision better than 10 keV. The accuracy is excellent for both yielding partial consistency factors of $F=1.0$ for the IMP-CSR, slightly less for the GSI-ESR set-up with $F=1.5$.

6.2.7 Cooled beam cyclotron frequency

Storage rings could also be used with cooled beams to measure the cyclotron frequency as has been demonstrated since 2003 at the GSI-ESR storage ring, with precisions sometimes as good as a 12 keV. Many of the measured nuclides belong to known α-decay chains. Thus, the available information on masses for proton-rich nuclides is considerably extended.

It must be mentioned that in the first group of mass values as given by GSI authors [2000Ra23], several could not be accepted without changes. The reason is that in their derivation α-decay energies between two or more of the occurring nuclides have been used. Evidently, they could therefore not without correction be included in our calculations, where they are again combined with these Q_α's. Remarks added to the data in Table I warn for this matter where important. This point is added here to show a kind of difficulty we meet more often in this work. Fortunately, for this group of data it is only of historical interest since all their data are outdated by more recent measurements [2005Li24] with the same instruments and with a much higher precision. Since then, a wealth of measurements of very high quality were published using this technique, see e.g. [2012Ch19] and references therein.

6.2.8 Isomeric mixtures

As stated above, many mass-spectrometer results yield an average mass value M_{exp} for a mixture of isomers. Here, we use a special treatment for the possible mixture of isomers (see Appendix B) and those changes are duly included in remarks accompanying these data.

The mass M_0 of the ground state can be calculated if both the excitation energy E_1 of the upper isomer, and the relative intensities of the isomers are known. But often this is not the case. If E_1 is known but not the intensity ratio, one must assume equal probabilities for all possible relative intensities. In the case of one excited isomer, see Appendix B, the mass estimate for M_0 becomes $M_{exp}-E_1/2$, and the part of the error due to this uncertainty $0.29E_1$ (see Appendix B, Section B.4). This policy was defined and tested first for the GSI-ESR cooled beam cyclotron frequency data and was discussed with the authors of the measurements. In eight cases, more than two isomers contribute to the measured line. They are treated as indicated in Appendix B.

A further complication arises if E_1 is not known. This, in addition to questions related to α-decay chains involving isomers, was a reason for us to consider the matter of

isomers with even more attention than was done before. Part of the results of our estimates (as always, flagged with '#') are incorporated in the NUBASE evaluation. In estimating the E_1 values, we first look at experimental data possibly giving lower limits: e.g. if it is known that one of two isomers decays to the other; or if γ rays of known energy occur in such decays. If not, we try to interpolate between E_1 values for neighboring nuclides that can be expected to have the same spin and configuration assignments (for odd A: isotones if Z is even, or isotopes if Z is odd). If such a comparison does not yield useful results, indications from theory were sometimes accepted, including upper limits for transition energies following from the measured half-lives. Values estimated this way were provided with somewhat generous errors, dutifully taken into account in deriving final results.

In several of these measurements, an isomer can only contribute if its lifetime is relatively long (hundreds of milliseconds or longer). However, half-life values given in NUBASE are those for neutral atoms. For bare nuclides, where all electrons are fully stripped from the atom, the lifetimes of such isomers can be considerably longer, since the decay by conversion electrons is switched off. Examples are the reported mass measurements [2005Li24] of the 580 ms ^{151}Er^m isomer at E_1=2586.0 keV excitation energy; and of the 103 ms ^{117}Te^m isomer at E_1=296.1 keV.

6.3 Mass of unbound nuclides

In the light mass region, many nuclides beyond the driplines can be accessed in nowadays experiments. They can decay by direct proton or neutron emission. The half-lives of these unbound nuclides are too short for them to acquire their outer electrons (which takes around 10^{-14} s), and to form atoms. However, we still convert their masses to "atomic masses" to have them treated consistently with other nuclides and be used conveniently in our tables. It's an experimental challenge to study these unbound nuclides far from stability: only very few events can be observed. Most often, theoretical calculations are required to extract their properties from the experimental data.

On the proton rich side, resonant states could be formed due to the Coulomb barrier. There are different approaches to study these states: transfer reaction with missing mass spectrum, proton scattering, and complete kinematic measurement with invariance mass spectrum. For a broad resonant state, the definition of the resonance energy and width is not unique. For example, in Ref. [2004Go15], ^{15}F is studied by using the inverse kinematical measurement of proton elastic scattering on ^{14}O. From the same experimental data, the proton decay energy of ^{15}F is obtained to be $1.29^{+0.08}_{-0.06}$ MeV where the energy at which the magnitude of the internal wave function is a maximum, or $1.45^{+0.16}_{-0.10}$ MeV where the nuclear phase shift has the value $\delta = \pi/2$. Since the latter value is consistent with values obtained by transfer reactions and complete kinematic measurements, it is adopted in our evaluation.

Some single proton resonant states could be accessed through the two proton decay. Their properties can be used or extracted from the two proton decay studies. In [2008Mu13], the authors quoted the value of $Q_p = 1560 \pm 130$ keV from [2004Le12] as the ground state of ^{15}F to study the 2p decay of ^{16}Ne; Similarly, $Q_p = 1300 \pm 170$ keV for ^{18}Na from [2004Ze05] to study the 2p decay of ^{19}Mg. In [2012Mu05], the same experimental data were reanalyzed and the resonant state of ^{18}Na is reconstructed from p+^{17}Ne independently. The ambiguous interpretation of the ^{18}Na states in [2004Ze05] is also clarified.

On the neutron rich side of the nuclear chart, the mass of unbound nuclides close to the stability line can be determined with missing mass method using transfer reactions, or with invariant mass method using radioactive ion (RI) beams. Recently the RI beams and detection techniques have been developed impressively and new masses of unbound nuclides in this region are obtained by using invariant mass method.

Since there is no Coulomb barrier, it is the centrifugal barrier that will play an important role to have a resonant state. For an s-wave neutron, no barrier exists, and an asymmetric peak situated at the threshold is a general feature of spectra obtained in s-wave elastic neutron-nucleus scattering. This state is usually referred to as a virtual state, which has no definite lifetime and thus differs strongly from a real resonance state. The virtual state can be characterized by the scattering length; its eigen energy is approximately $\hbar^2/2\mu {a_s}^2$, where μ is the reduced mass and a_s is the scattering length.

In AME2003, a $1/2^+$ s-state was assigned as the g.s. for ^{13}Be, based on [2001Th01], where this virtual state is found unbound with respect to ^{12}Be and a neutron by < 200 keV from the scattering length of $a_s < -10$ fm. Later work of [2008Ch07] seems to support this result with $a_s = -10$ fm. However, these results have been questioned by [2010Ko17], where the authors state: *"a mimic resonant peak may appear in a two-body relative energy spectrum obtained in an experiment with limited neutron-detection efficiency via a breakup reaction in which more than one neutron can be emitted. The sequential neutron decay spectroscopy measurements [2001Th01], [2008Ch07] where ^{13}Be was produced by the breakup of ^{18}O and ^{48}Ca may have suffered from this*

problem." In [2010Ko17], the reaction ^{1}H(^{14}Be,^{12}Be+n) was studied, which is expected to be a clear way to populate the unbound ^{13}Be. A scattering length a_s=-3.4(0.6) fm was obtained in this experiment. This result is supported by [2007Si24], where fragmentation of ^{14}Be on a carbon target was used and $a_s = -3.2^{+0.9}_{-1.1}$ fm was obtained. From these results, we assign now the $1/2^-$ state to be the g.s. of ^{13}Be, whereas it was the ^{13}Be^p state in NUBASE2003.

6.4 Isobaric Analogue states IAS

Definitions and notation For isobars around the $N = Z$ line, and in particular for mirror nuclides, the main difference between their masses can be attributed to the charge symmetry of the nucleon-nucleon interaction [1971Be29]. A more extensive mass relationship can be observed in isobars belonging to the same isospin multiplet around $N = Z$. In this case the ground state of a given nuclide may be identified as an excited state in the multiplet members. These isobaric analogue states (IAS) therefore have, by definition, the same spin-parity and isospin attributions. Their relative masses may be used to explore the charge-symmetry and charge-independence of the nuclear interaction via the isobaric mass multiplet equation (IMME) [53], and with calculations of the Coulomb Displacement Energy (CDE) (see for example [40], and references therein).

The localization of IAS multiplets on the chart of the nuclides is illustrated in Fig. 3.

$T = 1$ and $T = 2$ multiplets

In Fig. 3, the line going from bottom left to top right designates the $N = Z$ axis. The black line joining ^{38}Ca, ^{38}K, and ^{38}Ar are members of the same T=1 isospin triplet. By convention, the IAS multiplet is defined by its lowest Z member, and in this example it is ^{38}Ar. We therefore expect to find an excited state in ^{38}K which is the IAS of ground state ^{38}Ar. To differentiate between ground states (*gs*), isomers (m,n,$\cdots$), and IAS, the IAS is labeled ^{38}K^i.

Members of the $A = 38$, $T = 2$ multiplet are shown by the red line extensions to the black line. The IAS of ground state ^{38}Cl should exist in ^{38}Ar, ^{38}K, and ^{38}Ca. Since ^{38}K has levels which could be part of either the $T = 1$ or $T = 2$ isospin multiplets for $A = 38$, extra notation is required to distinguish between the two expected IAS. The triplet and quintuplet IAS in ^{38}K are written as ^{38}K^i and ^{38}K^j, respectively. The superscripts i and j designating successively higher multiplet members. The j levels are commonly called *double IAS's*.

$T = 3/2$ and $T = 5/2$ multiplets

To complete the illustration of the IAS multiplet location on the nuclide chart, a case for odd-A is also shown. The $A = 39$ IAS quadruplet is composed of Ar, K, Ca, and Sc as shown by the blue connecting line. The Ar ground state should show up as an excited IAS in K and Ca. The green extensions connect the $T = 5/2$ sextuplet members, Cl and Ti, and so in this IAS multiplet it is the analogue ground state of Cl that is looked for in the multiplet members. The lower $T = 3/2$ IAS members in both K and Ca are denoted with the superscript i (^{39}K^i and ^{39}Ca^i), and the $T = 5/2$ IAS by j (^{39}K^j and ^{39}Ca^j).

Exceptions

In general, IAS multiplets are naturally delimited by ground state mirror nuclides. However, the relationship between ground state masses being the main subject of the AME, these configurations have always been naturally included in the evaluation. We do not label these states in any particular way, and they are not included in the IAS statistics of the following paragraphs.

In two cases, ^{16}N^m and ^{26}Al^m, it turns out that the IAS also happens to be an excited isomeric state. In these cases we have given preference to the isomeric notation.

IAS updates The most recent IAS evaluation in the AME dates back to 1993 [3]. In the present edition we reintroduce and update the IAS experimental data. The evaluation procedure is the same as for ground state masses and isomers, the global mass matrix being minimized in a single step.

Nuclides from $A = 6$ to $A = 74$, and mainly for isospins T = 1, 3/2, 2, and 5/2 were studied. Roughly 117 nuclear excited states were retained as being experimentally identified IAS, of which around 50 are precise enough to survive through to the final evaluated mass table.

In most cases, when reaction data has been evaluated, the precision of IAS masses has been bettered. However, in the case of ^{73}Rb^i, even though the excited IAS level is known to $\pm$40 keV, the ground state has not yet been measured, and can only be estimated. Hence the final estimate for the excitation energy is given with a precision of 100# keV.

Only one new IAS has been included in this evaluation, ^{44}V^i, from recent experimental measurements of beta-delayed proton emission [2007Do17].

Beta-delayed proton emitters In general, when an IAS decays via internal transitions, even with a low branching ratio, the associated gamma measurements will generally provide more precise data than that obtained through external relationships with other nuclides. In the current evaluation, 33 cases of beta-delayed IAS proton emission are considered, most of which provide a more precise IAS mass evaluation as compared to previous ones.

Figure 3: Excerpt from the chart of nuclides. The ground state spin-parities are given for each nuclide. The ground state isospin T is given when it deviates from the expected value based on a charge independent nuclear force. Members of the same multiplet naturally show up through the symmetry of the $N = Z$ axis.

The biggest change in precision comes from the recently published results on $^{45}V^{i}$ [2007Do17] where a proton-gamma coincidence method provides a 9 keV precision on the Q-value, as compared to the previous, first identification of this IAS by Jackson *et al.* in 1974, with a 50 keV precision [1974Ja10].

Fragmented states Fragmented IAS levels have been seen to occur in eleven cases evaluated here. They are $^{8}Be^{i}$, $^{44}Ti^{j}$, $^{48}Cr^{j}$, $^{56}Co^{i}$, $^{56}Ni^{j}$, $^{57}Ni^{i}$, $^{58}Co^{i}$, $^{59}Ni^{i}$, $^{59}Cu^{i}$, $^{61}Cu^{i}$, and $^{64}Cu^{i}$. In these cases the IAS is spread over several isospin mixed levels. The first phenomenological description of fragmented IAS was given by A.M. Lane [54] using a spectral line broadening theory; a full description of the experimental application can be found in [1971Be29] (and references therein).

In this case the simple relationship between isobaric multiplet members breaks down, since there is no longer a single IAS level observed, but several isospin impure fragments. The sum of the individual IAS fragments, and their relative intensities, are considered in the final IAS mass evaluation. Our choice is to use the main experimentally observed mass fragment ("strongest fragment" in Table I) in the current evaluation. The excitation energies of the other fragments, along with their relative intensity when known, are provided in the associated comment. The original experimental observations are thus reported as accurately as possible.

6.5 Proton- and α-decays

In some cases, proton-decay energies can be estimated from proton-decay half-lives. Estimates for the following nuclides could thus be obtained:

Nuclide	$T_{1/2}$	S_p (keV)	Adopted S_p
^{64}As	40±30 ms	>-100	20# ± 300#
^{68}Br	<1.5 μs	<-500	-850# ± 300#
^{73}Rb	<30 ns	<-570	-570# ± 100#
^{77}Y	63±17 ms	>-180	-180# ± 50#
^{81}Nb	<80 ns	<-1000	-1280# ±1540#
^{89}Rh	>1.5 μs	>-860	-1080# ± 200#

These limits were used as a guide, but not the only one, to set our estimated S_p, thus masses, for these nuclides.

Experimental data are now available for many proton-rich nuclides, from $^{97}_{47}$Ag to $^{185}_{83}$Bi; among them for all intermediary odd-Z nuclides with the exception of $_{49}$In and $_{61}$Pm.

These results are important for two main reasons. Firstly, knowledge of proton separation energies just beyond the proton drip line is quite valuable in allowing estimate of mass values for nuclides for which no experimental data is available. Secondly, there are several cases where proton-decay energies from both members of an isomeric pair were measured, so one can determine the energy of a particular excited isomer. In addition, the lifetime of a proton-emitting nuclide is sensitive to the l value carried out by the proton and this can be used in turn to obtain reliable information about the spins and parities of the parent, and daughter states. This feature is even more valuable, since often the α-decay of both members is observed. Combination of long α-decay chains with proton decays offers a somewhat complete view of extended regions of the chart in the neighborhood of the proton dripline. These studies showed that several decays earlier assigned to ground states do belong in reality to upper isomers. Also, these measurements are found to yield good values for the excitation energies of the isomers among the descendants. We here follow the judgment of the authors, including their judgment about the final levels fed in those α-decays.

Often in α-decay studies of odd-N(Z) and odd-odd nuclides, the level fed directly by the α particle is not known. A comprehensive investigation that we have performed some time ago suggested, that in most cases when the decay does not go directly to the ground state, the final level is relatively close to the ground state. In such cases, we adopted the policy of accepting the measured E_α as feeding the ground state, but assigning a special label (not given in Table I) to indicate that a close-lying excited level may be also fed. This label will indicate to our computer program that the uncertainty, after possible pre-averaging of data of the same kind (also given in Table I), is to be increased to 50 keV.

The above mentioned results of proton decay analysis have been a reason to omit the mentioned label in several cases. One has to be also careful with the use of this label if mass-spectrometry results with a precision of about 50 keV or better are known for the parent and daughter nuclides. Comparison with theoretical models may also suggest to drop the mentioned above label; or just reversely to not accept a reported α energy.

In some cases, TMS estimates and theoretical predictions of α-decay energies indicate that the excitation energy E_1 of the final level may be much higher. Then, an estimate for the excited level energy (provided with a generous error) is added as an input value.

In regions where the Nilsson model for deformed nuclides applies, it is expected that the most intense α transition connects parent and daughter levels that have the same quantum numbers and configurations. (It is not rarely the only observed α-ray.) In such a case, adding an estimate for E_1 is attractive. Frequently, the energy difference between the excited and ground states can be estimated by comparison with the energy differences between the corresponding Nilsson levels in nearby nuclides.

Unfortunately, some authors derive a value they call Q_α from the measured α-particle energy by not only correcting for the recoil energy, but also for screening by atomic electrons (see Appendix A). In our calculations, the latter corrections have been removed.

Finally, some measured α-particle energies are affected by the coincidence summing between the α particle that feeds an excited level of the daughter nuclide and the conversion electrons that follow the decay of this level. This is sometimes apparent from the reported α spectra, since the width of the observed line is larger than that of other ones. In some cases, spurious α peaks can be observed. When deriving the corresponding Q_α values, appropriate (small) corrections are made for the escaping X-rays. Those are mentioned in a remark added to such a case.

6.6 Decay energies from capture ratios and relative positron feedings

For allowed transitions, the ratio of electron capture in different shells is proportional to the ratio of the squares of the energies of the emitted neutrinos, with a proportionality constant dependent on Z and quite well known [55]. For (non-unique) first forbidden transitions, the ratio is not notably different; with few exceptions. The neutrino energy mentioned is the difference of the transition energy Q with the electron binding energy in the pertinent shell. Especially if the transition energy is not too much larger than the binding energy in, say, the K shell, it can be determined rather well from a measurement of the ratio of capture in the K and L shells.

The non-linear character of the relation between Q and

the ratio introduces two problems. In the first place, a symmetrical error for the ratio is generally transformed in an asymmetrical one for the transition energy. Since our least-squares program cannot handle them, we have symmetrized the probability distribution by considering the first and second momenta of the real probability distribution (see NUBASE2012, Appendix A, p. 1173). The other problem is related to averaging of several values that are reported for the same ratio. Our policy, since AME1993, is to average the capture ratios, and calculate the decay energy following from that average. An example is ^{139}Ce(ε)^{139}La (see p. 1482), where the 10 results that are averaged are all given in the following remarks. In this procedure we used the best values [55] of the proportionality constant. We also recalculated older reported decay energies originally calculated using now obsolete values for this constant.

The ratio of positron emission and electron capture in the transition to the same final level also depends on the transition energy in a known way (anyhow for allowed and not much delayed first forbidden transitions). Thus, the transition energy can be derived from a measurement of the relative positron feeding of the level, which is often easier than a measurement of the positron spectrum endpoint (e.g. ^{147}Tb(β^+)^{147}Gd, now labeled 'U', p. 1494). For several cases we made here the same kind of combinations and corrections as mentioned for capture ratios. But in this case, a special difficulty must be mentioned. Positron decay can only occur when the transition energy exceeds $2m_ec^2 = 1022$ keV. Thus, quite often, a level fed by positrons is also fed by γ-rays coming from higher levels fed by electron capture. Determination of the intensity of this *side* feeding is often difficult. Cases exist where such feeding occurs by a great number of weak γ-rays easily overlooked (the *pandemonium* effect [11]). Then, the reported decay energy may be much lower than the real value. In judging the validity of experimental data, we kept this possibility in our mind.

6.7 Q_β far from β-stability

In the present work, the mass surface for nuclides far away from the valley of β-stability is observed to be located much higher than was previously believed. This is largely due to an underestimation of the Q_β decay energies, which were measured in the past using the end-point energy method. For nuclides far from the valley of stability,the decay energies become very large offering accessibility to many states in the daughter nuclide. The combination of many individual continuous β-decay spectra renders the analysis very difficult. The maximum energy analysis method is also not reliable, since there is no guarantee that the ground state is significantly fed. Also the $\beta - \gamma$ coincidence method can suffer from the 'pandemonium' effect [11].

As an example, in AME2003 the mass excess of the proton-rich nuclide ^{85}Nb was determined as $M - A$=-67150±220 keV. This value was derived from the measured Q_β in [1988Ku14], where the authors already noticed that their experimental Q_β was "noticeably lower than predicted values from mass formulae". The masses of ^{85}Nb and ^{85}Zr were recently measured with high precision using a Penning trap, and the Q_β value was thus determined to be about 900 keV higher than obtained in [1988Ku14]. The masses of ^{85}Nb and ^{85}Zr are now respectively 870 keV higher and 25 keV lower than in AME2003 with 2 orders of magnitude higher precisions.

The deduced higher values of atomic masses for exotic nuclides in the present work will have important consequences for nuclear astrophysics and nuclear energy applications, see the discussion in Ref. [56].

To conclude, for nuclei very far from the valley of stability, results from Q_β end-point measurements should be treated with caution. In such cases, data available from Penning traps and/or storage rings facilities should always be given a priority.

6.8 Superheavy nuclides

The search for superheavy nuclides (SHE) and elucidation of their properties is one of the prominent areas of the modern nuclear physics research. In the last several years the nuclear chart was extended impressively in the heaviest mass region up to the element with an atomic number of $Z = 118$. However, the exactness of the mass surface built with the available data is far from being perfect (see Part II, Fig. 9, p. 1835 and also Fig. 36, p. 1862).

Names and symbols At the time when AME2003 was published, SHE up to $Z = 109$ were officially named by The Commission on Nomenclature of Inorganic Chemistry of the International Union of Pure and Applied Chemistry (IUPAC) [57]. However and to be complete, if the user is to compare AME2012 with some older versions of AME or NUBASE, he should be aware that in the past some confusion occured in the naming of elements, due to IUPAC revising in 1997 some earlier proposals (see also NUBASE2012, Section 2, p. 1159) and changing symbols and names for $Z = 104$, 105, 106 and 108 elements as follows:

104	rutherfordium	Rf	replacing	Db
105	dubnium	Db	"	Jl
106	seaborgium	Sg	"	Rf
108	hassium	Hs	"	Hn

Since then, the names of five additional SHE were also approved: the $Z = 110$, 111 and 112 elements were named

Darmstadtium, Roentgenium and Copernicium, respectively, as proposed by the SHIP group at GSI; while the elements 114 and 116 were named Flerovium and Livermorium, respectively, following the proposal by the Dubna-Livermore collaboration. The provisional symbols Ed, Ef, Eh, and Ei are used in AME2012 for the yet unnamed elements 113, 115, 117, and 118, respectively.

Experimental methods Since α decay is the dominant decay mode in the region of super-heavy nuclides, knowledge of masses of SHE is most often obtained from measured E_α energy in α decay chains going down to a nuclide with known mass. Spatial and time-correlated α-decay (and SF) spectroscopy measurements of SHE continue to provide useful information about their properties. However, it often happens that α chains end-up on a nuclide decaying only by spontaneous fission (SF), offering thus no link to known masses. For example, the SF decay of ^{266}Sg does not allow to determine the mass of the doubly magic nuclide ^{270}Hs.

A very important development in this mass region since AME2003 was the first direct mass measurements of several isotopes of No ($Z = 102$) and Lr ($Z = 103$) at the SHIPTRAP facility at GSI. Those results provided anchor points for the values of atomic masses in this remote region of the nuclear chart. In general, the newly measured masses agree reasonably well with those deduced from known Q_α values of long α chains, thus giving confidence not only for the reliability of masses for SHE reported in the present work, but also for the Q_α obtained up to here and to the treatment and policies we used.

Alpha decay of superheavy nuclides For even-even nuclides, the strongest (favored) decays connect the parent and daughter ground states, and hence, those are directly related to the α-decay Q values. As a result, masses determined this way are quite reliable. Unfortunately, even-even nuclides are prone to spontaneous fission decay rendering these "good" cases relatively rare.

For many odd-A nuclides, and especially for odd-odd ones, the assignments are frequently complicated. In the present region of deformed nuclides, α-decays preferentially feed levels with the same Nilsson model assignments as the mother, which in the daughter are most often excited states, with unknown excitation energies E_1. Thus, in order to find the corresponding mass difference, we have to estimate these E_1's. For somewhat lighter nuclides, one may estimate them, as said above, from known differences in excitation energies for levels with the same Nilsson assignments in other nuclides. But such information is lacking in the region under consideration. In its place, one might consider to use values obtained theoretically [58]. We have not done so, but used their values as a guide-line. Finally, we choose values in such a way that diagrams of α-energies and the mass surface looked acceptable. Important for this purpose were the experimental α-decay energies for the heaviest isotopes for $Z = 112$, 114 and 116, especially for the even-A isotopes among them. The errors we assigned to values thus obtained may be somewhat optimistic; but we expect them not to be ridiculous.

This is especially true near sub-shell closures, since the favored alpha decay occurs between states that have the same quantum numbers and configurations. The presence of excited, long-lived isomers can also lead to severe complications. While many dedicated $\alpha - \gamma$ coincidence studies have been performed for nuclides in the light actinide region, such spectroscopy information needs to be extended to the heavier nuclides. In the last several years new results were published in the No-Lr-Rf region, which resolved some of the ambiguities. However, high quality data are still in demand and such studies would be very beneficial to future determination of masses for SHE.

A weak α-decay branch was recently observed in the decay of ^{262}Sg [2010Ac.A], which allowed experimental determination of the mass of ^{270}Ds, the heaviest nuclide that has an experimental mass value in AME2012. The new data allowed to establish unambiguously the existence of a significant deformed sub-shell gap at $N = 162$ and $Z = 108$. This gap appears to be much larger than the well known one at $N = 152$ and $Z = 100$.

In the AME2003 mass table, the heaviest nuclide with known mass was ^{265}Sg, where the highest α decay group $E_a = 8940 \pm 30$ keV of [1998Tu01] was adopted as gs-gs transition. This is a common policy if the α decay energies spread too much, because even if this group is formed due to α-electron summing, it is still the closest one to the real gs-gs Q value. With more events accumulated, the status has been changed for ^{265}Sg and the former α decay group assigned to ^{266}Sg is reassigned to ^{265}Sg^m state. In present evaluation we use the strongest group, which may be the unhindered transition, assuming this transition goes to one excited state in the daughter nuclide ^{261}Rf with unknown energy, which is estimated from the trends in the neighboring nuclides. Then in the present mass table, the mass of ^{265}Sg is estimated rather than experimental in AME2003, although the mass value doesn't change much.

With exception of the nuclide ^{278}113, all of the nuclides with atomic number from 113 to 118 are produced by using the "hot fusion" method, decaying with α emission eventually to some fissile nuclides whose masses are unknown experimentally, thus forming a floating island with none of the nuclides having known mass.

7 Special cases

In AME2003, some special cases have been discussed. Since new experimental information emerged in recent years, some of them have been resolved, while for others new issues were raised.

7.1 ^{9}He and ^{10}He

The knockout reaction on ^{11}Be has been used to produce ^{9}He [2001Ch31] and an $l = 0$ state has been assigned as its lowest state. An upper limit of the s-wave scattering length a_s=–10 fm has been obtained, corresponding to an energy for the virtual state below 0.2 MeV. In [2007Go24], the spectrum of ^{9}He was studied by means of the ^{2}H(^{8}He,p)^{9}He reaction. The lowest resonant state of ^{9}He was found at 2.0 ± 0.2 MeV with a width of 2 MeV and has been identified as a $1/2^-$ state. For the virtual $1/2^+$ state, a lower limit $a_s > -20$ fm has been obtained, which is not inconsistent with the result in [2001Ch31]. This assignment has been questioned in [2010Jo06], where ^{9}He was studied by using knockout reaction from ^{11}Li. The ^{8}He+n relative-energy spectrum is dominated by a strong peak-like structure at low energy, which may be interpreted within the effective-range approximation as the result of an s-wave interaction with a neutron scattering length $a_s = -3.17 \pm 0.66$ fm, thus conflicting with [2001Ch31]. It is argued that the s-state might not be the g.s. of ^{9}He.

This argument is supported by the structure of ^{10}He, which is highly dependent on the structure of ^{9}He. If a virtual state in ^{9}He as seen in [2001Ch31] really existed, a narrow near-threshold 0^+ state in ^{10}He with a $[s1/2]^2$ structure would exist in addition to the $[p1/2]^2$ state [59, 60], in contradiction to the available experimental data on ^{10}He.

Based on these experimental results, we adopt the $1/2^-$ as the ground state of ^{9}He. In earlier work [1987Se05], [1988Bo20], and [1991Bo.B], transfer reactions were used, yielding values of E_r (resonance energy) of this state around 1.1 MeV. More recently, [1999Bo26] and [2010Jo06] determined $E_r \sim 1.3$ MeV. In [2007Go24], the $1/2^-$ state of ^{9}He was found at $E_r = 2.0 \pm 0.2$ MeV with a width ~ 2 MeV in this work, significantly higher than in the other work. The energy resolution of this experiment was 0.8 MeV (FWHM), which is quite large compared to the energy difference of $\sim$1.1 MeV between the $1/2^-$ and $3/2^-$ states [1988Bo20], [1999Bo26], [2010Jo06]. Therefore, we suspect this state to be a mixture due to the poor energy resolution in this experiment.

Finally, we adopt the results of [1999Bo26] and [2010Jo06] to define the resonance energy of the g.s. of ^{9}He.

Four experimental results are known concerning the mass of ^{10}He, as listed below:

Reference	Q_{2n}(in keV)	Method of production
1994Os04	1070 ± 70	^{10}Be(^{14}C,^{14}O)^{10}He
1994Ko16	1200 ±300	C(^{11}Li,^{10}He)
2010Jo06	1420 ±100	^{1}H(^{11}Li,^{10}He)
2012Si07	2100 ±200	^{3}H(^{8}He,p)^{10}He

The mass of ^{10}He from [1994Os04] is significantly lower than the others. In this work the statistics are poor compared to the high background. The values obtained in two invariant mass measurements agree with each other, both using ^{11}Li to produce ^{10}He. In the most recent work the value is higher than the others, while the authors stated that "the results reported in Refs. [1994Ko16] and [2010Jo06] do not contradict the g.s. energy of ^{10}He obtained in the present work", based on the calculations of Ref. [60]. They argued that due to the strong initial state effect, the observable g.s. peak position in [1994Ko16] and [2010Jo06] is shifted towards lower energy because of the abnormal size of ^{11}Li possessing one of the most developed known neutron halos.

The argument is based on theoretical calculations in a three-body ^{8}He+n+n model from [60]. The structure of ^{10}He is highly dependent on the structure of ^{9}He. Based on the ^{9}He spectrum from [2007Go24], the ^{10}He g.s. with structure $[p1/2]^2$ is predicted to be at about 2.0 – 2.3 MeV. However, the result of ^{9}He from [2007Go24] is not adopted, as discussed earlier. The model has problems in interpreting all of the experimental data, indicating the states may have a more complex structure. In the present evaluation, we choose the result from [2010Jo06] provisionally and call for more experiments to clarify this case.

Note added in proof: very recently, a group from MSU has studied ^{10}He using the fragmentation of ^{14}Be. Their result supports our choice. The discrepancy with the result in [2012Si07] could not be explained simply by the exotic structure of ^{11}Li, which was the argument used in the previous experiment, since, in the present case, a different reaction channel is explored.

7.2 The masses of ^{26}Al and ^{27}Al

In AME2012, the mass excess of ^{26}Al is -12210.112 ± 0.064 keV, which is more than 3 σ away from the AME2003 value of -12210.31 ± 0.06 keV. The origin of this difference lies in the new ^{26}Al-^{26}Mg Penning trap measurement at JYFLTRAP [2009Er02], which is in strong conflict with the older ^{26}Mg(p,n)^{26}Al measurement [1994Br11] as used in AME2003.

Prior to AME2003, the two results of the ^{25}Mg(n,γ) reaction were not in absolute agreement, either with

one another, or when combined with the average of non-conflicting values, such as that constructed from ^{25}Mg(p,γ) and the two values for ^{26}Mg(p,n)^{26}Al. The older Penning trap mass values for ^{24}Mg and ^{26}Mg [2003Be02], combined with the average of the very nicely agreeing values for the ^{24}Mg(n,γ) reaction, gave a value halfway between the ones just mentioned. In AME2003 we considered this compromise but concluded that the mass of ^{26}Al was not reliable. This situation was thought unfortunate, especially because of the special interest of the ^{26}Mg(p,n)^{26}Al reaction for problems connected with the intensity of allowed Fermi β-transitions. Therefore, the new result from JYFLTRAP mentioned above is mostly welcome in the present adjustment.

This result also helped solving the difficulty we had with the mass of ^{27}Al (see AME2003), due to its connections with all the nuclides just mentioned and, also with ^{28}Si through the (p,γ) reaction.

The new mass for ^{26}Al fix the problem by discarding definitively the ^{26}Mg(p,n)^{26}Al results [1992Ba.A], [1984Ba.B], and [1994Br11], all from the same group. However, no clear explanation can be given here for these discrepancies.

7.3 The mass of ^{32}Si

In AME2003, the mass excess of ^{32}Si was -24080.91 ± 0.05 keV. The value was determined, by the PTB group in Braunschweig, from an extraordinarily precise (n,γ) measurement [2001Pa52], originally given with a precision (5 eV) we judged, at that time already, to be excessively optimistic. Moreover, the publication did not provide spectra or any other detailed information. By comparison to well established (n,γ) from other groups, we could evaluate a calibration error of 30 eV and derive the above value in AME2003.

However, recently, the MSU group [2009Kw02] measured the masses of several nuclides including ^{32}Si, in a Penning trap. Their result is 3.25 keV away from the PTB result, and with a precision of 0.30 keV for ^{32}Si. The MSU measurements were internally cross-checked by combining various molecules and comparing to different references.

In general, and until otherwise proven, (n,γ) measurements have the reputation of being quite reliable. We have tried to contact the PTB group, but without success, to discuss their measurement. Until this issue is resolved, it has been decided, provisionally at least, not to use the (n,γ) data, but rather the Penning trap values.

7.4 The ^{35}S(β^-)^{35}Cl decay energy

This case has been investigated several times in connection with the report that a neutrino might exist with a mass of 17 keV.

Up until AME2003, the reported decay energies were so different from each other (with a Birge ratio of $\chi_n = 3.07$), that we decided at that time to use all nine datasets, irrespective of their claimed precision. We applied then the procedure described in Section 5.4.1 to establish the arithmetic average, and uncertainty, derived from the dispersion of the 9 data, at 167.222 ± 0.095 keV.

A new value, that was unfortunately missed in AME2003 is now adopted, at 167.334 ± 0.027 keV [2000Ho13]. It outweighs all previous ^{35}S(β^-)^{35}Cl measurements. Moreover it agrees quite nicely with the two accepted ^{34}S(n,γ)^{35}S results in [1983Ra04] and [1985Ke08].

7.5 The masses of ^{35,37}Cl and ^{36}Ar

The SMILETRAP ^{36}Ar result [2003Fr08] was some 1.2 keV lower than the value accepted until 2003, for which an error of 0.3 keV was claimed. The latter value was essentially due to mass-spectrometry results for ^{35}Cl and ^{37}Cl, combined with reaction energies for five reactions. These data agreed quite well if combined in a least squares analysis: $\chi_n = 1.13$. Combining with the [2003Fr08] mass value for ^{36}Ar increases χ_n to 2.00. But this value could be reduced to a reasonable 1.35 if, of the two available values for the ^{36}Ar(n,γ)^{37}Ar reaction energy, the oldest, not well documented one is no longer used. Also, this removed an earlier hardness in the connection with ^{40}Ar, of which the mass was already known with high precision. This problem is considered definitively settled.

7.6 The masses of ^{100}Sn

Determination of the mass of ^{100}Sn has been subject of discussion in AME2003. This result is particularly interesting due to the doubly magic character of ^{100}Sn which is, moreover, the heaviest known nuclide with $N = Z$.

The adopted mass in AME2003 was -56780 ± 710 keV, due to β^+ decay, and is 1060 keV less bound than indicated by the GANIL result [1996Ch32]. Earlier estimate from trends in the mass surface (TMS), were -56860#(430#) keV in AME1995, and -56460#(450#) keV in AME1993. The differences are not particularily large as compared to the claimed or estimated precisions. It is therefore interesting to note that the new result in [2012Hi07], also from β^+ decay, yields -57280(300) keV, that is almost half-way between the above values.

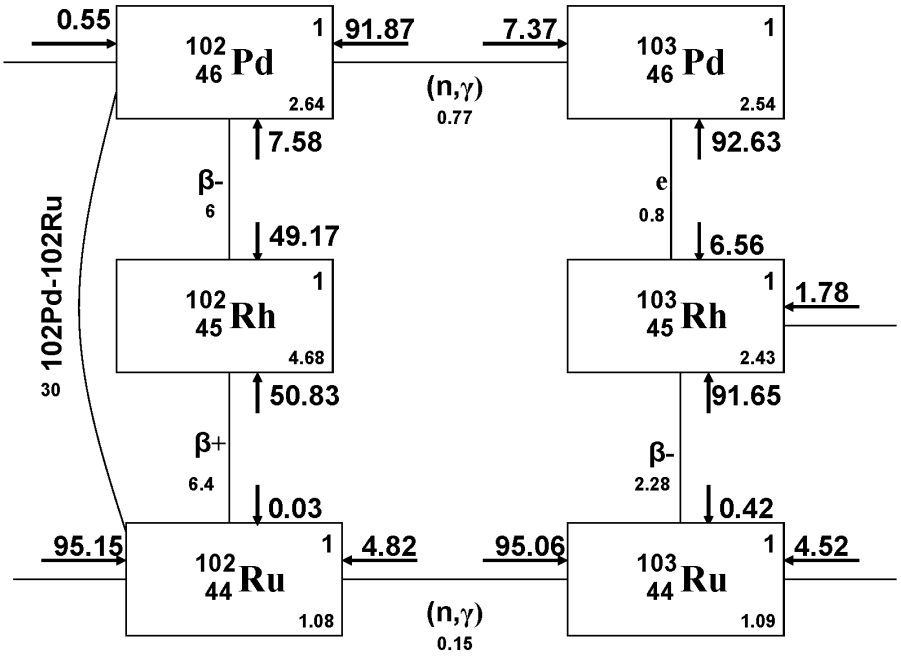

Figure 4: Flow of information diagram displaying the three "routes" between ^{102}Pd and ^{102}Ru. Each square box represents an individual nuclide. Its mass precision (keV) is given in the lower right corner, its degree in the upper right corner. Along each connection between two nuclides is the type of relation, its precision and on both sides are arrows indicating the flow of information to the two connected nuclides.

7.7 The ^{102}Pd double-electron capture energy

The double β or ε energy of some nuclides is an important parameter to study the neutrino properties. In recent years this measurement has attracted at lot attention, mainly in high-precision Penning traps. The mass difference between ^{102}Pd and ^{102}Rh, equivalent to the double-electron capture energy of ^{102}Pd, has been measured recently by SHIPTRAP yielding $Q_{\varepsilon\varepsilon} = 1203.27 \pm 0.36$ keV [2011Go23]. This result differs from the AME2003 value 1173.0±2.4 keV by 30 keV, i.e., more than 10 standard deviations. Besides this measurement, this $Q_{\varepsilon\varepsilon}$ value can be determined by local links established experimentally, as shown in Fig. 4. The two nuclides involved are not only linked via ^{102}Rh, but also are connected with higher mass isotopes through (n,γ) with lower uncertainty. The $Q_{\varepsilon\varepsilon}$ values obtained with these two different links agree with each other perfectly. All these connections, except ^{102}Rh(β^-)^{102}Pd, are determined by two or more different groups, sometimes with different methods. Their results are in good agreement with each other, and no reason can be found to suspect any individual measurement. Details of the input data is displayed in Table I. It should be recalled that Penning trap measurements have generally been quite reliable. In the present evaluation, the new Penning trap result is provisionaly not used. We call for more measurements to clarify this issue.

7.8 The mass of ^{105}Sb

The nuclide ^{105}Sb was reported in [1994Ti03] to be a proton emitter with $E_p = 478 \pm 15$ keV (thus $Q_p = 482.6 \pm 15$ keV) and a branching ratio of 1%. However, the later work of [1997Sh13] and [2005Li47], using different experimental methods, were unable to confirm the [1994Ti03] result. In fact, the production yield in the [2005Li47] work was significantly higher than in the previous studies, yielding an upper limit of 0.1% for the proton branching ratio (∼150 decay events of ^{105}Sb were expected, but none were seen), indicating that the activity observed in [1994Ti03] did not belong to ^{105}Sb. In more recent work, [2007Ma35] reported a weak α-decay branch for the ground state decay of ^{109}I with an energy of $E_\alpha = 3774 \pm 20$ keV. Because of the existing relationship between proton and α-decay Q values, $Q_\alpha(^{109}\text{I})+Q_p(^{105}\text{Sb})=Q_p(^{109}\text{I})+Q_\alpha(^{108}\text{Te})$, one can determine $Q_p(^{105}\text{Sb}) = 322 \pm 22$ keV. This value is in severe disagreement with the result (483±15 keV) of [1994Ti03] It is difficult to conclude unambiguously from the trends in the mass surface alone, which value is correct. Consequently, the Q_p value deduced from the Q_α measurement in [2007Ma35] was adopted in the present evaluation, and will determine the mass of ^{105}Sb. Direct proton-decay studies of ^{105}Sb are desirable in order to clarify this case.

7.9 The ^{163}Ta(α)^{159}Lu(α)^{155}Tm decay chain

This α-decay chain was discussed in the previous AME2003 publication, because it presented special difficulties.

The chain starts at ^{179}Tl and undergoes a series of consecutive α decays from both the ground state and excited isomer, which are associated with the $s_{1/2}$ and $h_{11/2}$ proton orbitals. It terminates at ^{147}Tb, which decays entirely by β^+ decay and whose ground state spin is measured directly as J=1/2, with a higher spin isomeric state, J^π=11/2$^-$, located at 50.6 $\pm$ 0.9 keV.

Mass-spectrometer data with precisions ranging from 28 to 68 keV are available [2005Li24] for the ^{147}Tb, ^{151}Ho, ^{155}Tm, ^{159}Lu and ^{163}Ta members of the chain. The first 3 ones carry no weight, but agree within their precision with values deduced from α decays. The directly measured mass of ^{159}Lu, with a precision of 57 keV, agrees with, and is combined with the Q_α measurement within the adjutment procedure.

Only ^{163}Ta (48 keV precision) strongly disagrees (3.6 σ) and is not accepted in our calculation. The α decay of ^{163}Ta yields Q(α)=4749$\pm$6 keV whereas combining masses from [2005Li24] one can derive Q(α)=4656$\pm$40 keV. In order to resolve this discrepancy, an isomeric state needs to be introduced in ^{163}Ta, and which α decays to the ^{159}Lu ground state.

In fact, such an isomer is now established at 130# $\pm$ 20# keV above the ground state from the measured α-decay energies and parent-daughter correlations in decays of the ^{179}Tl^m(α)^{175}Au^m(α)^{171}Ir^m(α)^{167}Re^gs(α)^{163}Ta^m chain nuclides and the estimated excitation energies 825# $\pm$ 10# for the ^{179}Tl^m isomer. The latter estimate is derived from interpolation of similar (11/2$^-$) states in Tl isotopes 177, 181 and 183. The isomer in ^{163}Ta is assigned $J^\pi = (9/2^-)$, following the favorite α decay from the $J^\pi = (9/2^-)$ ^{167}Re ground state.

To summarize, by combining all available information, and by discarding only one piece of data, we were able to build up a scenario for the double (ground states and excited isomers) ^{147}Tb-^{179}Tl decay chain. However most of the adopted values for excitation energies, and also for the ^{167}Re ground state are still labeled with the '#' flag, due to the estimated excitation energy of ^{179}Tl^m. Experimental determination of any of the excitation energy in ^{159}Lu, ^{163}Ta, ^{167}Re, ^{171}Ir, ^{175}Au, or ^{179}Tl will allow to access all other ones. Future measurements would be beneficial not only in order to firmly establish these excitation energies, but even more importantly, to provide also useful parent-daughter correlations on α decays that feed the ^{159}Lu ground state and decays out of the excited isomer.

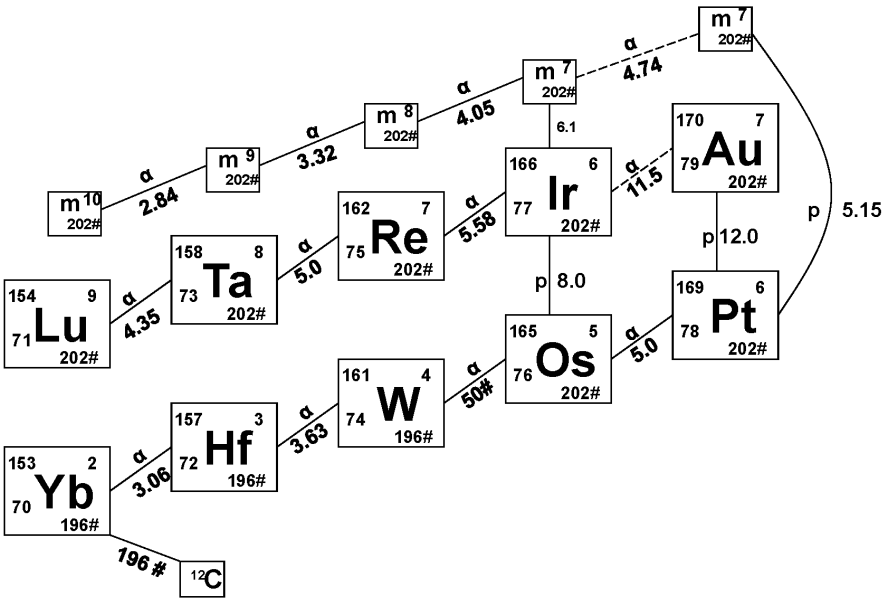

Figure 5: Loops created by two alpha decay chains interconnected by proton decays. See caption of Fig. 4. 'm' stands for the excited isomer of the nuclide below it.

Table D. Input data and adjusted values around the ^{170}Au-^{165}Os loop.

Item	Input AME2003	Output AME2003	Adjusted LSM	Input AME2012	adjusted value
^{166}Ir(p)^{165}Os	1152(8)	1152(8)	1150.6(7.1)	1152(8)	1154(6)
^{166}Ir^{m}(IT)^{166}Ir	171.5(6.1)	172(6)	170.8(5.6)	171.5(6.1)	172(6)
^{169}Pt(α)^{165}Os	6846.233(12.869)	6846(13)	6849.8(8.9)	6857.4(5.)	6856(5)
^{170}Au(p)^{169}Pt	1473.8(15.)	1474(15)	1475(10)	1471.7(12.)	1470(9)
^{170}Au^{m}(p)^{169}Pt	1747.9(6.247)	1748(6)	1748.9(5.7)	1751.356(5.145)	1751(5)
^{170}Au(α)^{166}Ir	7174.1(11.)	7168(21)	7173.7(9.3)	7170(12)	7172(9)
^{170}Au^{m}(α)^{166}Ir^{m}	7277.5(6.)	7271(17)	7276.9(5.6)	7278.5(9.)	7280(7)

7.10 The ^{170}Au(α) and ^{169}Pt(α) decay chains

It has been previously mentioned that some proton-rich nuclides can decay by both α and proton emission. In some cases, a loop of interconnected nuclides can be formed. Two long α-decay chains illustrate this case:

^{170}Au - ^{166}Ir - ^{162}Re - ^{158}Ta - ^{154}Lu and

^{169}Pt - ^{165}Os - ^{161}W - ^{157}Hf - ^{153}Yb - ^{149}Er,

which are connected by ^{170}Au(p)^{169}Pt and ^{166}Ir(p)^{165}Os, thus forming a loop as shown in Fig. 5. Unfortunately, none of the masses shown in Fig. 5 has been measured. If the mass of at least one nuclide is measured in the future, then all of the masses along the above two decay chains will be determined.

The general difficulty here, is that if all of the experimental information is used in the evaluation, then a closed loop would be formed, and all nuclides involved would be primary. The consequence is that some estimated (non-experimental) values would then automatically become primary data. For example, to avoid this, the ^{170}Au(α)^{166}Ir value was not used in AME2003, despite its good precision. A local evaluation is carried out in this region, involving all the corresponding nuclides, using least-squares method. The input and adjusted values are listed in Table D. The sources of the input data can be found in main Table I. As can be seen, the adjusted value of ^{170}Au(α)^{166}Ir would be 7173.7$\pm$9.3 instead of 7168$\pm$21, as listed in Table I of AME2003, if the full-scale least-squares method had been employed. Other values are also influenced by this new evaluation, as discussed in the following paragraph.

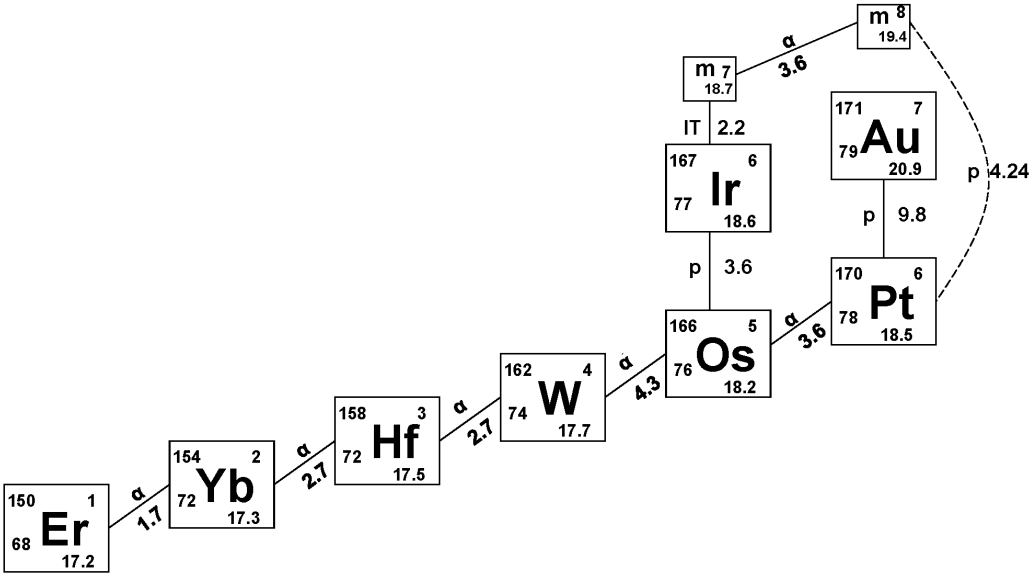

Figure 6: The loop and decay chains from ^{171}Au^{m} down to ^{150}Er, when replacing ^{171}Au^{m}(p)^{170}Pt by an equivalent ^{167}Ir(p)^{166}Os, as treated in AME2003. In the AME2012 treatment, the dotted connection has been restored. See caption of Fig. 4. 'm' stands for the excited isomer of the nuclide below it.

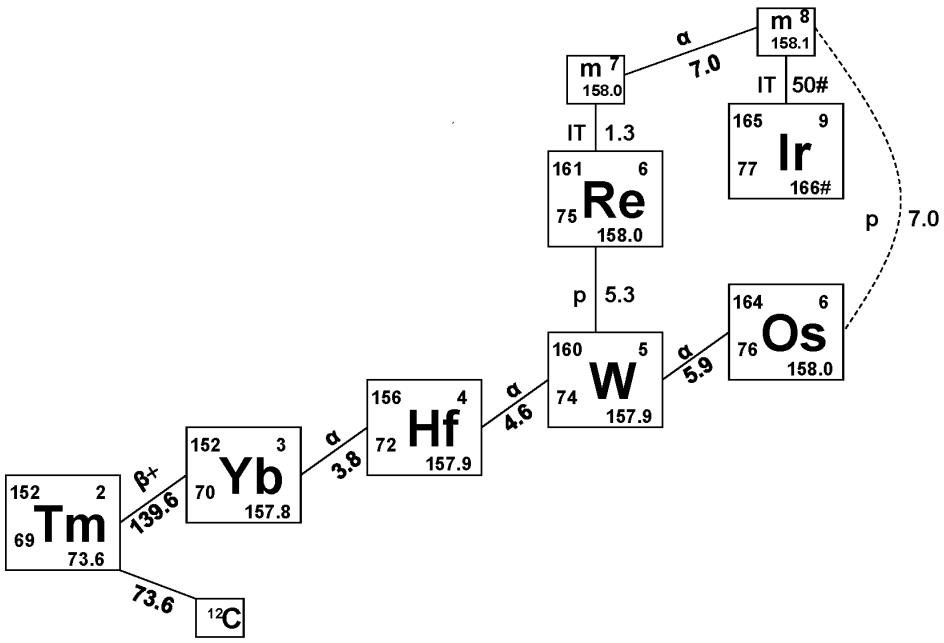

Figure 7: The loop and decay chains from $^{165}Ir^{m}$ down to ^{152}Tm, when replacing $^{165}Ir^{m}(p)^{164}Os$ by an equivalent $^{161}Re(p)^{160}W$, as treated in AME2003. In the AME2012 treatment, the dotted connection has been restored. See caption of Fig. 4. 'm' stands for the excited isomer of the nuclide below it.

Table E. Input data and adjusted values around the ^{165}Ir-^{160}W loop.

Item	Input Value AME2003	Output AME2003	Reference	Output AME2012
$^{161}Re(p)^{160}W$	1199.5 ± 6.0	1197.2 ± 5.3	97Ir01	1197.3 ± 5.3
$^{161}Re(p)^{160}W$	1188.9 ± 11.5	1197.2 ± 5.3	replacement	
$^{161}Re^{m}(IT)^{161}Re$	123.8 ± 1.3	123.8 ± 1.3	97Ir01	123.4 ± 1.3
$^{164}Os(\alpha)^{160}W$	6473.2 ± 10.0	6477.2 ± 5.9	96Bi07	6479.4 ± 5.3
$^{164}Os(\alpha)^{160}W$	6479.4 ± 7.0	6477.2 ± 5.9	96Pa01	6479.4 ± 5.3
$^{165}Ir^{m}(p)^{164}Os$	1717.5 ± 7.0	1725.9 ± 10.8	97Da07	1720.5 ± 5.9
$^{165}Ir^{m}(\alpha)^{161}Re^{m}$	6882.1 ± 7.0	6882.1 ± 7.0	97Da07	6878.9 ± 6.0

Here is a similar, but slightly different exemple. In our previous adjustments, following our policy of replacement to avoid loops, we also replaced in some rare cases a connection that did not obey the conditions defined in Section 5.4.2, by an equivalent connection, accepting a (slight) loss of precision. For example, in AME2003, the 1717.5±7.0 for $^{165}Ir^{m}(p)^{164}Os$ was replaced (see Table E) by an equivalent 1188.9±11.5 for $^{161}Re(p)^{160}W$, to avoid having 7 secondary masses to become primary as illustrated in Fig. 7. The increase in the uncertainty reflects the combination with other connections in the loop which uncertainties are not negligible.

There is no new experimental data since the publication of AME2003. We however decided in AME2012, taking advantage of computer's increased power, to restore original data, making thus all the nuclides in the chain down to ^{152}Tm to become primaries. Table E displays comparison of the two treatments and the restored precision of the $^{165}Ir^{m}(p)^{164}Os$ datum.

The only other case of this type is illustrated in Fig. 7. The interested reader will find in the main Table I all details and rebuild easily an equivalent of Table E.

7.11 The problem of the stable Hg isotopes

In our earlier evaluations we did not accept the 1980 Winnipeg measurements of the atomic masses of stable Hg isotopes, reported with errors of only about 1 keV. Since AME2003 the situation is stabilized. Here we recall the reasons for this.

In [1980Ko25], mass differences were measured between stable Hg isotopes and $^{12}C_2$ Cl_5 molecules, for $A = 199$ and 201, or $^{12}C^{13}C$ Cl_5, for $A = 200$, 202 and 204. The resulting Hg masses values were 22 μu high (odd A) and 17 μu high (even-A), compared to values from mass-spectrometry results for both lighter and heavier nuclides combined with experimental reaction and decay energies, see Fig. 1 in [34]. The difference suggested an influence due to the intensities of the ion beams, since ^{13}C is much less abundant than ^{12}C. Therefore, both sets of results were judged questionable.

In 2003, the Winnipeg group reported a new value for ^{199}Hg [2003Ba49], 7 μu lower than their 1980 result. In addition, measurements with the Stockholm Penning trap spectrometer SMILETRAP gave results for ^{198}Hg and ^{204}Hg, essentially agreeing with the 1980 Winnipeg even-mass values. Thus, the latter appear to be reasonable.

We therefore accepted these data, and also included old and new nuclear reaction and decay results.

The relation with the higher-A mass-spectrometry results (Th and U isotopes) is acceptable, but the differences are nearly equal to the old ones but with a change in sign. With lower-A, Winnipeg provided further information through new measurements of the mass of ^{183}W and its difference with ^{199}Hg. These essentially confirmed the mass values around ^{183}W given in earlier evaluations [3, 7]. For completeness, we observe that the new ^{183}W result is 15 μu higher than the 1977 Winnipeg result (error 2.7 μu), which was one of the items that helped to suggest the lower Hg masses.

Closer scrutiny, shows that nuclear reaction energies, in the region between these two nuclides, have discrepancies which, as yet, are not resolved. The upshot is, that the earlier difficulty in the connection of the stable Hg's to lower A data appears to be due to errors in the mass-spectrometer data used at the time. We therefore think that the most recent mass values for these Hg isotopes as adopted since 2003 are definitely more dependable than earlier ones.

7.12 Other special cases

Other special cases are presented and discussed on the AMDC web site [8].

8 General information and acknowledgments

The full content of the present issue is accessible online at the AMDC website [8]. In addition, on the site, there are several localized mass analyses that were carried out, but could not be given in the printed version. Also, several graphs representing the mass surface, beyond the main ones in Part II, are also available.

As before, the table of masses (Part II, Table I) and the table of nuclear reaction and separation energies (Part II, Table III) are available in plain ASCII format to simplify their input to computer programs using standard languages. The headers of these files give information on the formats. The first file, named **mass_rmd.mas12**, contains the table of masses. The next two files correspond to the table of reaction and separation energies, in two parts of 6 entries each, as in Part II, Table III: **rct1_rmd.mas12** for S_{2n}, S_{2p}, Q_α, $Q_{2\beta}$, $Q_{\varepsilon p}$ and $Q_{\beta n}$ (odd pages in this issue); and **rct2_rmd.mas12** for S_n, S_p, $Q_{4\beta}$, $Q_{d,\alpha}$, $Q_{p,\alpha}$ and $Q_{n,\alpha}$ (facing even pages). As explained in Section 4.2, since AME2003, we no longer produce any more special tables for experimental data which we do not recommend.

We wish to thank our many colleagues who answered our questions about their experiments and those who sent us preprints of their papers. Continuous interest, discussions, suggestions and encouragements from K. Blaum, D. Lunney, G. Savard, Zhang Yuhu, Zhongzhou Ren, and Ch. Scheidenberger were highly appreciated.

This work was performed in the frame and with the help of the French-Chinese collaboration under the PICS programme. M.W. acknowledges support from the Max-Planck Society, from the International Atomic Energy Agency, IAEA-Vienna and from the National Natural Science Foundation of China through Grant No.10925526, 11035007. The work at ANL was supported by the U.S. Department of Energy, Office of Nuclear Physics, under Contract No. DE-AC02-06CH1357.

Appendix A The meaning of decay energies

Conventionally, the decay energy in an α-decay is defined as the difference in the atomic masses of mother and daughter nuclides:

$$Q_\alpha = M_{\text{mother}} - M_{\text{daughter}} - M_{^4\text{He}} \qquad (8)$$

This value equals the sum of the observed energy of the α particle and the easily calculated energy of the recoiling nuclide (with only a minor correction for the fact that the cortège of atomic electrons in the latter may be in an excited state). Very unfortunately, some authors quote as resulting Q_α a value 'corrected for screening', which essentially means that they take for the values M in the above

equation the masses of the bare nuclides (the difference is essentially that between the total binding energies of all electrons in the corresponding neutral atoms).

This bad custom is a cause of confusion; even so much that in a certain paper this "correction" was made for some nuclides but not for others.

A similar bad habit has been observed for some proton decay energies. We very strongly object to this custom; at the very least, the symbol Q should not be used for the difference in nuclear masses!

Appendix B Mixtures of isomers or of isobars in mass-spectrometry

In cases where two or more unresolved lines may combine into a single one in an observed spectrum, while one cannot decide which ones are present and in which proportion, a special procedure has to be used.

The first goal is to determine what is the most probable value M_{exp} that will be observed in the measurement, and what is the uncertainty σ of this prediction. We assume that all the lines may contribute and that all contributions have equal probabilities. The measured mass reflects the mixing. We call M_0 the mass of the lowest line, and $M_1, M_2, M_3, \ldots$ the masses of the other lines. For a given composition of the mixture, the resulting mass m is given by

$$m = (1-\sum_{i=1}^{n} x_i)M_0 + \sum_{i=1}^{n} x_i M_i \qquad \text{with} \begin{cases} 0 \le x_i \le 1 \\ \sum_{i=1}^{n} x_i \le 1 \end{cases} \tag{9}$$

in which the relative unknown contributions $x_1, x_2, x_3, \ldots$ have each a uniform distribution of probability within the allowed range.

If $P(m)$ is the normalized probability of measuring the value m, then :

$$\overline{M} = \int P(m)\, m\, dm \tag{10}$$

$$\text{and} \quad \sigma^2 = \int P(m)\, (m-\overline{M})^2\, dm \tag{11}$$

It is thus assumed that the experimentally measured mass will be $M_{exp} = \overline{M}$, and that σ, which reflects the uncertainty on the composition of the mixture, will have to be quadratically added to the experimental uncertainties.

The difficult point is to derive the function $P(m)$.

B.1 Case of 2 spectral lines

In the case of two lines, one simply gets

$$m = (1-x_1)M_0 + x_1 M_1 \quad \text{with} \quad 0 \le x_1 \le 1 \tag{12}$$

The relation between m and x_1 is biunivocal so that

$$P(m) = \begin{cases} 1/(M_1 - M_0) & \text{if } M_0 \le m \le M_1, \\ 0 & \text{elsewhere} \end{cases} \tag{13}$$

i.e. a rectangular distribution (see Fig. 8*a*), and one obtains :

$$M_{exp} = \frac{1}{2}(M_0 + M_1) \tag{14}$$

$$\sigma = \frac{\sqrt{3}}{6}(M_1 - M_0) = 0.290\ (M_1 - M_0)$$

B.2 Case of 3 spectral lines

In the case of three spectral lines, we derive from Eq. 9:

$$m = (1-x_1-x_2)M_0 + x_1 M_1 + x_2 M_2 \tag{15}$$

$$\text{with} \begin{cases} 0 \le x_1 \le 1 \\ 0 \le x_2 \le 1 \\ 0 \le x_1 + x_2 \le 1 \end{cases} \tag{16}$$

The relations (15) and (16) may be represented on a x_2 vs x_1 plot (Fig. 9). The conditions (16) define a triangular authorized domain in which the density of probability is uniform. The relation (15) is represented by a straight line. The part of this line contained inside the triangle defines a segment which represents the values of x_1 and x_2 satisfying all relations (16). Since the density of probability is constant along this segment, the probability $P(m)$ is proportional to its length. After normalization, one gets (Fig. 8*b*):

$$P(m) = \frac{2k}{M_2 - M_0} \tag{17}$$

$$\text{with} \begin{cases} k = (m-M_0)/(M_1-M_0) & \text{if } M_0 \le m \le M_1 \\ k = (M_2-m)/(M_2-M_1) & \text{if } M_1 \le m \le M_2 \end{cases} \tag{18}$$

and finally:

$$M_{exp} = \frac{1}{3}(M_0 + M_1 + M_2) \tag{19}$$

$$\sigma = \frac{\sqrt{2}}{6}\sqrt{M_0^2 + M_1^2 + M_2^2 - M_0M_1 - M_1M_2 - M_2M_0}$$

B.3 Case of more than 3 spectral lines

For more than 3 lines, one may easily infer $M_{exp} = \sum_{i=0}^{n} M_i/(n+1)$, but the determination of σ requires the knowledge of $P(m)$. As the exact calculation of $P(m)$ becomes rather difficult, it is more simple to do simulations.

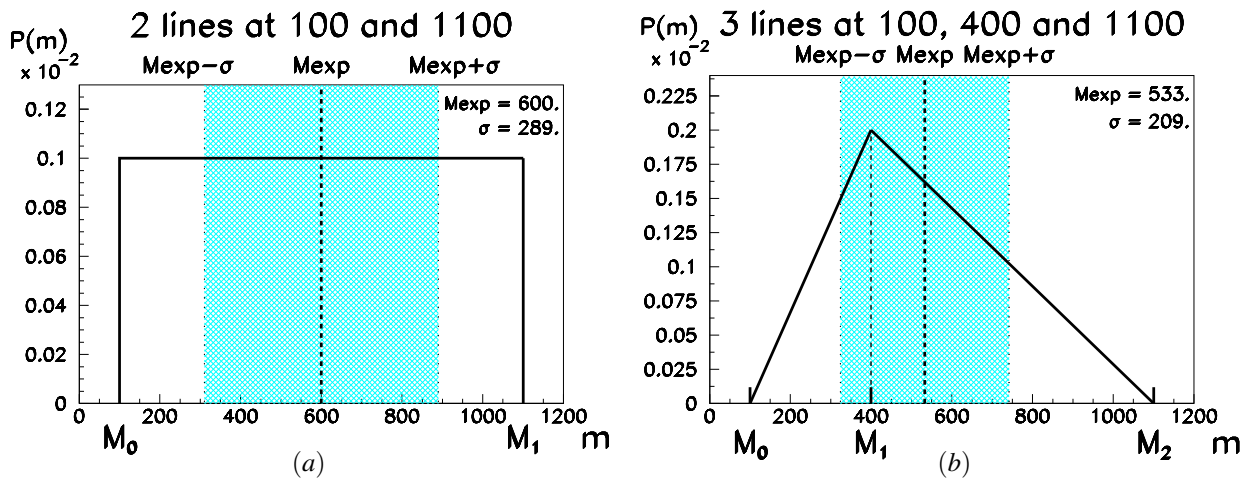

Figure 8: Examples of probabilities to measure m according to an exact calculation in cases of the mixture of two (a) and three (b) spectral lines.

However, care must be taken that the values of the x_i's are explored with an exact equality of chance to occur. For each set of x_i's, m is calculated, and the histogram $N_j(m_j)$ of its distribution is built (Fig. 10). Calling *nbin* the number of bins of the histogram, one gets :

$$P(m_j) = \frac{N_j}{\sum_{j=1}^{nbin} N_j} \quad (20)$$

$$M_{exp} = \sum_{j=1}^{nbin} P(m_j) m_j$$

$$\sigma^2 = \sum_{j=1}^{nbin} P(m_j)(m_j - M_{exp})^2$$

A first possibility is to explore the x_i's step-by-step: x_1 varies from 0 to 1, and for each x_1 value, x_2 varies from 0 to $(1-x_1)$, and for each x_2 value, x_3 varies from 0 to $(1-x_1-x_2)$, ... using the same step value for all.

A second possibility is to choose x_1, x_2, x_3, ... randomly in the range [0,1] in an independent way, and to keep only the sets of values which satisfy the relation $\sum_{i=1}^{n} x_i \leq 1$. An example of a Fortran program based on the CERN library is given below for the cases of two, three and four lines. The results are presented in Fig. 10.

Both methods give results in excellent agreement with each other, and as well with the exact calculation in the cases of two lines (see Fig. 8*a* and 10*a*) and three lines (see Fig. 8*b* and 10*b*).

The Fortran program used to produce the histograms in Fig. 10.

```
      program isomers

c-------------------------------------------------------------------
c-   October 15, 2003              C.Thibault
c-   Purpose and Methods : MC simulation for isomers (2-4 levels)
c-   Returned value      : mass distribution histograms
c-------------------------------------------------------------------

      parameter (nwpawc=10000)
      common/pawc/hmemor(nwpawc)
      parameter (ndim=500000)
      dimension xm(3,ndim)
      data e0,e1,e31,e41,e42/100.,1100.,400.,200.,400./
      call hlimit(nwpawc)
c histograms 2, 3, 4 levels
      call hbook1(200,'',120,0.,1200.,0.)
      call hbook1(300,'',120,0.,1200.,0.)
      call hbook1(400,'',120,0.,1200.,0.)
      call hmaxim(200,6500.)
```

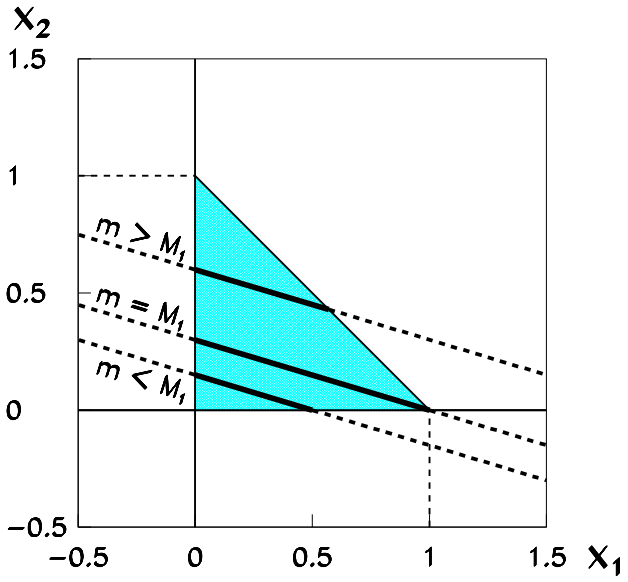

Figure 9: Graphic representation of relations 15 and 16. The length of the segments (full thick lines) inside the triangle are proportional to the probability $P(m)$. Three cases are shown corresponding respectively to $m < M_1$, $m = M_1$, and to $m > M_1$. The maximum of probability is obtained when $m = M_1$.

```
      call hmaxim(300,6500.)
      call hmaxim(400,2500.)
      w=1.
c random numbers [0,1]
      ntot=3*ndim
      iseq=1
      call ranecq(iseed1,iseed2,iseq,' ')
      call ranecu(xm,ntot,iseq)
      do i=1,ndim
c 2 levels :
         t=1-xm(1,i)
         e = t*e0 + xm(1,i)*e1
         call hfill(200,e,0.,w)
c 3 levels :
         if ((xm(1,i)+xm(2,i)).le.1.) then
           t=1.-xm(1,i)-xm(2,i)
           e= t*e0 + xm(1,i)*e31 + xm(2,i)*e1
           call hfill(300,e,0.,w)
         end if
c 4 levels
         if ((xm(1,i)+xm(2,i)+xm(3,i)).le.1.) then
           t=1.-xm(1,i)-xm(2,i)-xm(3,i)
           e = t*e0 + xm(1,i)*e41 + xm(2,i)*e42 + xm(3,i)*e1
           call hfill(400,e,0.,w)
         end if
      end do
      call hrput(0,'isomers.histo','N')
      end
```

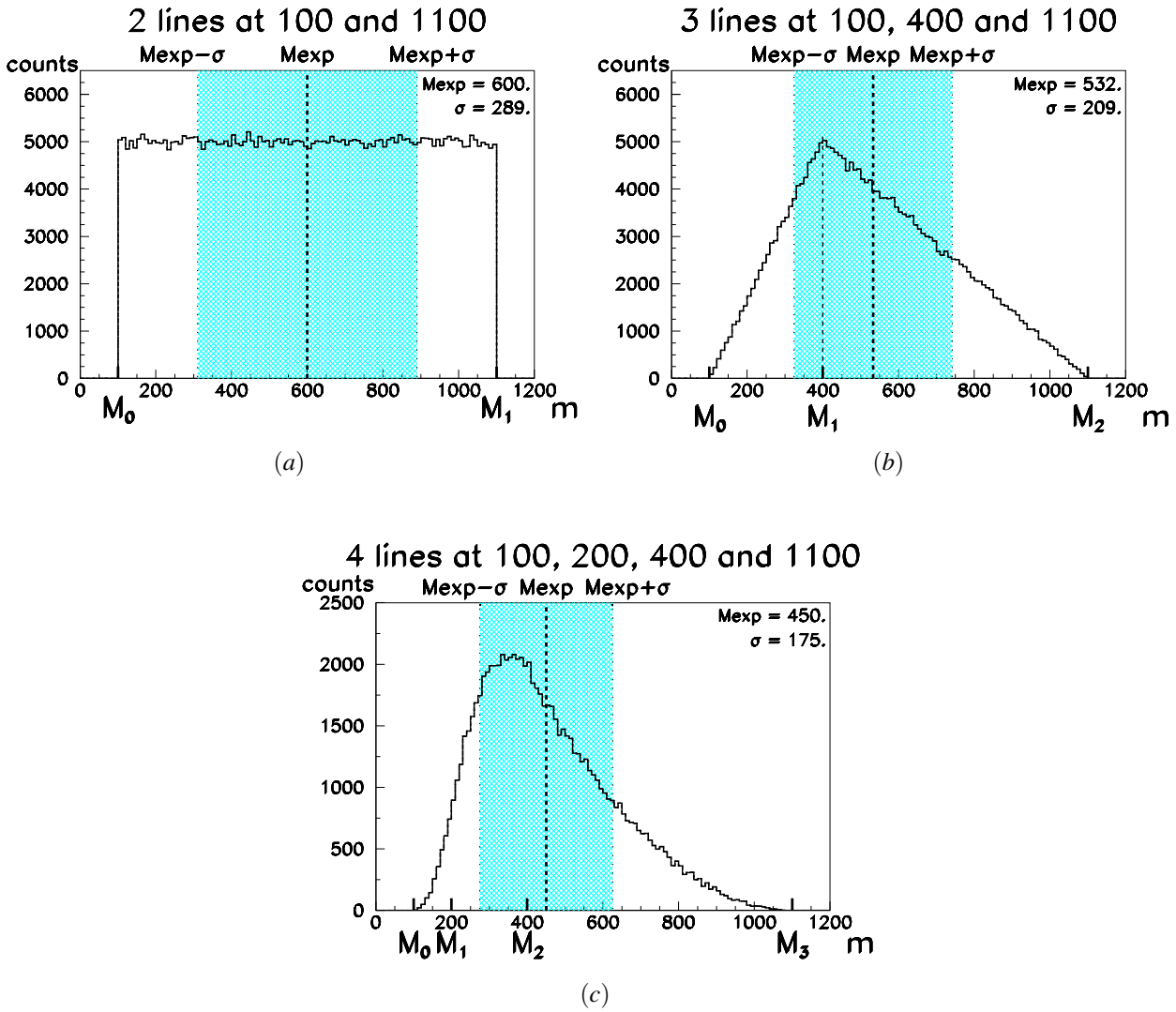

Figure 10: Examples of Monte-Carlo simulations of the probabilities to measure m in cases of two (a), three (b) and four (c) spectral lines.

B.4 Example of application for one, two or three excited isomers

We consider the case of a mixture implying isomeric states. We want to determine the ground state mass $M_0 \pm \sigma_0$ from the measured mass $M_{exp} \pm \sigma_{exp}$ and the knowledge of the excitation energies $E_1 \pm \sigma_1, E_2 \pm \sigma_2, \ldots$

With the above notation, we have

$M_1 = M_0 + E_1,$

$M_2 = M_0 + E_2, \ldots$

For a single excited isomer, Equ. (14) can be written:

$$\begin{aligned} M_0 &= M_{exp} - \frac{1}{2}E_1 \\ \sigma^2 &= \frac{1}{12}E_1^2 \qquad \text{or} \qquad \sigma = 0.29\,E_1 \\ \sigma_0^2 &= \sigma_{exp}^2 + (\frac{1}{2}\sigma_1)^2 + \sigma^2 \end{aligned}$$

For two excited isomers, Equ. (19) lead to :

$$\begin{aligned} M_0 &= M_{exp} - \frac{1}{3}(E_1 + E_2) \\ \sigma^2 &= \frac{1}{18}(E_1^2 + E_2^2 - E_1E_2) \\ &\text{or} \qquad \sigma = 0.236\sqrt{E_1^2 + E_2^2 - E_1E_2} \\ \sigma_0^2 &= \sigma_{exp}^2 + (\frac{1}{3}\sigma_1)^2 + (\frac{1}{3}\sigma_2)^2 + \sigma^2 \end{aligned}$$

If the levels are regularly spaced, *i.e.* $E_2 = 2E_1$,

$$\sigma = \frac{\sqrt{6}}{12}E_2 = 0.204\,E_2$$

while for a value of E_1 very near 0 or E_2,

$$\sigma = \frac{\sqrt{2}}{6}E_2 = 0.236\,E_2$$

For three excited isomers , the example shown in Fig. 10*c* leads to:

$$\begin{aligned} M_0 &= M_{exp} - \frac{1}{4}(E_1+E_2+E_3) = 450. \\ \sigma &= 175. \\ \sigma_0^2 &= \sigma_{exp}^2 + (\frac{1}{4}\sigma_1)^2 + (\frac{1}{4}\sigma_2)^2 + (\frac{1}{4}\sigma_3)^2 + \sigma^2 \end{aligned}$$

Appendix C Converting frequency ratios to linear equations

In the following, quantities with the subscript r describe the charateristics of the reference ion in the Penning Trap. Equivalent quantities, with no subscript, describe characteristics of the ion being measured. The ratio R of frequencies f between the reference and newly measured ion is written:

$$R = \frac{f_r}{f} = \frac{\mathscr{M} - m_e\, q + B}{\mathscr{M}_r - m_e\, q_r + B_r}\ \frac{q_r}{q} \tag{21}$$

where q is the charged state of the given ion, B is the electron binding energy, m_e is the mass of the electron and $\mathscr{M}$ the total atomic mass. All masses and energies are in atomic mass units (u) and so, u=1.

This expression can be written in terms of the mass excess M and atomic mass number A:

$$\begin{aligned} A + M \;-\; & R\,\frac{q}{q_r}\,A_r - R\,\frac{q}{q_r}\,M_r = \\ = \;& m_e\, q(1-R) + B_r\, R\,\frac{q}{q_r} - B \end{aligned}$$

or, alternatively:

$$\begin{aligned} M - R\,\frac{q}{q_r}\,M_r \;=\; & m_e\, q(1-R) \;+\; A_r\left(\frac{q}{q_r}\,R - \frac{A}{A_r}\right) \\ & +\; B_r\, R\,\frac{q}{q_r} - B \end{aligned}$$

The general aim is to establish some quantity y and its associated precision dy. We define C to be a truncated, three-digit decimal approximation of the ratio A to A_r, and then we can write:

$$y \;=\; M - C\, M_r \tag{22}$$

and so

$$y \;=\; y_1 + y_2 + y_3 + y_4 \tag{23}$$

where

$$y_1 \;=\; M_r\left(R\,\frac{q}{q_r} - C\right) \tag{24}$$

$$y_2 \;=\; m_e\, q(1-R) \tag{25}$$

$$y_3 \;=\; A_r\left(\frac{q}{q_r}\,R - \frac{A}{A_r}\right) \tag{26}$$

and

$$y_4 \;=\; B_r\, R\,\frac{q}{q_r} - B \tag{27}$$

To fix relative orders of magnitude, M_r is generally smaller than 0.1 u, $R-C$ is a few 10^{-4}, $(1-R)$ is usually smaller than unity (and typically 0.2 for a 20% mass change), $R - \frac{A}{A_r}$ varies from 1 to 100×10^{-6} and A_r is typically 100 u for atomic mass $A = 100$. The four terms y_1, y_2, y_3, and y_4 take values of the order of 10 μu, 100 μu, 10 to 10000 μu, and 0.1 μu, respectively.

The associated precision dy is written:

$$dy \;=\; dy_1 + dy_2 + dy_3 + dy_4 \tag{28}$$

where

$$dy_1 \;=\; \frac{q}{q_r}\,M_r\,dR + \left(R\,\frac{q}{q_r} - C\right)\,dM_r \simeq dR\times10^5\ \mu u \tag{29}$$

$$dy_2 \;=\; m_e\, q\, dR \simeq dR\times10^3\ \mu u \tag{30}$$

$$dy_3 \;=\; \frac{q}{q_r}\,A_r\,dR \simeq dR\times10^8\ \mu u \tag{31}$$

and

$$dy_4 \;=\; \frac{q}{q_r}\,B_r\,dR + R\,\frac{q}{q_r}dB_r + dB \simeq dR\times10^{-1}\ \mu u \tag{32}$$

Consequently, only the 3rd term contributes significantly to the precision of the measurement, and so we write: $dy \;=\; dy_3$

If the two frequencies are measured with a typical precision of 10^{-7} for ions at $A = 100$, then the precision on the frequency ratio R is 1.4×10^{-7} and the precision on the mass is approximatively 14 μu.

C.1 Program for frequency conversion

Primary data from Penning Trap measurement are typically given in the form of an experimental frequency ratio. An example is given here for a series of nuclides with respect to a various reference nuclides and various charge states. Below is the Fortran frequency conversion program, followed by sample input file and corresponding output file.

The frequency conversion program

```
c                              PTrap15publ      G.Audi    m 06 nov 2012
c
c  Conversion of Frequency Ratios to Linear Equations
c
      real*8 xzero,mel,mref,smref,mrefk,rap,srap,coef
      real*8 prov,membre,sigmem,m118,sm118
      integer q118,qref
      character txref*4,tx118*4,rev*2
      character*30 filea,fileb
c
c        mel : electron mass in micro-u
c        mref, smref : Mass and uncert. for reference (ref)
c        m118, sm118 : Mass and uncert. for mesured (118)
c        qref, q118  : charge states of the ions
c
      filea='ptkl.equat                     '                ! output file
      fileb='ptkl.freq                      '                ! input file
      open(unit=1,file=filea,form='formatted',status='new')
      open(unit=3,file=fileb,form='formatted',status='old',readonly)
c
      mel   = 548.5799110
      xzero = 9.314940090d-1                                 ! conversion factor micro-u to keV
   12 read(3,1001,err=99) iaref,txref,qref,mref,rev,smref    ! read reference, mass in micro-u
 1001 format(i4,a4,i4,f17.6,a2,f11.6)
      mrefk = mref  * xzero
c
   15 read(3,1001,end=90,err=99) ia118,tx118,q118,rap,rev,srap ! read frequency ratio
      if(tx118.eq.'NEW ') go to 12                           ! reset reference
      if(rev.eq.'  ') then                                   ! if reversed freq. ratio: rev=-1
        rap  = rap  / 1.d+6
        srap = srap / 1.d+6
      else
        rap  = 1.d+6 / rap
        srap = rap*rap * srap/1.d+6
      endif
      coef = anint(1000.*ia118/iaref) / 1000.                ! calculate 3-digit coefficient
c
      prov = (ia118*1.d+0)/iaref - rap*q118/qref
      membre = mref*(rap*q118/qref-coef) + mel*q118*(1-rap)
     *         - iaref*1.d+6*prov                            ! value (in micro-u) for the equation
      sigmem = srap * iaref * 1.d+6 * q118/qref              ! its uncertainty
      write (1,1020) ia118,tx118,iaref,txref,coef,membre,sigmem
 1020 format(5x,i6,a4,'-',i4,a4,'*',
     *                   f6.3,' =', f13.3,' (',f9.3,')')
      m118  = membre + coef*mref
      sm118 = sqrt(sigmem**2 + (coef*smref)**2)
      write (1,1030) ia118,tx118,m118,sm118
 1030 format(13x,i4,a4,' =',f14.5,' +/-',f10.5,' micro-u')
      m118  = m118  * xzero
      sm118 = sm118 * xzero
      write (1,1032) m118,sm118
 1032 format(13x,8x,' =',f14.5,' +/-',f10.5,' keV',/)
c
      go to 15
c
   90 write (1,1990)
 1990 format(1H0,'Normal End of Freq.Ratios to Equations Conversion')
      stop
   99 write(1,1999)
 1999 format(1H0,'Error in File Reading')
      stop
      end
```

A typical frequency ratio input file

```
 6Li    +1     15122.885   ..   0.029     1st line : reference nuclide
 4He    +1    665392.8420       0.0077    following lines : frequency ratios
 7Li    +1   1166409.2053       0.0131    NEW : new set with new ref. follows
 8Li    +1   1333749.8620       0.0180
  NEW                        ..            column 1 : nuclidic name
 7Li    +1     16003.42560      0.00455   column 2 : ionic charge
10Be    +1    700635.628   -1   0.009     column 3 : mass excess for ref. (micro-u)
11Be    +1    636546.859   -1   0.036             or frequency ratio *10^6
  NEW                        ..            column 5 : -1 for inverse ratio
39K     +4    -36293.410   ..   0.085     column 4 : uncertainty
44K     +4    886306.8169  -1   0.0444
  NEW                        ..
85Rb    +9    -88210.26200 ..   0.00535
74Rb    +8    979689.6094       0.0858
76Rb    +8   1006067.4141       0.0223
  NEW                        ..
85Rb   +13    -88210.26200 ..   0.00535
99Sr   +15   1009776.3077       0.0451
```

Corresponding output file

```
         4He  -   6Li  * 0.667 =    -7483.694 (    0.046)
               4He   =    2603.27019 +/-   0.05009 micro-u
                     =    2424.93058 +/-   0.04665 keV

         7Li  -   6Li  * 1.167 =    -1644.991 (    0.079)
               7Li   =   16003.41533 +/-   0.08558 micro-u
                     =   14907.08550 +/-   0.07971 keV

         8Li  -   6Li  * 1.333 =     2327.424 (    0.108)
               8Li   =   22486.22932 +/-   0.11471 micro-u
                     =   20945.78789 +/-   0.10685 keV

        10Be  -   7Li  * 1.429 =    -9334.156 (    0.128)
              10Be   =   13534.73895 +/-   0.12850 micro-u
                     =   12607.52825 +/-   0.11970 keV

        11Be  -   7Li  * 1.571 =    -3479.829 (    0.622)
              11Be   =   21661.55299 +/-   0.62197 micro-u
                     =   20177.60683 +/-   0.57936 keV

        44K   -  39K   * 1.128 =     2529.206 (    2.204)
              44K    =  -38409.76074 +/-   2.20643 micro-u
                     =  -35778.46201 +/-   2.05527 keV

        74Rb  -  85Rb  * 0.871 =    21096.382 (    6.483)
              74Rb   =  -55734.75669 +/-   6.48267 micro-u
                     =  -51916.59195 +/-   6.03857 keV

        76Rb  -  85Rb  * 0.894 =    13930.883 (    1.685)
              76Rb   =  -64929.09141 +/-   1.68490 micro-u
                     =  -60481.05966 +/-   1.56947 keV

        99Sr  -  85Rb  * 1.165 =    35661.650 (    4.423)
              99Sr   =  -67103.30571 +/-   4.42327 micro-u
                     =  -62506.32725 +/-   4.12025 keV

0Normal End of Freq.Ratios to Equations Conversion
```

References

References such as 1984Sc.A, 1989Sh10 or 2003Ot.1 are listed under "References used in the AME2012 *and the* NUBASE2012 *evaluations", p. 1863.*

[1] A.H. Wapstra, G. Audi and C. Thibault, Nucl. Phys. **A 729** (2003) 129; http://amdc.in2p3.fr/masstables/Ame2003/Ame2003a.pdf

[2] G. Audi, A.H. Wapstra and C. Thibault, Nucl. Phys. **A 729** (2003) 337; http://amdc.in2p3.fr/masstables/Ame2003/Ame2003b.pdf

[3] G. Audi and A.H. Wapstra, Nucl. Phys. **A 565** (1993) 1; http://amdc.in2p3.fr/masstables/Ame1993/

[4] G. Audi and A.H. Wapstra, Nucl. Phys. **A 565** (1993) 66.

[5] C. Borcea, G. Audi, A.H. Wapstra and P. Favaron, Nucl. Phys. **A 565** (1993) 158.

[6] G. Audi, A.H. Wapstra and M. Dedieu, Nucl. Phys. **A 565** (1993) 193.

[7] G. Audi and A.H. Wapstra, Nucl. Phys. **A 595** (1995) 409; http://amdc.in2p3.fr/masstables/Ame1995/

[8] The AME2012 files in the electronic distribution and complementary documents can be retrieved from the Atomic Mass Data Center (AMDC) through the *Web*: http://amdc.in2p3.fr/ and http://amdc.impcas.ac.cn/

[9] G. Audi, O. Bersillon, J. Blachot and A.H. Wapstra, Nucl. Phys. **A 624** (1997) 1; http://amdc.in2p3.fr/nubase/nubase97.pdf

[10] A.H. Wapstra and K. Bos, At. Nucl. Data Tables **20** (1977) 1.

[11] J.C. Hardy, L.C. Carraz, B. Jonson and P.G. Hansen, Phys. Lett. **B71** (1977) 307.

[12] K.-N. Huang, M. Aoyagi, M.H. Chen, B. Crasemann and H. Mark, At. Nucl. Data Tables **18** (1976) 243.

[13] P.J. Mohr, B.N. Taylor and David B. Newell, http://arxiv.org/pdf/1203.5425

[14] T.P. Kohman, J.H.E. Mattauch and A.H. Wapstra, J. de Chimie Physique **55** (1958) 393.

[15] John Dalton, 1766-1844, who first speculated that elements combine in proportions following simple laws, and was the first to create a table of (very approximate) atomic weights.

[16] E.R. Cohen and A.H. Wapstra, Nucl. Instrum. Methods **211** (1983) 153.

[17] E.R. Cohen and B.N. Taylor, CODATA Bull. **63** (1986), Rev. Mod. Phys. **59** (1987) 1121.

[18] T.J. Quin, Metrologia **26** (1989) 69; B.N. Taylor and T.J. Witt, Metrologia **26** (1989) 47.

[19] P.J. Mohr and B.N. Taylor, J. Phys. Chem. Ref. Data **28** (1999) 1713.

[20] A. Rytz, At. Nucl. Data Tables **47** (1991) 205.

[21] A.H. Wapstra, Nucl. Instrum. Methods **A292** (1990) 671.

[22] http://amdc.in2p3.fr/masstables/Ame2003/recalib

[23] R.G. Helmer and C. van der Leun, Nucl. Instrum. Methods **422** (1999) 525.

[24] Nuclear Data Sheets.

[25] M.L. Roush, L.A. West and J.B. Marion, Nucl. Phys. **A147** (1970) 235.

[26] P.M. Endt, C.A. Alderliesten, F. Zijderhand, A.A. Wolters and A.G.M. van Hees, Nucl. Phys. **A510** (1990) 209.

[27] D.P. Stoker, P.H. Barker, H. Naylor, R.E. White and W.B. Wood, Nucl. Instrum. Methods **180** (1981) 515.

[28] A.H. Wapstra, unpublished.

[29] G. Audi, M. Epherre, C. Thibault, A.H. Wapstra and K. Bos, Nucl. Phys. **A378** (1982) 443.

[30] G. Audi, Hyperfine Interactions **132** (2001) 7; École Internationale Joliot-Curie 2000, Spa, p.103; http://amdc.in2p3.fr/masstables/hal.pdf

[31] Systematic errors are those due to instrumental drifts or instrumental fluctuations, that are beyond control and are not accounted for in the error budget. They might show up in the calibration process, or when the measurement is repeated under different experimental conditions. The experimentalist adds then quadratically a systematic error to the statistical and the calibration ones, in such a way as to have consistency of his data. If not completely accounted for or not seen in that experiment, they can still be observed by the mass evaluators when considering the mass adjustment as a whole.

[32] C.F. von Weizsäcker, Z. Phys. **96** (1935) 431; H.A. Bethe and R.F. Bacher, Rev. Mod. Phys. **8** (1936) 82.

[33] C. Borcea and G. Audi, Rev. Roum. Phys. **38** (1993) 455; *CSNSM Report* **92-38**, Orsay 1992: http://amdc.in2p3.fr/extrapolations/bernex.pdf

[34] A.H. Wapstra, G. Audi and R. Hoekstra, Nucl. Phys. **A432** (1985) 185.

[35] D. Lunney, J.M. Pearson and C. Thibault, Rev. Mod. Phys. **75** (2003) 1021.

[36] R.G. Thomas, Phys. Rev. **80** (1950) 136, **88** (1952) 1109; J.B. Ehrman, Phys. Rev. **81** (1951) 412.

[37] E. Comay, I. Kelson and A. Zidon, Phys. Lett. **B210** (1988) 31.

[38] M.C. Pyle, A. García, E. Tatar, J. Cox, B.K. Nayak, S. Triambak, B. Laughman, A. Komives, L.O. Lamm, J.E. Rolon, T. Finnessy, L.D. Knutson and P.A. Voytas, Phys. Rev. Lett. **B88** (2002) 122501.

[39] A.H. Wapstra, Proc. Conf. Nucl. Far From Stability/AMCO9, Bernkastel-Kues 1992, Inst. Phys. Conf. Series 132 (1993) 125.

[40] M.S. Antony, J. Britz, J.B. Bueb and A. Pape, At. Nucl. Data Tables **33** (1985) 447;
M.S. Antony, J. Britz and A. Pape, At. Nucl. Data Tables **34** (1985) 279;
A. Pape and M.S. Antony, At. Nucl. Data Tables **39** (1988) 201;
M.S. Antony, J. Britz and A. Pape, At. Nucl. Data Tables **40** (1988) 9.

[41] J. Jänecke, in D.H. Wilkinson, *'Isospin in Nuclear Physics'*, North Holland Publ. Cy. (1969) eq. 8.97; J. Jänecke, Nucl. Phys. **61** (1965) 326.

[42] L. Axelsson, J. Äystö, U.C. Bergmann, M.J.G. Borge, L.M. Fraile, H.O.U. Fynbo, A. Honkanen, P. Hornshøj, A. Jonkinen, B. Jonson, I. Martel, I. Mukha, T. Nilsson, G. Nyman, B. Petersen, K. Riisager, M.H. Smedberg, O. Tengblad and ISOLDE, Nucl. Phys. **A628** (1998) 345.

[43] Y.V. Linnik, Method of Least Squares (Pergamon, New York, 1961); Méthode des Moindres Carrés (Dunod, Paris, 1963).

[44] G. Audi, W.G. Davies and G.E. Lee-Whiting, Nucl. Instrum. Methods **A249** (1986) 443.

[45] Particle Data Group, 'Review of Particle Properties', Phys. Rev. **D66** (2002) 10001.

[46] M.U. Rajput and T.D. Mac Mahon, Nucl. Instrum. Methods **A312** (1992) 289.

[47] M.J. Woods and A.S. Munster, NPL Report RS(EXT)95 (1988).

[48] G. Audi, Int. J. Mass Spectr. **251** (2006) 85-94;
http://dx.doi.org/10.1016/j.ijms.2006.01.048

[49] G. Bollen, H.-J. Kluge, M. König, T. Otto, G. Savard, H. Stolzenberg, R.B. Moore, G. Rouleau and G. Audi Phys. Rev. **C46** (1992) R2140.

[50] Each group of mass-spectrometric data is assigned a factor F according to its partial consistency factor χ_n^p, due to the fact that its statistical uncertainties and its internal systematic error alone do not reflect the real experimental situation. From comparison to all other data and more specially to combination of reaction and decay energy measurements, we have assigned factors F of 1.5, 2.5 or 4.0 to the different labs. Only Penning trap data have almost all been assigned a factor $F = 1.0$. Example: the group of data H25 has been assigned $F = 2.5$, this means that the total uncertainty assigned to ^{155}Gd ^{35}Cl$-^{153}$Eu ^{37}Cl is $2.4\mu u \times 2.5$. The weight of this piece of data is then very low, compared to $0.79\mu u$ derived from all other data. This is why it is labelled "U".

[51] A. Gillibert, L. Bianchi, A. Cunsolo, A. Foti, J. Gastebois, Ch. Grégoire, W. Mittig, A. Peghaire, Y. Schutz and C. Stéphan, Phys. Lett. **B176** (1986) 317.

[52] D.J. Vieira, J.M. Wouters, K. Vaziri, R.H. Krauss, Jr., H. Wollnik, G.W. Butler, F.K. Wohn and A.H. Wapstra, Phys. Rev. Lett. **57** (1986) 3253.

[53] E.P. Wigner, in Proceedings of the Robert A. Welch Foundation Conference on Chemical Research, edited by W.0. Milligan (Welch Foundation, Houston, 1958), Vol. 1, p. 88.

[54] A.M. Lane, in D.H. Wilkinson, *'Isospin in Nuclear Physics'*, North Holland Publ. Cy. (1969), p. 509

[55] W. Bambynek, H. Behrens, M.H. Chen, B. Crasemann, M.L. Fitzpatrick, K.W.D. Ledingham, H. Genz, M. Mutterrer and R.L. Intemann, Rev. Mod. Phys. **49** (1977) 77.

[56] G. Audi, M. Wang, A.H. Wapstra, B. Pfeiffer and F.G. Kondev, J. Korean Phys. Soc. **59** (2011) 1318-1321.

[57] Commission on Nomenclature of Inorganic Chemistry, Pure and Applied Chemistry **69** (1997) 2471.

[58] S. Cwiok, S. Hofmann and W. Nazarewicz, Nucl. Phys. **A573** (1994) 356;
S. Cwiok, W. Nazarewicz and P.H. Heenen, Phys. Rev. Lett. **63** (1999) 1108.

[59] S. Aoyama, Phys. Rev. Lett. **89** (2002) 052501.

[60] L.V. Grigorenko and M.V. Zhukov, Phys. Rev. **C77** (2008) 034611.